1-16453

ASPECTS OF GALLIUM GEOCHEMISTRY

IN

UPPER MANTLE-DERIVED LHERZOLITE XENOLITHS

AND

CONTINENTAL ALKALINE VOLCANIC ROCKS

BY

DOUGLAS BRUCE McKAY©

SUBMITTED AS PARTIAL FULFILLMENT OF THE REQUIREMENTS

FOR THE DEGREE OF MASTER OF SCIENCE

FACULTY OF SCIENCE

LAKEHEAD UNIVERSITY

THUNDER BAY, ONTARIO, CANADA

SEPTEMBER, 1987

ISBN 0-315-44795-8

ABSTRACT

Various aspects of the geochemistry of Ga in upper mantle-derived garnet lherzolite xenoliths (from the Bultfontein Floors mine dump in Kimberley, South Africa), spinel lherzolite xenoliths (from Mount Porndon, Australia), and continental alkaline volcanic rocks (from the Freemans Cove, Balcones, Urach and Hegau suites of Canada, the U.S.A., and Germany, respectively) have been investigated. Ga abundances were determined by RNAA. The feasibility of using epithermal INAA to generate accurate Ga data was investigated. Analysis of U.S.G.S. standard granite G-2 suggests that epithermal INAA utilizing 630.1 KeV ^{72}Ga data has the potential to produce geologically useful Ga data.

The abundance of Ga in the lherzolite xenoliths varies by a factor of approximately 10 from 0.52 ± 0.14 ppm to 5.23 ± 0.44 ppm. The spinel lherzolite xenoliths contain appreciably more Ga (2.78 ± 0.26 ppm to 5.23 ± 0.44 ppm) than the garnet lherzolite xenoliths (0.52 ± 0.14 ppm to 1.44 ± 0.18 ppm). The sequence of enrichment of Ga in the minerals comprising the lherzolites is, from lowest to highest Ga content, olivine (0.20 ± 0.04 ppm to 0.72 ± 0.11 ppm), clinopyroxene (1.31 ± 0.13 ppm to 4.92 ± 0.32 ppm), garnet, if present (3.71 ±0.16 ppm to 6.03 ±0.48 ppm), phlogopite, if present (7.65 ±0.21 ppm), and spinel, if present (43.49 ±

0.91 ppm to 65.91 ± 2.10 ppm). Ga mineral/mineral distribution coefficients have been calculated. Preliminary results suggest the distribution of Ga between certain mineral pairs (e.g., $D_{Ga}^{opx/cpx}$) is temperature dependent and might be profitably utilized as a geothermometer.

The abundance of Ga in the continental alkaline volcanic rocks varies by a factor of approximately 3.5 from 12.14 ± 0.32 ppm to 41.97 ± 1.20 ppm. Ga behaved as an incompatible trace element during the genesis of these rocks. Model-derived constraints for Ga bulk-solid/melt distribution coefficients vary from 0.16 (Balcones suite) to 0.28 (Hegau suite). Intrasuite variations in the Ga/Al ratios of the mafic continental alkaline volcanic rocks range from approximately 14% (Hegau and Urach suites) to approximately 20% (Freemans Cove suite). Ga/Al ratios of primary melts from the Freemans Cove and Balcones suites decrease slightly (from 2.86 ± 0.16 to 2.28 ± 0.13, and from 4.12 ± 0.24 to 3.35 ± 0.19 respectively) with increasing degrees of partial melting.

ACKNOWLEDGEMENTS

The author would like to thank Dr. R. H. Mitchell for his guidance and constructive criticism during his supervision of this research study. Financial support was provided by an NSERC scholarship to the author and by NSERC Grant # A8706 to Dr. Mitchell. Credit is also due to Dr. J. Crockett and Dr. S. Landsburger for providing facilities, staff, and guidance to the author during a summer of research at McMaster University. Many thanks to the friends and fellow graduate students who have offered aid and encouragement at this time and in the past. Special thanks to the faculty and staff, especially Maureen Downey, of the Geology Department at Lakehead University for helping me along the way. Last, but not least, I would like to thank Linda Henriques for typing the manuscript.

TABLE OF CONTENTS

CHAPTER 4 (Cont'd) Page

CHAPTER 5 (Cont'd) Page

CHAPTER 5 (Cont'd) Page

LIST OF FIGURES

LIST OF FIGURES (Cont'd) Page

LIST OF TABLES

LIST OF TABLES (Cont'd) Page

LIST OF TABLES (Cont'd) Page

LIST OF TABLES (Cont'd) Page

LIST OF APPENDICES

LIST OF APPENDICES (Cont'd) Page

CHAPTER ONE

RATIONALE OF THESIS WORK

Although considerable progress has been made in recent years, many aspects of Ga geochemistry are still poorly understood and/or have never been investigated. The present thesis was undertaken in an attempt to expand our knowledge of Ga geochemistry and to promote future studies of Ga geochemistry.

The major objectives of this thesis are outlined below and discussed in detail in following chapters.

1. Accurate determination (better than ±5% (1σ)) of the abundance of Ga at the ppm level in geological materials is presently a relatively complicated procedure. As a consequence, few accurate Ga data have been published and our knowledge of Ga geochemistry is incomplete. It is of interest, therefore, to develop simpler analytical techniques. A major objective of this thesis is to assess the feasibility of using epithermal instrumental neutron activation analysis (a relatively simple analytical technique) to determine accurately the Ga content of geological materials.
2. The present data base for the abundance of Ga in upper mantle-derived ultramafic xenoliths is small and biased towards spinel lherzolites. A major objective of this thesis is to expand this data base by accurately

analyzing both garnet lherzolite and spinel lherzolite xenoliths.

3. Very few accurate Ga mineral/mineral distribution coefficients exist for upper mantle-derived xenoliths. A major objective of this thesis is to determine accurate Ga mineral/mineral distribution coefficients for garnet lherzolite and spinel lherzolite xenoliths and to assess the feasibility of using these distribution coefficients to estimate equilibration conditions of pressure and temperature.

4. Very few accurate Ga data for mafic volcanic rocks have been published. This is especially so for continental alkaline volcanic rocks. A major objective of this thesis is to expand the data base for the abundance of Ga in continental alkaline volcanic rocks by accurately analyzing four different volcanic suites (all of which contain rocks believed to be primary partial melts of the upper mantle) from widely separated geographical localities.

5. Very little is known about the geochemical behaviour of Ga during the genesis of continental alkaline volcanic rocks. A major objective of this thesis is to compare the Ga data obtained for these rocks to other trace element data in order to assess the geochemical behaviour of Ga during the genesis of these rocks.

6. Recent studies (discussed below) of mafic oceanic volcanic rocks suggest that Ga/Al ratios in these rocks

might be used to infer mantle source Ga/Al ratios, to differentiate basalts derived from different mantle sources, and to map mantle heterogeneities. A major objective of this thesis is to determine the Ga/Al ratios of mafic continental alkaline volcanic rocks in order to assess the validity of these suggestions.

7. The final major objective of this thesis is to develop possible constraints for the Ga bulk-solid/melt distribution coefficients associated with the genesis of the primary partial melts of the continental alkaline volcanic suites studied.

CHAPTER TWO

INTRODUCTION TO GALLIUM GEOCHEMISTRY

Gallium (Ga) was discovered by LeCoq De Boisbaudran in 1875 and named after the Latin word for France (Mellor, 1924). Ga is a soft, silvery white metal that melts in your hand. It is the only metal that expands as it freezes (Schiller, 1987).

The principal use of Ga is in the electronics industry where it is used in the production of light emitting diodes, lasers, bubble memories and microwave equipment (Schiller, 1987). Ga is essential for building superfast, supercool computer chips (Maurice, 1987).

Ga is presently recovered as a by-product of zinc reprocessing and bauxite refining, and from certain rare and unique sulphide ores (Schiller, 1987). Major producers of Ga are Alcan and Cominco in Canada and smelters in Europe, Russia and Japan. Fargo Resources Limited of Vancouver are presently performing experiments in attempts to extract Ga from British Columbian coals (Schiller, 1987). The annual consumption of Ga in the Western World is believed to be approximately 50 tons (Wittur, 1987).

General aspects of Ga geochemistry have been reviewed by Shaw (1957) and Vlasov (1966). Ga is a transition element located in Group III of the Periodic Table. Some of the physical properties of Ga are given in Table 1.

TABLE 1

Physical Properties of Gallium

Property	Value	References
Atomic Number	31	
Atomic Weight	69.72	
Natural Isotopes	69 (60.2%)	Day, 1963
	71 (39.8%)	Day, 1963
Valency	1+, 2+, 3+	
Specific Gravity (20°C)	5.91 g/cc	Vlasov, 1966
Melting Point	29.78°C	Vlasov, 1966
Boiling Point	2070°C	Vlasov, 1966

Although stable in air at normal temperatures, Ga does not naturally occur in the native state (Shaw, 1957). Ga is a typical dispersed element that very rarely forms its own mineral phases. Examples of the abundance of Ga in some common minerals are given in Table 2.

The only independent Ga mineral reported to exist, gallite ($CuGaS_2$), occurs in negligible amounts in association with sphalerite, renierite, germanite and chalcopyrite in only two known ore deposits: Tsumeb (Southwest Africa) and Kipushi (Congo) (Vlasov, 1966).

The solar abundance of Ga has been estimated to be approximately 38 atoms/10^6 Si atoms (Cameron, 1982; Anders and Ebihara, 1982). The average crustal abundance of Ga has been estimated to be approximately 19 ppm (Shaw, 1957; Vinogradov, 1962).

Ga is crystallochemically similar (Table 3) to aluminum (Al^{3+}), zinc (Zn^{2+}) and iron (Fe^{3+}) and can isomorphously replace these elements in many minerals.

TABLE 2

Examples of the Abundance of Ga in Some Common Minerals

Mineral	Ranges in Ga Content (ppm)	References
Beryl	0 - 30	1
Biotite	0 - >100	1
Cassiterite	0 - 50	1
Clinopyroxene	4.0 - 5.0	2
Chlorite	0 - 100	1
Garnet	0 - 30	1
Ilmenite	1.1	3
Lepidolite	10 - 300	1
Magnetite	48.9 - 110.0	3
Muscovite	0 - >100	1
Nepheline	0 - 1000	1
Orthopyroxene	2.6 - 3.8	2
Phlogopite	10 - 50	1
Plagioclase	31.0 - 38.0	3
Sericite	0 - 50	1
Sphalerite	0 - 10000	1
Spinel	40	2
Spodumene	10 - 700	1
Tourmaline	10 - 100	1

Reference abbreviations: 1 - Vlasov, 1966;
2 - Kurat *et al.*, 1980;
3 - Vincent and Nightingale, 1974.

TABLE 3

Valency, Ionic Radii and Ionization Potentials of Ga, Al, Fe and Zn

Element	Ionic Radius (Å) (Whittaker and Muntus, 1970)		Ionization Potential (eV) (Vlasov, 1966)
	Tetrahedral Coordination	Octahedral Coordination	
Ga^{3+}	0.55	0.70	57.02
Al^{3+}	0.47	0.61	53.14
Fe^{3+}	0.57	0.73	55.42
Zn^{2+}	0.68	0.83	27.41

The geochemical coherence of Ga and Al during partial melting and fractional crystallization has been noted by many geochemists (e.g., Goldschmidt, 1937; Ringwood, 1955; Ahrens, 1965; and De Argollo, 1974) and may be attributed to the similarity of the ionic radii, valency, and ionization potentials of these two elements.

Ga is siderophile, lithophile, and chalcophile in its geochemical behaviour.

The siderophile nature of Ga is revealed by its abundance and distribution in iron meteorites. In these meteorites, the bulk of the Ga occurs in the metallic phases where it attains concentrations of up to 90 ppm (Wasson, 1970).

The lithophile nature of Ga is revealed by its abundance and distribution in silicate rocks. In these rocks the distribution of Ga is primarily dependent upon the aluminum content of the major mineral phases present (Shaw, 1957). Ga can replace Al at both octahedral and tetrahedral lattice sites in common rock forming minerals. The substitution of Ga for Al at tetrahedral sites accounts for approximately 50 - 75% of the Ga present in most rocks (Vlasov, 1966).

Although iron also occurs in four-fold and six-fold coordination with oxygen, it appears that Ga^{3+} will only replace Fe^{3+} at tetrahedral lattice sites (Burton *et al*, 1959; Vincent and Nightingale, 1974). It is not presently understood why Ga^{3+} does not replace Fe^{3+} at octahedral lattice sites.

The chalcophile nature of Ga is revealed by its occurrence in sulphide minerals. The mineral gallite, for example, contains up to 35 wt.% Ga (Vlasov, 1966). Ga also occurs as a common minor constituent of sphalerite (Moller *et al*, 1983). Vlasov (1966) states there is apparently no Ga-Zn isomorphism in oxygen compounds -- silicates, oxides, carbonates, etc., since Ga is virtually nonexistent in calamine, willemite and smithsonite. It appears that the coherence of Ga and Zn is weak and mainly restricted to sulphides (Shaw, 1957).

The dispersion of Ga in the major rock forming minerals results in its ubiquitous occurrence in all igneous rocks. Examples of the abundance of Ga in different igneous rock types are given in Table 4.

TABLE 4

Examples of the Abundance of Ga in Different Igneous Rock Types

Rock Type	Range in Ga Content (ppm)	References
Ultramafic	1.92 - 3.70	Jagoutz *et al.* (1979)
Mafic	16.4 - 27.1	De Argollo (1974)
Intermediate	12.2 - 35.6	Vincent and Nightingale (1974)
Felsic	29.6 - 36.7	Vincent and Nightingale (1974)

Ultramafic igneous rocks only contain significant amounts of Ga when aluminous minerals (biotite, kalsilite, leucite, melilite) are present (Shaw, 1957). The differences between the abundances of Ga in mafic, intermediate and felsic igneous rocks are small. Alkalic and pegmatitic igneous rocks common-

ly contain the greatest concentrations of Ga (Vlasov, 1966).

Ga generally behaves as a moderately incompatible trace element and tends to concentrate in the liquid phases associated with igneous processes (Vlasov, 1966; De Argollo, 1974; Vincent and Nightingale, 1974; Frey *et al.*, 1985).

CHAPTER THREE

ANALYSIS OF GALLIUM

3.1 INTRODUCTION

Trace amounts of Ga in geological materials have been determined using a variety of analytical techniques. These include spectrographic (Goldschmidt and Peters, 1931; Oftedal, 1940; Gabrielson, 1945; Strock, 1945; Mukherjee, 1948; Ahrens, 1951), fluorimetric (Sandell, 1947 and 1949), atomic absorption spectrometric (Van Der Walt and Strelow, 1984), and neutron activation techniques (Morris and Chambers, 1960; Vincent and Nightingale, 1974; De Argollo and Schilling, 1978(a)). Of these, neutron activation is, in general, the most sensitive, accurate and precise analytical method (Morris and Brewer, 1954; Meinke, 1955; Morris and Chambers, 1960; Smales, 1965).

The general principles of neutron activation analysis (NAA) are discussed by De Soete *et al.* (1972), Muecke (1980), Steinnes (1971). A brief summary is given in Appendix 1.

NAA of Ga is based on the nuclear reaction $^{71}Ga(n,\gamma)^{72}Ga$. ^{72}Ga is radioactive and decays with a half-life of 14.1 hours. A decay scheme for ^{72}Ga is given in Figure 1. The activities of the 630.1 KeV and 834.1 KeV gamma rays (relative intensities of 10% and 40% respectively) are used to calculate Ga contents. A worked example is given in Appendix 1.

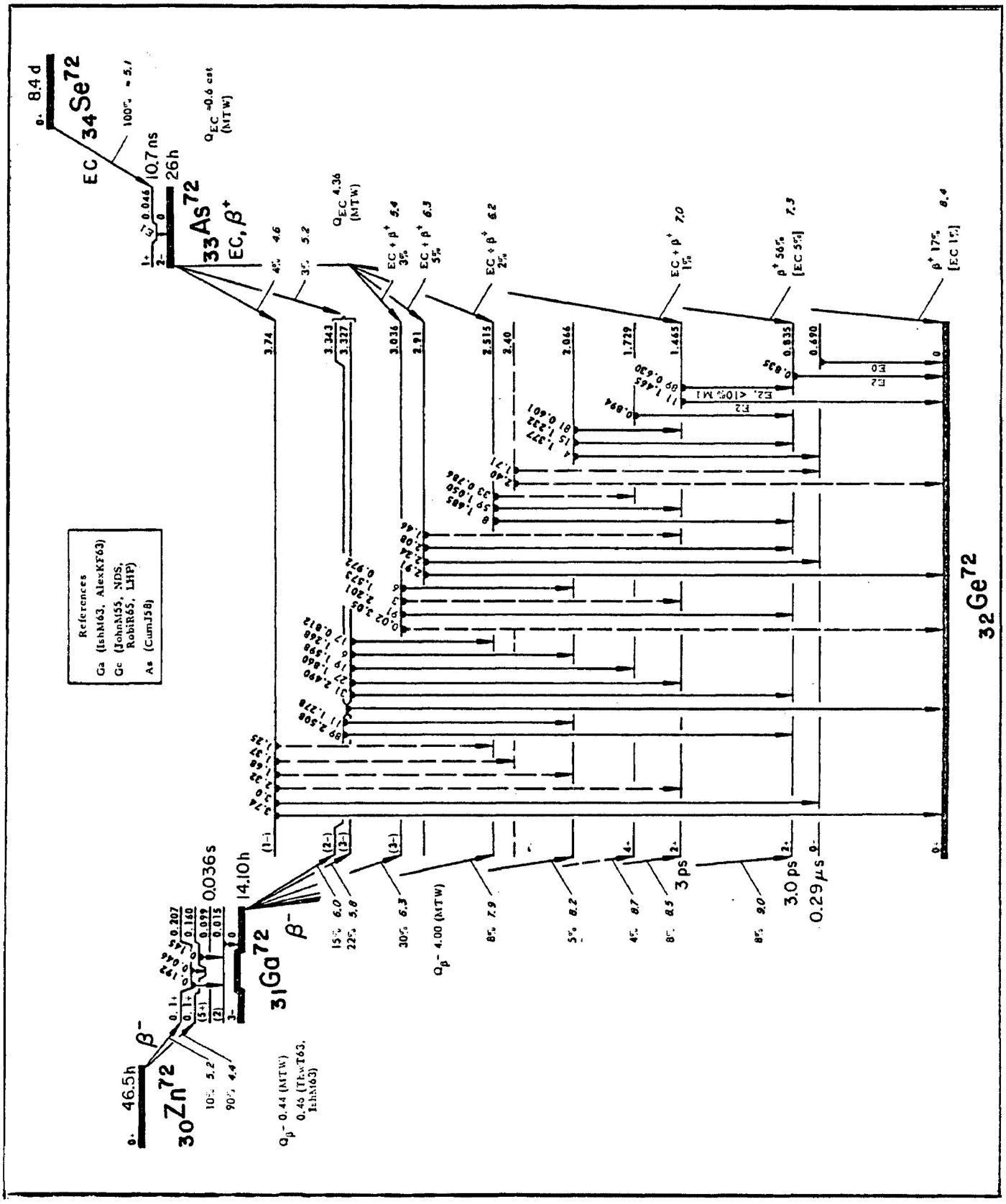

Figure 1. Decay scheme for ^{72}Ga (from Lederer et al., 1967).

In the present study, two types of NAA of Ga are compared:

1. radiochemical neutron activation analysis (RNAA) involving activation by thermal neutrons;
2. instrumental neutron activation analysis (INAA) involving activation by epithermal neutrons.

The general advantages of INAA involving activation by epithermal neutrons rather than thermal neutrons are discussed by Steinnes (1971). The primary advantage is that elements which contribute significantly to the compton continuum of thermally activated samples (i.e., ^{23}Na, ^{27}Al, ^{31}P, ^{41}K, ^{45}Sc, ^{50}Cr, ^{55}Mn, ^{58}Fe, ^{139}La, ^{151}Eu, etc.) have low resonance activation integrals compared to their thermal activation cross-sections. This permits determination of elements such as Ga, Cs, or U that would otherwise have their photopeaks obscured by matrix activity.

3.2 ANALYTICAL METHODS

3.2.1. RNAA

The RNAA method used is a modification of the methods described by Culkin *et al.* (1958), Morris and Chambers (1960), Wasson *et al.* (1966), and De Argollo (1974). The method is described in detail in Appendix 1. Briefly, approximately 100 mg of powdered sample are irradiated for 7 hours in a thermal neutron flux of 5×10^{12} $n/cm^2/sec$ and allowed to "cool" for approximately 84 hours. Ga carrier is

added and the sample decomposed in a mixture of HF and HNO_3. The sample is dried, adjusted to 6N in HCl, and transferred to a separatory funnel. Ga is extracted into isopropyl ether and back extracted into H_2O. The activity of the extract is measured and Ga content calculated relative to standard samples. Chemical yields are determined by re-irradiation (see Appendix 1) and are, in general, better than 90%. Trace amounts of Na, Sc, Co, Fe, and REE's are present in the Ga extract but do not significantly affect measurement of the ^{72}Ga photopeaks.

3.2.2 Epithermal INAA

The INAA method used is based upon the methods described by Baedecker *et al.* (1977) and Brunfelt and Steinnes (1969). The method is described in detail in Appendix 1. Briefly, approximately 300 mg of powdered sample are irradiated in a cadmium shield for 30 minutes in an epithermal neutron flux of 2×10^{11} $n/cm^2/sec$. The sample is allowed to "cool" for approximately 12 hours. ^{72}Ga activity is measured and Ga content calculated relative to standard samples.

3.3 RNAA vs. EPITHERMAL INAA

3.3.1 Accuracy and Precision

The accuracy and precision of the techniques were assessed by performing replicate analyses of the U.S.G.S. standard granite G-2 using synthetic gallium standards. The results are given in Tables 5 and 6.

The RNAA data are more accurate, relative to Abbey's

TABLE 5

RNAA Ga Data for G-2 (quoted uncertainties, 1δ, due to counting statistics of gamma ray spectrometry)

Sample G-2, 23 ppm Ga (Abbey, 1983)				
Analysis	Analytical Peak			
	630.1 KeV		834.1 KeV	
	Calculated Ga Content (ppm)	Accuracy (%)	Calculated Ga Content (ppm)	Accuracy (%)
1	22.02 ± 1.30	-4.26	23.49 ± 0.64	+2.13
2	24.82 ± 1.49	+7.91	22.99 ± 0.79	-0.04
3	23.10 ± 1.34	+0.43	22.55 ± 0.76	-1.96
4	20.83 ± 1.23	-9.43	22.40 ± 0.65	-2.61
5	21.18 ± 1.27	-7.91	23.31 ± 0.77	+1.35
6	23.43 ± 1.38	+1.87	24.53 ± 0.81	+6.65
7	24.43 ± 1.41	+6.22	22.04 ± 0.77	-4.17
8	22.57 ± 1.35	-1.87	22.11 ± 0.82	-3.87
9	20.92 ± 1.38	-9.04	23.52 ± 0.85	+2.26
10	22.74 ± 1.40	-1.13	22.46 ± 0.72	-2.32
Mean	22.60 ± 1.40	-1.74	22.94 ± 0.76	-0.26
Standard Deviation (1δ)	1.32 ppm (5.76%)		0.78 ppm (3.39%)	

TABLE 6

Epithermal INAA Ga Data for G-2 (quoted uncertainties, 1δ, due to counting statistics of gamma ray spectrometry)

Sample G-2, 23 ppm Ga (Abbey, 1983)				
Analysis	Analytical Peak			
	630.1 KeV		834.1 KeV	
	Calculated Ga Content (ppm)	Accuracy (%)	Calculated Ga Content (ppm)	Accuracy (%)
1	22.19 ± 3.33	-3.65	32.48 ± 2.21	+41.22
2	25.12 ± 3.12	+9.22	32.99 ± 2.28	+43.43
3	22.93 ± 2.75	+0.31	29.10 ± 2.31	+26.52
4	29.89 ± 3.56	+12.99	32.35 ± 2.23	+40.65
5	27.89 ± 3.84	+12.13	30.71 ± 2.03	+33.52
6	23.34 ± 3.26	+1.48	28.25 ± 2.11	+22.83
7	22.49 ± 3.37	-2.27	28.50 ± 2.25	+23.91
Mean	24.84 ± 3.32	+8.00	30.63 ± 2.20	+33.17
Standard Deviation (1δ)	1.32 ppm (5.76%)		0.78 ppm (3.39%)	

(1983) recommended value of 23 ppm, and more precise than the epithermal INAA data. The 834.1 KeV RNAA data are the most accurate (mean accuracy of -0.26%) and most precise (3.39% at 1σ).

The 630.1 and 834.1 KeV RNAA data are similar (mean values of 22.60 ± 1.40 and 22.94 ± 0.76 ppm Ga respectively). This suggests spectral interference has not affected measurement of either ^{72}Ga photopeak.

The 630.1 and 834.1 KeV epithermal INAA data are significantly different (mean values of 24.84 ± 3.32 and 30.63 ± 2.20 ppm Ga respectively). This difference suggests that spectral interference has affected measurement of the 834.1 KeV ^{72}Ga photopeak.

^{54}Mn emits 834.8 KeV gamma rays (100% intensity) and is a possible source of the observed interference. Unfortunately, ^{54}Mn does not emit any other gamma rays that can be used to detect its presence. As a result, it is difficult to determine whether or not the observed interference of the 834.1 KeV ^{72}Ga photopeak is due to ^{54}Mn. ^{54}Mn is generated by the nuclear reaction ^{54}Fe (n, p) ^{54}Mn. ^{54}Mn has a half-life of 291 days (De Soete *et al.*, 1972).

In order to assess the possibility that ^{54}Fe derived ^{54}Mn is produced during epithermal neutron activation, 5 Fe solutions (Fe contents ranging from 482.69 μg to 17980.57 μg) were prepared, irradiated, and analyzed. The results are given in Table 7.

TABLE 7

Epithermal INAA Activity Data for Fe Solutions
(quoted uncertainties, 1δ, due to counting statistics of gamma ray spectrometry)

Sample Solution	Fe Content (μg)	Activity (Net Area Counts/4000sec)	
		630.1 KeV	834.1 KeV
1	482.69	0 ± 0	11 ± 18
2	2226.39	0 ± 0	60 ± 27
3	3768.78	0 ± 0	173 ± 24
4	8561.87	46 ± 35	353 ± 29
5	17980.57	36 ± 42	526 ± 35

The 630.1 KeV and 834.1 KeV activities of the samples are compared in Figure 2.

The 834.1 KeV activities (net area) increase systematically (from 11 ± 18 to 526 ± 35) with increasing Fe content. The 630.1 KeV activities (net area) are negligible (0 ± 0 to 46 ± 35) and, in all but one sample (sample 4), below the minimum detection limit (Woldseth, 1973) for the technique. The measured 630.1 KeV activities (net area) of samples 4 (46 ± 35) and 5 (36 ± 42) may reflect the presence of small quantities of contaminating Ga in these samples. The large differences between the 630.1 KeV and 834.1 KeV activities preclude the possibility of ^{72}Ga as the major 834.1 KeV activity source (if ^{72}Ga was the activity source, the 834.1 KeV activity would only be approximately 4 times that of the 630.1 KeV activity). The data suggest ^{54}Mn is the major 834.1 KeV activity source and demonstrates that ^{54}Mn is produced from ^{54}Fe during epithermal neutron activation.

In order to assess the effect of ^{54}Fe derived ^{54}Mn on

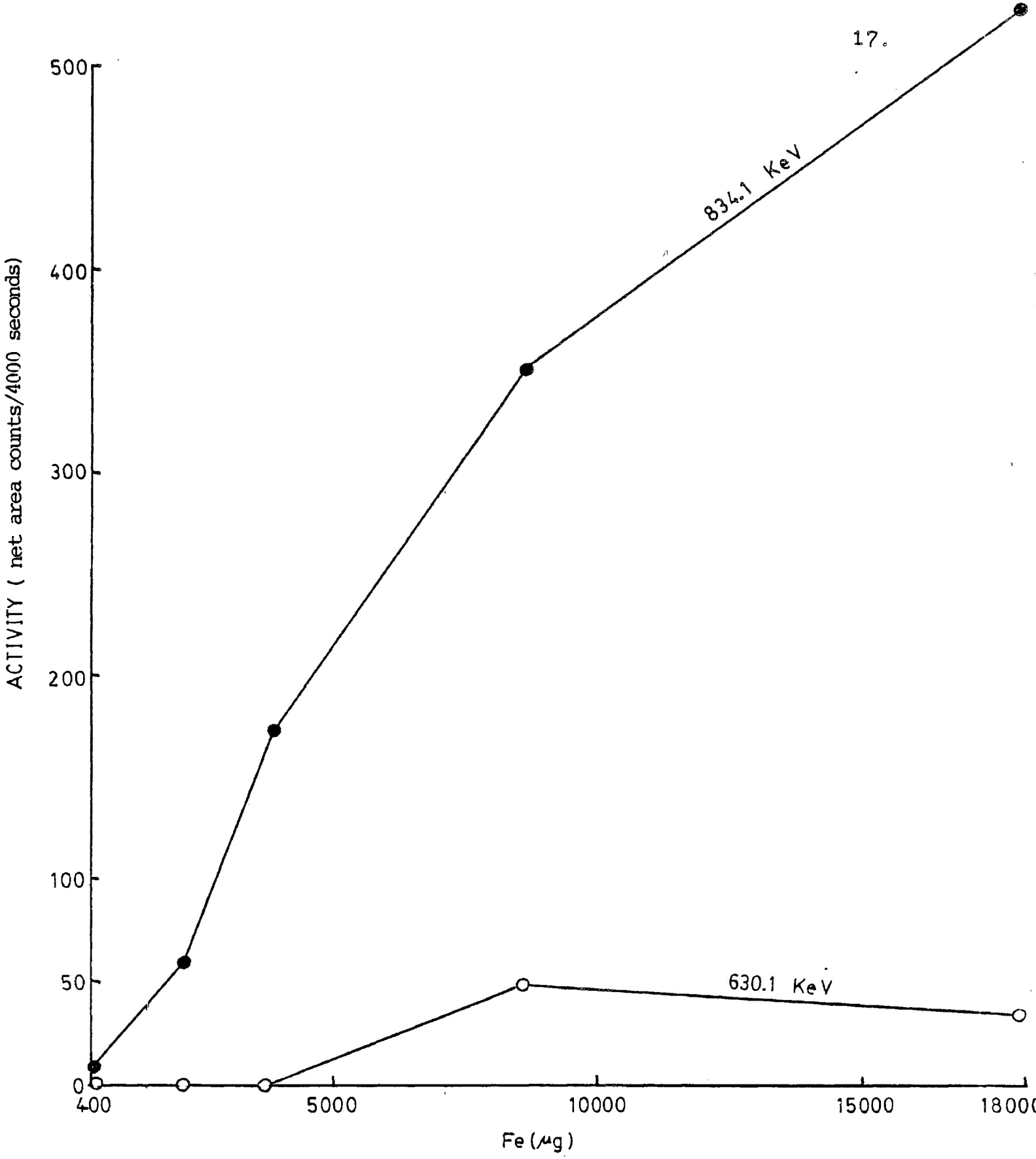

FIGURE 2 Activity vs. Fe(μg) plot for Epithermal INAA of Fe solutions.

the measurement of 834.1 KeV ^{72}Ga photopeaks, Ga solutions (average Ga content of approximately 18.5 ppm) containing varying quantities of Fe (from 0.16 wt.% to 4.54 wt.%) were prepared, irradiated and analyzed. The results are given in Table 8.

TABLE 8
Epithermal INAA Data for Ga+Fe Solutions
(quoted uncertainties, 1σ, due to counting statistics of gamma ray spectrometry)

Sample Solution	Fe Content (wt. %)	True Ga Content (ppm)	Analytical Peak			
			630.1 KeV		834.1 KeV	
			Calculated Ga Content (ppm)	Accuracy (%)	Calculated Ga Content (ppm)	Accuracy (%)
1	0.16	17.24	16.98±0.44	−0.15	17.41±0.19	+0.99
2	0.68	18.64	18.33±0.46	−1.66	19.02±0.20	+2.04
3	1.20	19.24	19.20±0.40	−0.21	19.98±0.18	+3.85
4	2.38	18.82	18.94±0.40	+0.64	20.14±0.18	+7.55
5	4.54	18.63	18.66±0.39	+0.16	21.11±0.17	+13.31

The accuracies of the calculated Ga contents (relative to the true Ga contents) based on 834.1 KeV data range from +0.99% to +13.31% and become systematically poorer by approximately 3% for each weight % of Fe present (Figure 3). The accuracies of the calculated Ga contents (relative to the true Ga contents), based on 630.1 KeV data range from −1.66% to +0.64%, do not vary systematically with Fe content (Figure 3), and can be accounted for by the analytical errors due to counting statistics.

The epithermal INAA 630.1 KeV ^{72}Ga data collected during the present study, although not as accurate or precise as the 630.1 KeV or 834.1 KeV RNAA data, suggest that epithermal

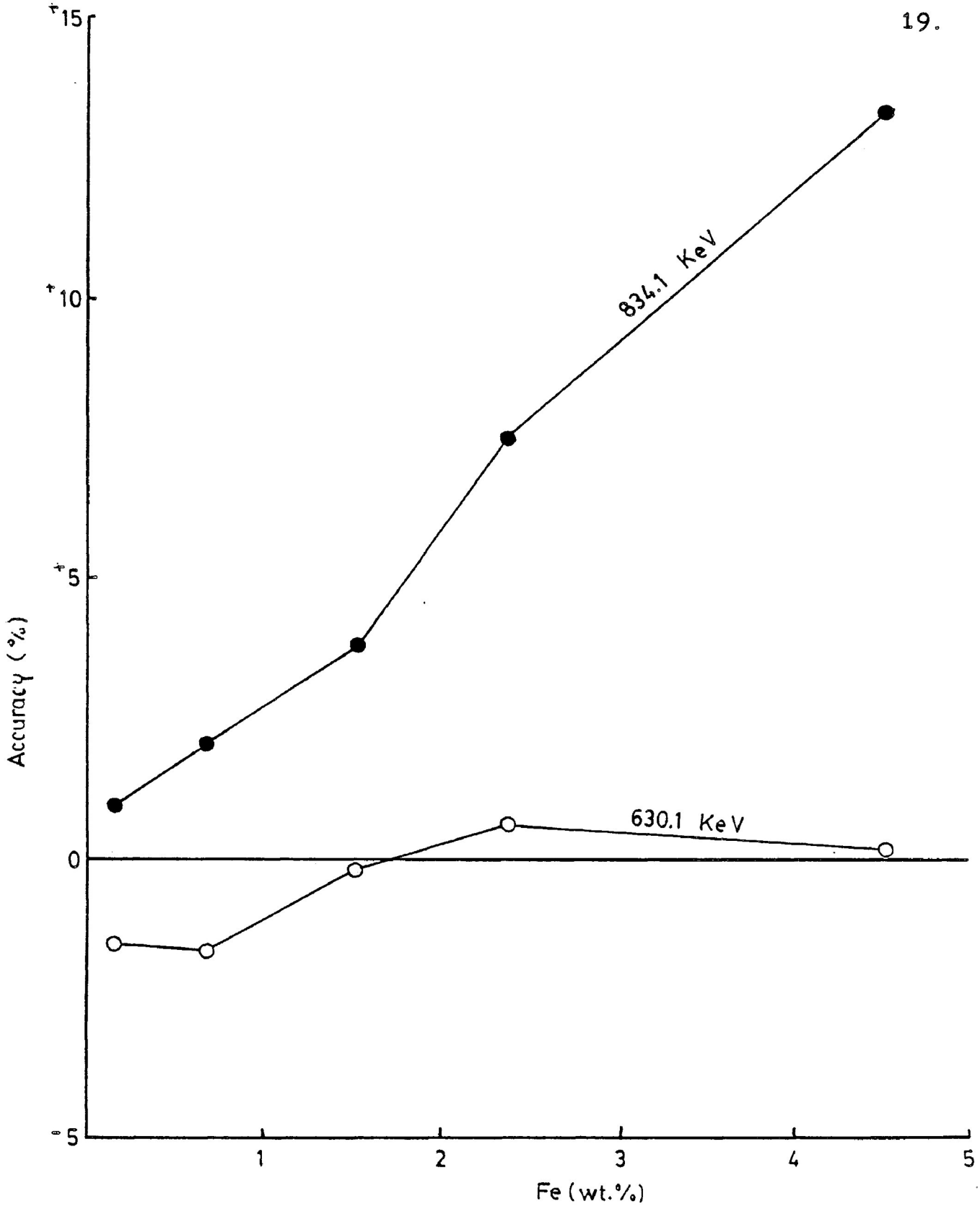

FIGURE 3 Accuracy vs. Fe(wt.%) plot for epithermal INAA of Ga + Fe solutions.

INAA based on measurement of the ^{72}Ga 630.1 KeV photopeak has the potential to produce geologically useful Ga data. If the Fe content of the rocks or minerals of interest are sufficiently low (<~1 wt. %) epithermal INAA based on measurement of the ^{72}Ga 834.1 KeV photopeak may be viable.

Activity data for representative epithermal INAA of G-2 and RNAA of G-2 are given in Table 9. The average background activity associated with epithermal INAA is approximately 10 times greater than that associated with RNAA. The peak apex to average background ratios associated with RNAA (2.3 and 5.6 for the 630.1 and 834.1 KeV ^{72}Ga photopeaks respectively) are greater than those associated with epithermal INAA (1.1 and 1.4 for the 630.1 and 834.1 KeV ^{72}Ga photopeaks respectively). These differences account, in part, for the differences in accuracy and precision associated with each technique.

TABLE 9

Activity Data for Representative Analyses of G-2

Technique	Count Time (sec)	Net Peak Area (counts)		Background Area (counts)		Peak Apex (counts/channel)		Average Background (counts/channel)	
		630.1 KeV	834.1 KeV	630.1 KeV	834.1 KeV	630.1 KeV	834.1 KeV	630.1 KeV	834.1 KeV
RNAA									
Sample	4000	1022	3049	1230	1800	487	1014	208	180
Standard	4000	3248	9464	980	810	1137	3421	156	90
Yield Sample	1000	2753	7548	8500	7217	2788	4552	1703	1512
Yield Standard	1000	3285	10405	10970	8500	3434	5894	1907	1752
INAA									
Sample	10000	1385	5027	16800	18900	2758	3334	2407	2400
Std.	10000	4517	12402	3320	1665	1470	3589	332	120

The U.S.G.S. standard rock BHVO-1, a basalt, was also analyzed by epithermal INAA. The results are given in Table 10. The 630.1 KeV data are more accurate, relative to Abbey's (1983) recommended value of 21 ppm Ga, than the 834.1 KeV data. The differences between the 630.1 and 834.1 KeV data are due to spectral interference in the region of the 834.1 KeV ^{72}Ga photo-peak.

TABLE 10
Epithermal INAA of BHVO-1 (uncertainties, 1δ, due to counting statistics of gamma ray spectrometry)

Sample BHVO-1, 21 ppm Ga (Abbey, 1983)				
Analysis	Analytical Peak			
	630.1 KeV		834.1 KeV	
	Calculated Ga Content (ppm)	Accuracy (%)	Calculated Ga Content (ppm)	Accuracy (%)
1	17.73 ± 1.82	-15.57	24.82 ± 0.82	+18.19
2	17.82 ± 1.92	-15.14	25.31 ± 0.83	+20.52
3	19.07 ± 1.93	-9.19	24.76 ± 0.85	+17.90
4	18.29 ± 1.98	-12.90	26.23 ± 0.90	+24.90
5	17.90 ± 2.04	-14.76	24.46 ± 0.86	+16.48
6	18.97 ± 2.42	-9.67	24.30 ± 0.98	+15.71
7	19.91 ± 2.19	-5.19	26.78 ± 1.08	+27.52
8	19.00 ± 2.39	-9.52	25.10 ± 0.99	+19.52
9	18.75 ± 2.34	-10.71	24.23 ± 1.07	+15.38
10	21.25 ± 2.74	+1.19	27.24 ± 1.27	+29.71
Mean	18.87 ± 2.18	-10.14	25.32 ± 0.97	+20.57
Standard Deviation (1δ)	1.08 ppm (5.73%)		1.07 ppm (4.21%)	

3.3.2 Relative Sensitivity

The sensitivity of each technique is largely dependent on the background activity in the region of the photopeaks of interest. An estimate of the minimum detection limit (MDL)

for each technique is given by Equation 1 (Woldseth, 1973).

$$MDL = 2\sqrt{B} \qquad (1)$$

where: MDL: is the minimum detection limit in net area counts,

B: is the background activity at the photopeak of interest in counts.

Table 11 gives a comparison of estimated minimum detection limits for Ga in representative samples of G-2 (calculations based on activity data given in Table 9).

TABLE 11
Comparison of Estimated Minimum Detection Limits for Ga in Representative Samples of G-2

Technique	Estimated MDL	
	Net Area Counts	Corresponding Ga Content (ppm)
RNAA		
630.1 KeV	70	1.70
834.1 KeV	85	0.61
Epithermal INAA		
630.1 KeV	259	4.17
834.1 KeV	275	1.57

The estimated minimum detection limits for Ga in G-2 are lower for RNAA than for epithermal INAA; 834.1 KeV RNAA has the lowest minimum detection limit for Ga in G-2 (0.61 ppm).

The estimated minimum detection limits for Ga in G-2 do not necessarily apply to analysis of other materials. In mineral samples, for example, the background activities are lower than those associated with G-2 and the estimated minimum detection limits for Ga would be lower than those given in Table 11. Table 12 gives some estimated minimum

detection limits for Ga in mineral samples analyzed using 834.1 KeV RNAA (calculations based on activity data collected during the present study).

TABLE 12
Estimated Minimum Detection Limits for Ga in Mineral Samples Analyzed Using 834.1 KeV RNAA

Mineral Sample	Estimated MDL	
	Net Area Counts	Corresponding Ga Content (ppm)
Olivine	75	0.13
OPX	57	0.10
CPX	106	0.18
Garnet	89	0.15
Spinel	111	0.19
Phlogopite	104	0.18

Accuracy and precision decrease as the minimum detection limit is approached.

3.3.3 Cost

3.3.3.1 Labour Cost

The approximate labour costs associated with each technique, expressed in "man-hours", are given in Table 13.

TABLE 13
Approximate Labour Costs

		Cost (man-hours/sample)	
		Epithermal INAA	RNAA
Sample preparation prior to irradiation:	Rock Samples	0.35	0.35
	Yield Samples	-	0.15
Sample preparation prior to spectrometry:	Rock Samples	0.05	0.55
	Yield Samples	-	0.05
Total Cost		0.40	1.10

3.3.3.2 Chemical Cost

The approximate costs of chemicals used in processing are given in Table 14. The costs are expressed in Canadian dollars according to 1985 price estimates.

TABLE 14
Approximate Costs of Chemicals Used in Processing

Chemical	Cost ($ per sample)	
	Epithermal INAA	RNAA
HNO_3	-	0.06
HF	-	0.70
HCl	-	0.36
$TiCl_3$	-	0.12
Isopropyl Ether	-	1.41
Gallium Carrier	-	0.05
Total Cost	-	2.70

3.3.3.3 Irradiation Cost

The approximate irradiation costs are given in Table 15.

TABLE 15
Approximate Irradiation Costs

Technique		Cost ($ per sample)
RNAA	Sample Exposure	7.50
	Yield Exposure	7.50
	Total	15.00
Epithermal INAA		
	Sample Exposure	10.70
	Total	10.70

Spatial and temporal constraints associated with epithermal INAA restrict the maximum number of samples that can be irradiated together to 7. This increases the sample exposure cost relative to RNAA.

RNAA of Ga costs approximately 7 dollars more, per sample, and requires approximately 0.7 more man-hours to perform, per sample, than epithermal INAA of Ga.

3.4 CONCLUSIONS

1. RNAA of Ga in G-2 is more accurate and precise than epithermal INAA of Ga in G-2. RNAA utilizing 834.1 KeV ^{72}Ga activity data is the most accurate and precise analytical technique.
2. During epithermal INAA of Ga, ^{54}Fe-derived ^{54}Mn activity interferes with accurate measurement of the 834.1 KeV ^{72}Ga photopeak.
3. Epithermal INAA 630.1 KeV ^{72}Ga data, although not as accurate or precise as 630.1 KeV or 831 KeV RNAA ^{72}Ga data suggests that epithermal INAA has the potential to produce geologically useful Ga data.
4. The estimated sensitivity of RNAA of Ga is lower than the estimated sensitivity of epithermal INAA of Ga.
5. RNAA of Ga costs approximately 7 dollars (Canadian) more, per sample, and requires approximately 0.7 more man-hours to perform, per sample, than epithermal INAA of Ga.

RNAA utilizing 834.1 KeV ^{72}Ga activity data is judged the superior technique. All subsequent Ga data reported in this work were obtained using this technique. During analysis, the 630.1 KeV ^{72}Ga activity data was measured and

used to monitor the 834.1 KeV ^{72}Ga activity data for spectral interference. None was observed.

CHAPTER FOUR

ASPECTS OF GALLIUM GEOCHEMISTRY IN UPPER MANTLE-DERIVED GARNET AND SPINEL LHERZOLITE XENOLITHS

4.1 INTRODUCTION

4.1.1 Comments on Siderophile Element Geochemistry

Knowledge of the composition of the upper mantle is fundamental to our understanding of major Earth-forming processes. Numerous hypotheses and considerable controversy exist concerning the exact nature of such processes. In recent years, the abundance and distribution of siderophile (metal-loving) elements in the Earth's upper mantle have been used by geochemists to constrain models of basalt petrogenesis, the extent of core-mantle equilibration, and the amount of post core-formation meteoritic input to the mantle (e.g., Ringwood, 1965; Brett, 1970; Ringwood and Kesson, 1977; Chou, 1978; Mitchell and Keays, 1981; Keays *et al.*, 1984; Garuti *et al.*, 1984; Newson and Palme, 1984; and Morgan, 1986).

The rationale for using siderophile element abundances to constrain such hypotheses is based on the fact that siderophile elements tend to become strongly enriched in Fe-Ni phases (e.g., the core of the Earth) and depleted in silicate phases (e.g., the mantle of the Earth) if these phases are in equilibrium with one another. By determining the siderophile element abundances in the core and mantle of the Earth, it

may be possible to estimate the extent of core-mantle equilibration and to develop constraints for various Earth-forming processes such as those mentioned above.

The validity of hypotheses based upon the distribution of siderophile elements between the core and mantle of the Earth depend upon:

1. accurate determination of the abundances of siderophile elements in the mantle and core of the Earth; and
2. accurate determination of metal/silicate distribution coefficients for siderophile elements at core/mantle conditions of P, T, and composition.

It is presently impossible to determine directly either of the above parameters.

The abundances of siderophile elements in the Earth's mantle have generally been estimated by assuming the composition of the mantle corresponds to the composition of pyrolite (i.e., a mixture of 1 part of ocean-floor tholeiite to 5 parts of residual refractory peridotite (Ringwood, 1975).

The abundances of siderophile elements in the Earth's core have been estimated by assuming the composition of the bulk Earth corresponds to the composition of C1 carbonaceous chondrites. By subtracting the estimated siderophile element contributions of the crust and mantle from the bulk Earth estimate, an estimate of the abundances of siderophile elements in the core is obtained.

Metal/silicate distribution coefficients for siderophile elements have been estimated using:

1. data obtained from C1 carbonaceous chondrites; and
2. data obtained from experiments on simple systems at low pressures.

Chou (1978) has classified siderophile elements in the Earth's upper mantle into highly siderophile elements (e.g., PGE, Re, Au) which have metal/silicate distribution coefficients greater than 10,000, and moderately siderophile elements (e.g., Ga, Ni, Co, W, Mo) which have metal/silicate distribution coefficients less than 10,000. Figure 4 shows the estimated abundances of siderophile elements in the Earth's upper mantle relative to type C1 chondrites (Chou *et al.*, 1983).

The highly siderophile elements are depleted by factors ranging from about 120 to 150 relative to their abundances in C1 chondrites (Chou *et al.*, 1983). The moderately siderophile elements are depleted by factors ranging from 15 to 50 relative to their abundances in C1 chondrites (Chou, 1978).

The abundances of siderophile elements in the upper mantle are higher, by factors varying from 10 to 1000, than the abundances predicted on the basis of low pressure partitioning experiments of these elements between metal and silicate phases (Chou, 1978). Kimura *et al.* (1974), for example, have experimentally determined the Au metal/silicate distribution coefficient to be approximately 3.3×10^4, whereas Mitchell and Keays (1981) assuming a C1 carbonaceous chondrite parent and a spinel lherzolite based pyrolite have determined the Au core/mantle distribution coefficient

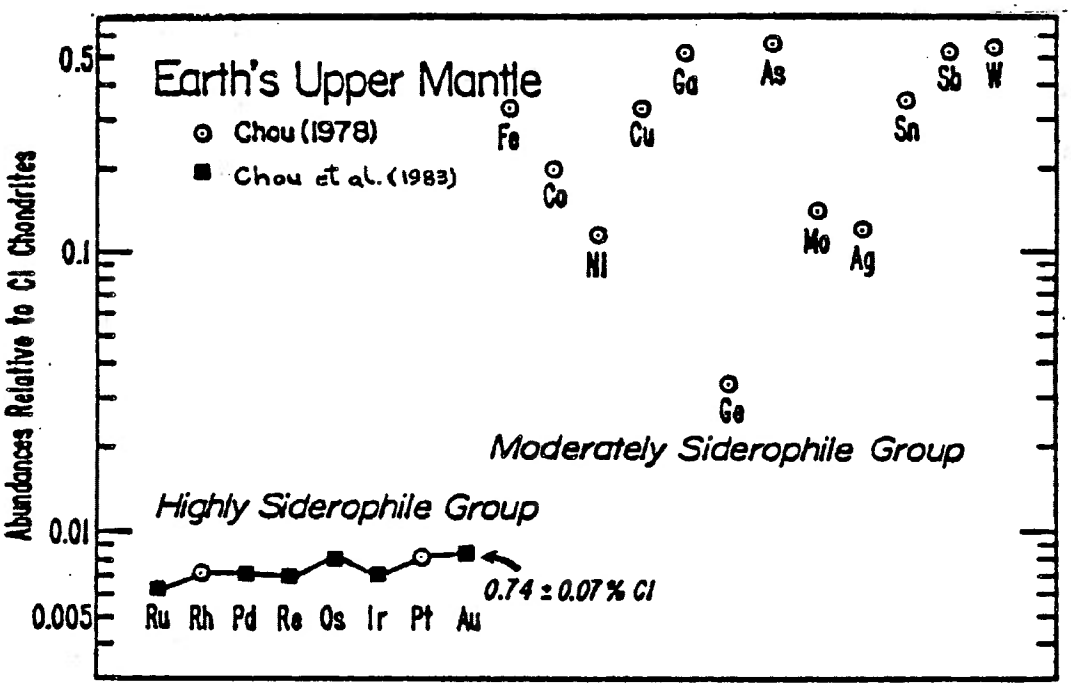

Figure 4. Estimated abundances of siderophile elements in the Earth's upper mantle relative to C1 chondrites (from Chou et al., 1983).

to be approximately 5×10^{2}. Thus, if the above distribution coefficients are valid, Au is over-abundant in the mantle by a factor of approximately 66.

Numerous models have been proposed in attempts to explain the apparent overabundance of siderophile elements in the Earth's upper mantle. Morgan *et al.* (1980) present the following summary of recent models:

1. segregation of metal from the upper mantle in the later stages of accretion was so rapid that equilibrium was not attained (Ringwood, 1966)

2. solution of FeO in the core raises the $f(O_2)$ conditions at the core-mantle interface sufficiently to increase the equilibrium concentration of the siderophile elements in the mantle (Ringwood, 1977);
3. heterogeneous accretion allowed siderophiles to be accumulated along with the Earth's complement of volatile elements, after the formation of the core, as a veneer of material somewhat resembling carbonaceous chondrites (Anders, 1968; Turekian and Clark, 1969; and Ganapathy and Anders, 1974);
4. pressure and temperature effects, calculated for Ni as an example, may shift the distribution coefficients in favour of the silicate phase (Brett, 1970, 1976); and
5. Meteoritic influx after planetary differentiation has clearly taken place on the Moon (Morgan, 1977; Hertogen *et al.*, 1977) and must surely have introduced at least

some siderophile elements to the Earth's crust (Kimura *et al.*, 1974; Chou, 1978; and Chou *et al.*, 1983).

Chou (1978) states that models 4 and 5 above provide the most viable mechanisms for explaining the "overabundance" of siderophile elements in the upper mantle.

Some geochemists (e.g., Mitchell and Keays, 1981; and Sun, 1981) have expressed concern regarding usage of siderophile element abundances in constructing and constraining the types of models described above. The siderophile element data base currently available for the upper mantle has been derived from very limited numbers of analyses. Doubts exist concerning the validity of calculating geochemical averages for the upper mantle based on such a limited data base (Mitchell and Keays, 1981). Sun (1981) cautions that various factors including chemical alteration, mantle metasomatism and magma generation processes can act together to complicate estimation of siderophile element abundances in the mantle. Jagoutz *et al.* (1979) caution that:

1. geologists do not really know what rock type comes closest in composition to primitive mantle material and therefore problems exist in estimating siderophile element abundances in the mantle using data obtained from the various rocks believed to be transported fragments of the upper mantle; and
2. problems exist in calculating siderophile element abundances in the mantle using data obtained from primary partial melts of the mantle because current

melting models do not fully explain observed trace element abundances in these rocks and many relevant trace element distribution coefficients are not known. In addition, little consideration has been given to the chalcophile (Arculus and Delano, 1981; and Mitchell and Keays, 1981) and lithophile (Chou *et al.*, 1973; and Morgan *et al.*, 1980) tendencies of "siderophile" elements during core-mantle fractionation.

As a result of the limitations discussed above, it is presently not possible to state categorically whether or not the core and mantle of the Earth were equilibrated and therefore whether or not any of the models created to explain the "overabundance" of siderophile elements in the upper mantle have real significance. In order to resolve these problems, much more data must be obtained. Towards this end, this work provides a detailed study of the abundance and distribution of the moderately siderophile element Ga in upper mantle-derived garnet and spinel lherzolite xenoliths.

4.1.2 Review of Recent Studies of Ga in Upper Mantle-derived Materials

Very few accurate (better than ±5% (1σ)) data exist for the abundance and distribution of Ga in upper mantle-derived materials.

4.1.2.1 Whole Rock Data

A summary of recent whole rock Ga abundances in upper mantle-derived materials is given in Table 16.

TABLE 16

Summary of Recent Whole Rock Ga Abundances in Upper Mantle-derived Materials

Rock Type	Range in Ga Content (ppm)	No. of Samples Analyzed	Quoted Accuracy	Analytical Technique	Source (see note)
Ultramafic Xenoliths					
- spinel lherzolite	1.4-3.4	4	± 10% (±5%)	INAA(RNAA)	(1)
- spinel lherzolite	1.92-3.70	6	±5%	RNAA	(2)
- garnet peridotite	2.3-3.7	7	not given	XRF	(3)
- garnet-free peridotite	1.5-3.6	11	not given	XRF	(3)
- Websterite	10.6	1	±5%	RNAA	(1)
Alpine Peridotites					
- spinel harzburgite	0.5-2.0	6	not given	XRF	(4)
- plag. harzburgite	1-2	2	not given	XRF	(4)
- spinel lherzolite	2.5-3.5	4	not given	XRF	(4)
- garnet lherzolite	4.5	1	not given	XRF	(4)
- plag. lherzolite	2.5	1	not given	XRF	(4)

Note: (1) Kurat *et al.* (1980)
(2) Jagoutz *et al.* (1979)
(3) Rhodes and Dawson (1975)
(4) Frey *et al.* (1985)

The abundance of Ga in most ultramafic xenoliths analyzed in previous studies varies from approximately 1.4 ppm to 3.7 ppm. The abundance of Ga in alpine peridotites

varies from 0.5 ppm to 4.5 ppm. Accurate (better than ±5% (1σ)) data for the abundance of Ga in garnet lherzolite xenoliths could not be found in the literature.

4.1.2.2 Mineral Data

Accurate data for the abundance of Ga in constituent mineral phases of upper mantle-derived materials are very scarce. The only recent data found in the literature are for mineral separates from 4 ultramafic xenoliths from Kapfenstein, Austria, (Kurat *et al.*, 1980). These data are given in Table 17.

TABLE 17

Abundances of Ga in Mineral Separates of Ultramafic Xenoliths from Kapfenstein, Austria, (N.A. = not analyzed)

Sample	Ga Content (ppm)					Analytical Techniques	Quoted Accuracy
	ol	opx	cpx	sp	amph		
Spinel lherzolite	NA	3.8	5.0	NA	-	INAA	±10%
Hbl-spinel lherzolite	NA	NA	4.0	NA	NA	INAA	±10%
Harzburgite	NA	2.6	NA	NA	-	INAA	±10%
Hornblendite	NA	NA	NA	40	14	INAA	±10%

Although the mineral data is incomplete, it appears that the sequence of enrichment from lowest to highest Ga content is orthopyroxene, clinopyroxene, amphibole (if present), and spinel. The only mineral/mineral distribution coefficient for Ga that can be calculated from the data is $D_{Ga}^{opx/cpx}$ for the spinel lherzolite ($D_{Ga}^{opx/cpx} = 0.75 \pm 0.11$).

4.1.2.3 Estimated Abundance of Ga in the Upper Mantle and Pyrolite

Most previous recent estimates of the abundances of Ga in the upper mantle and in pyrolite (e.g., Jagoutz *et al.*, 1979; Sun, 1981; and Brett, 1984) are based on the spinel lherzolite data of Jagoutz *et al.* (1979). Mitchell and Keays (1981) caution that spinel lherzolites are not necessarily representative of the mantle as a whole and mantle abundances based upon garnet lherzolites may be significantly different.

A summary of recent estimates of the abundance of Ga in the upper mantle and in pyrolite is given in Table 18.

TABLE 18

Summary of Recent Estimates of the Abundance of Ga in the Upper Mantle and in Pyrolite

Estimated Ga Content (ppm)		Data Base	Source
Upper Mantle	Pyrolite		
3.0 ± 0.29	6	6 spinel lherzolite xenoliths	Jagoutz *et al.* (1979)
2.5	5.5	Baedecker *et al.* (1971) Rhodes & Dawson (1975)	Chou (1978)
4	-	Jagoutz *et al.* (1979) Morgan & Wandless (1977)	Sun (1981)
4.5 - 5.0	-	Sun & Nesbitt (1977)	
3	6	De Argollo (1974) Baedecker *et al.* (1971) Goles (1967)	Ringwood & Kesson (1977)
5.0	-	Jones & Drake (1982)	Brett (1984)
4.5	-	Jagoutz *et al.* (1979)	

The estimated abundance of Ga in the upper mantle ranges from 2.5 ppm (Chou, 1978) to 5.0 ppm (Brett, 1984). The esti-

mated abundance of Ga in pyrolite ranges from 5.5 ppm (Chou, 1978) to 6 ppm (Ringwood and Kesson, 1977; Jagoutz *et al.*, 1979).

4.2 PETROGRAPHY OF THE XENOLITHS STUDIED

4.2.1 Garnet Lherzolites

Three garnet lherzolite xenoliths from the Bultfontein Floors mine dump in Kimberley, South Africa (Wagner, 1914; Boyd and Nixon, 1979) were examined. These xenoliths are believed to have come from the Bultfontein or Dutoitspan kimberlite diatremes (Boyd and Nixon, 1978). The xenoliths were rounded ovoids approximately 6 - 10 cm in diameter. Using Harte's (1977) classification, 2 of the xenoliths (385 and 390) were classified as porphyroclastic garnet lherzolite and the other (387) a coarse granular garnet lherzolite. Modal mineralogies were determined by point counting thin sections. The results are given in Table 19.

TABLE 19

Modal Mineralogies of Bultfontein Garnet Lherzolites

Sample	Total Counts	Modal Mineralogy (%)				
		Olivine	Opx	Cpx	Garnet	Phlogopite
385	9932	56.40	31.78	6.98	4.84	-
387	9528	63.54	19.43	12.26	3.12	1.65
390	9335	69.72	22.63	2.74	4.91	-

Samples 385 and 390 consist of large (2 - 5 mm), extensively fractured and strained, rounded porphyroclasts of olivine, orthopyroxene, clinopyroxene, and garnet set in a

poorly developed matrix of small (0.05 - 0.10 mm), strain-free olivine neoblasts. The olivine neoblasts have a granuloblastic mosaic texture. The olivine porphyroclasts are moderately serpentinized. Rare phlogopite and spinel form thin (0.01 mm), irregular mantles about the garnets which, in general, appear less deformed than the other porphyroclasts. Clinopyroxene is irregularly distributed as a lobate, interstitial phase.

Sample 387 consists primarily of large (2 - 5 mm), extensively fractured, rounded grains of olivine, opx, cpx, and garnet. Subhedral laths of strained phlogopite up to 3 mm in length occur as randomly oriented interstitial grains. Phlogopite also occurs as rare, thin (0.01 mm), irregular mantles surrounding garnet. Clinopyroxene is more abundant than in samples 385 and 390.

4.2.2 Spinel Lherzolites

Three spinel lherzolite xenoliths from the Quaternary Newer volcanics of Western Victoria, Australia, (Frey and Green, 1974) were examined. The xenoliths were collected from Mount Porndon. They were rounded, friable ovoids approximately 10 - 25 cm in diameter. Using Harte's (1977) classification, all 3 xenoliths were classified as coarse granular spinel lherzolite.

Modal mineralogies were determined by point counting thin sections. The results are given in Table 20.

All 3 xenoliths consist primarily of large (1 - 3 mm), slightly fractured and strained, rounded grains of olivine,

TABLE 20

Modal Mineralogies of Mt. Porndon Spinel Lherzolites

Sample	Total Counts	Modal Mineralogy (%)			
		Olivine	Opx	Cpx	Spinel
VSL-5	9608	67.09	23.49	7.40	2.02
VSL-6	9009	47.55	30.87	17.20	4.38
VSL-7	8035	65.15	18.65	10.51	5.69

opx and cpx. Spinel occurs as smaller (0.1 - 1.0 mm), irregularly distributed, red-brown grains. The olivine is rarely serpentinized.

4.3 ABUNDANCE AND DISTRIBUTION OF Ga

4.3.1 Whole Rock Data

The abundance of Ga in the lherzolite xenoliths is given in Table 21.

TABLE 21

Abundance of Ga in the Lherzolite Xenoliths (uncertainties (1σ) based on counting statistics of gamma ray spectrometry)

Sample	Ga Abundance (ppm)
Garnet Lherzolites	
385	1.44 ± 0.18
387	1.12 ± 0.21
390	0.52 ± 0.14
Spinel Lherzolites	
VSL-5	2.78 ± 0.26
VSL-6	5.23 ± 0.44
VSL-7	3.78 ± 0.36

The abundance of Ga in the xenoliths varies by a factor of ten from 0.52 ± 0.14 ppm (390) to 5.23 ± 0.44 ppm (VSL-6).

The spinel lherzolites contain more Ga (2.78 ± 0.26 ppm to 5.23 ± 0.44 ppm) than the garnet lherzolites (0.52 ± 0.14 ppm to 1.44 ± 0.18 ppm).

The range in the abundance of Ga in the spinel lherzolites of the present study (2.78 ± 0.26 ppm to 5.23 ± 0.44 ppm) is similar to the range in the abundance of Ga in other spinel lherzolites analyzed in recent studies (Table 16). The present analyses extend the upper limit for Ga in spinel lherzolite xenoliths from 3.7 ppm (Jagoutz *et al.*, 1979; Rhodes and Dawson, 1975) to 5.23 ± 0.44 ppm.

The range in the abundance of Ga in the garnet lherzolites of the present study (0.52 ± 0.14 ppm to 1.44 ± 0.18 ppm) is substantially lower than the range in the abundance of Ga in any of the xenolith types analyzed in recent studies (Table 16). The present analyses extend the lower limit for Ga in ultramafic xenoliths from 1.4 ppm (Kurat *et al.*, 1979) to 0.52 ± 0.14 ppm.

4.3.2 Mineral Data

The abundance of Ga in the major mineral phases comprising the lherzolite xenoliths is given in Table 22.

The mineral phases comprising the spinel lherzolites generally contain more Ga than similar phases in the garnet lherzolites.

The distribution of Ga between the minerals comprising the lherzolites is illustrated in Figures 5 and 6. The sequence of enrichment of Ga in the minerals is similar in all six lherzolite samples. The sequence of enrichment, from

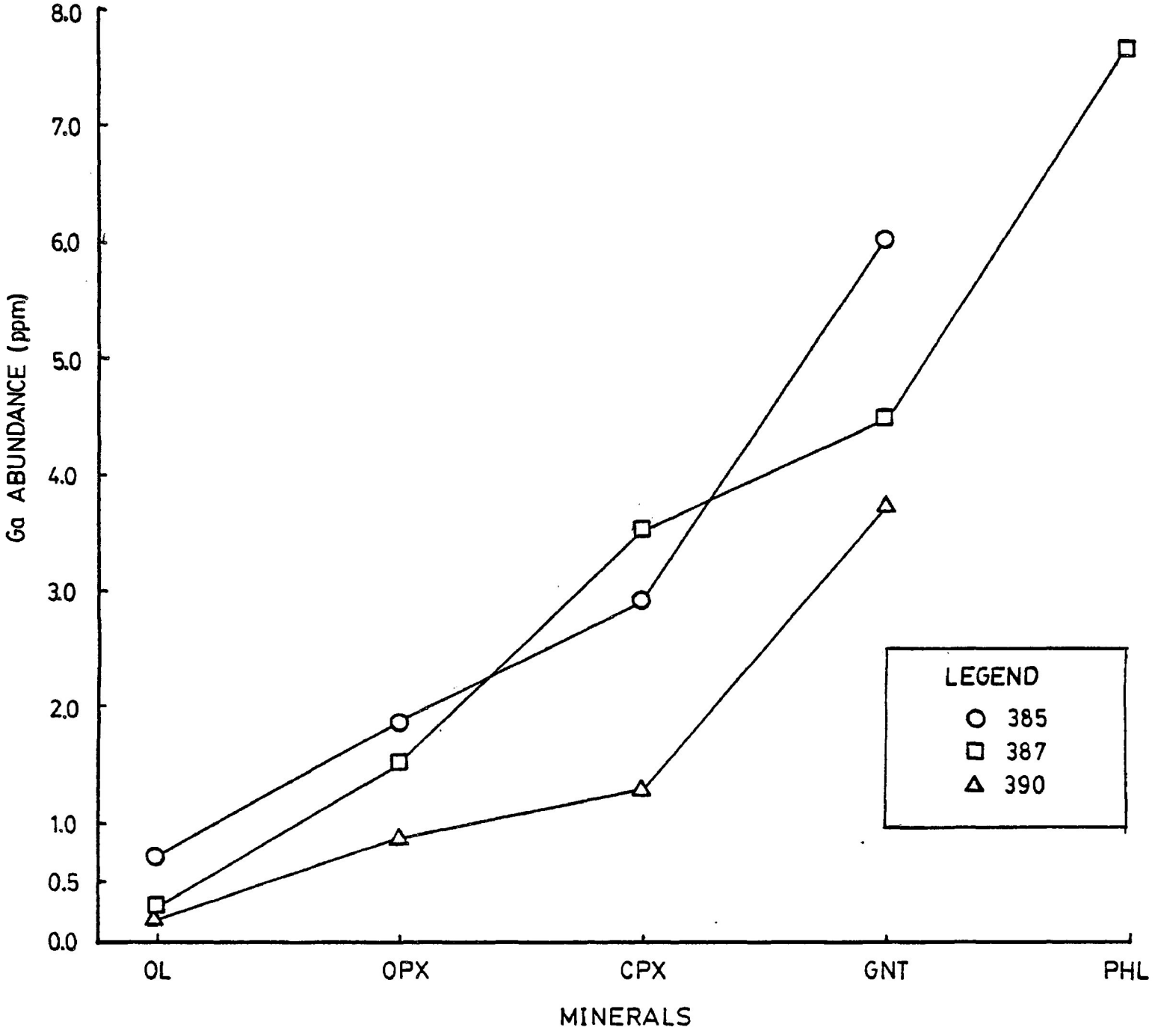

FIGURE 5. Distribution of Ga between major constituent mineral phases of garnet lherzolites. Abbreviations: OL- olivine, OPX- orthopyroxene, CPX- clinopyroxene, GNT- garnet, PHL- phlogopite.

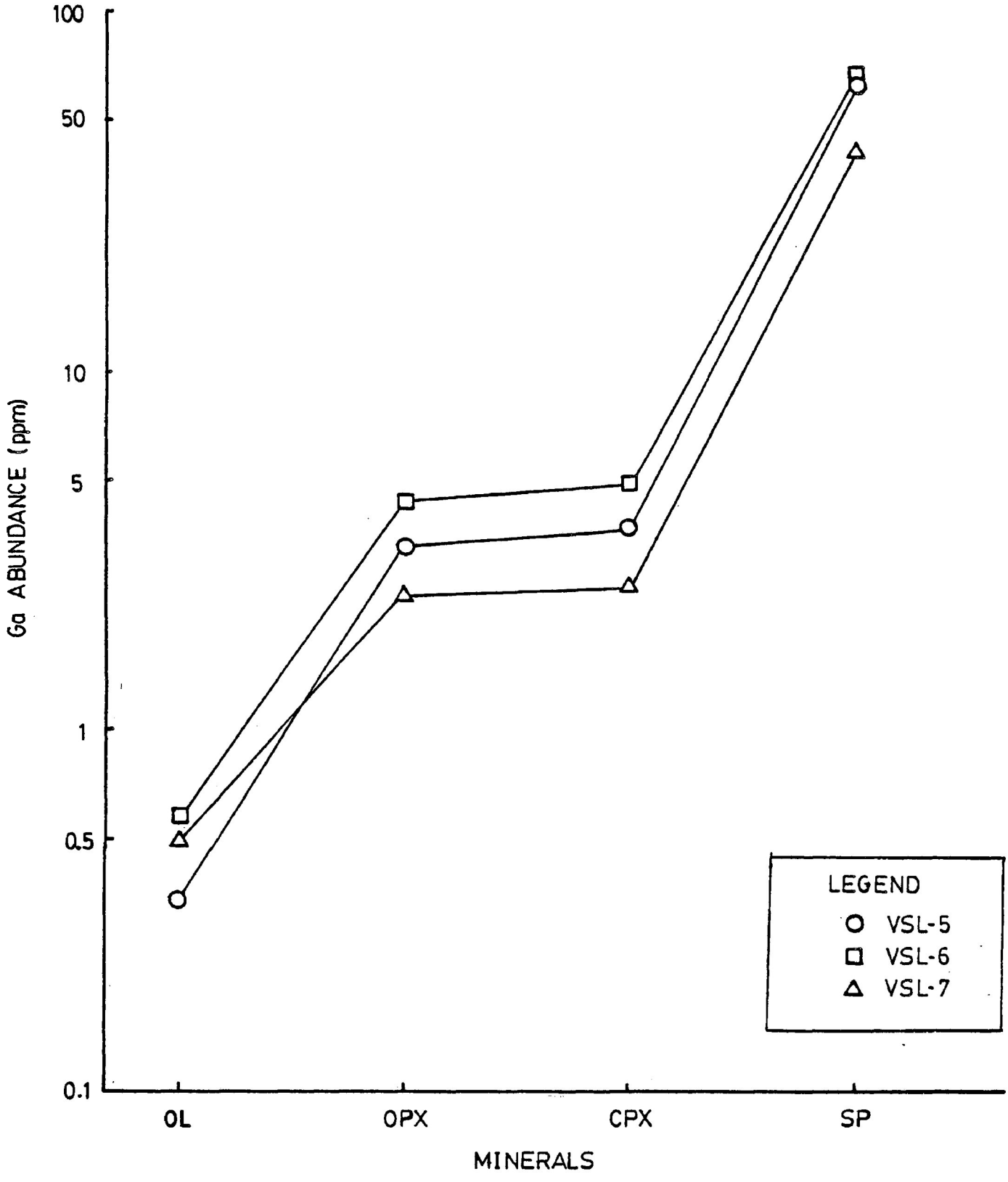

FIGURE 6. Distribution of Ga between major constituent mineral phases of spinel lherzolites. Abbreviations: OL- olivine, OPX- orthopyroxene, CPX- clinopyroxene, SP- spinel.

TABLE 22

The Abundance of Ga in the Major Mineral Phases Comprising the Lherzolite Xenoliths (uncertainties (1σ) based on counting statistics of gamma ray spectrometry)

Sample	Ga Abundance (ppm)					
	Olivine	Opx	Cpx	Spinel	Garnet	Phlogopite
Garnet Lherzolites						
385	0.72±0.11	1.89±0.12	2.93±0.21	-	6.03±0.48	-
387	0.30±0.05	1.54±0.09	3.52±0.22	-	4.46±0.25	7.65±0.21
390	0.20±0.04	0.90±0.07	1.31±0.13	-	3.71±0.16	-
Spinel Lherzolites						
VSL-5	0.34±0.06	3.35±0.11	3.65±0.18	63.92±1.09	-	-
VSL-6	0.58±0.09	4.42±0.18	4.92±0.32	65.91±2.10	-	-
VSL-7	0.50±0.11	2.43±0.13	2.49±0.21	43.49±0.91	-	-

lowest to highest Ga content, is olivine, orthopyroxene, clinopyroxene, garnet (if present), phlogopite (if present), and spinel (if present). This sequence of enrichment in Ga content is similar to the sequence observed by Kurat *et al.* (1979).

The consistency in the sequence of enrichment of Ga in the minerals comprising the lherzolite samples of the present study suggests there is a crystallochemical control on the distribution of Ga in these rocks.

4.3.3 Ga Mineral/Mineral Distribution Coefficients

Calculated Ga mineral/mineral distribution coefficients for the lherzolites are given in Table 23 and compared in Figure 7.

The Ga mineral/mineral distribution coefficients for the

TABLE 23

Calculated Ga Mineral/Mineral Distribution Coefficients for the Lherzolites (uncertainties (1δ) based on counting statistics of gamma ray spectrometry)

Sample	Mineral/Mineral Distribution Coefficients for Ga				
Garnet Lherzolites	ol/opx	ol/cpx	ol/gnt	ol/phl	opx/cpx
385	0.38±0.06	0.25±0.04	0.12±0.02	-	0.65±0.06
387	0.19±0.03	0.09±0.02	0.07±0.01	0.04±.007	0.44±0.04
390	0.22±0.05	0.15±0.03	0.05±0.01	-	0.69±0.08
	opx/gnt	opx/phl	cpx/gnt	cpx/phl	gnt/phl
385	0.31±0.03	-	0.49±0.03	-	-
387	0.35±0.03	0.20±0.01	0.79±0.07	0.46±0.03	0.58±0.04
390	0.24±0.03	-	0.30±0.04	-	-
Spinel Lherzolites	ol/opx	ol/cpx	ol/sp	opx/cpx	
VSL-5	0.10±0.02	0.09±0.02	.005±.0009	.82±0.06	
VSL-6	0.13±0.02	0.12±0.02	.009±.001	0.90±0.07	
VSL-7	0.21±0.05	0.20±0.04	.011±.003	0.98±0.09	
	opx/sp	cpx/sp			
VSL-5	.052±.002	.057±.003			
VSL-6	.067±.003	.075±.005			
VSL-7	.056±.003	.057±.005			

Abbreviations: ol - olivine
opx - orthopyroxene
cpx - clinopyroxene
gnt - garnet
sp - spinel
phl - phlogopite

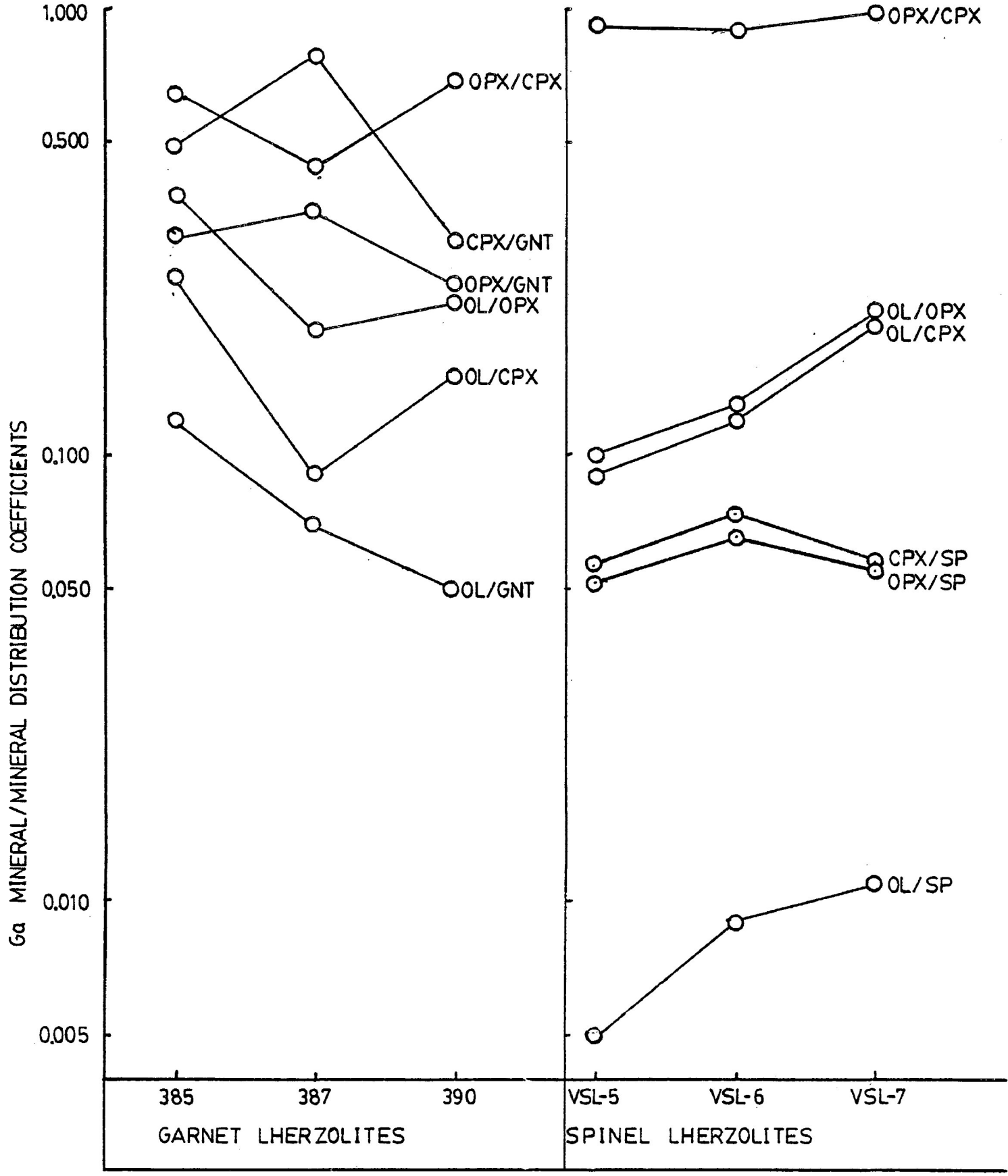

FIGURE 7. Comparison of Ga mineral/mineral distribution coefficients for the lherzolites. Abbreviations: OL- olivine, OPX- orthopyroxene, CPX- clinopyroxene, GNT- garnet, SP- spinel.

spinel lherzolites are slightly more consistent (they vary by factors of 1.1 for $D_{Ga}^{opx/cpx}$ to 2.2 for $D_{Ga}^{ol/cpx}$) than the Ga mineral/mineral distribution coefficients for the garnet lherzolites (these vary by factors of 1.5 for $D_{Ga}^{opx/gnt}$ to 2.8 for $D_{Ga}^{ol/cpx}$).

The Ga mineral/mineral distribution coefficients for mineral pairs common to both the spinel and garnet lherzolites (i.e., ol/opx, ol/cpx, and opx/cpx), if considered collectively, vary by factors of 2.2 for $D_{Ga}^{opx/cpx}$ to 3.8 for $D_{Ga}^{ol/opx}$.

The values of $D_{Ga}^{opx/cpx}$ for the spinel lherzolites of the present study (0.90 ± 0.07 to 0.98 ± 0.09) are slightly greater than the value of 0.76 ± 0.11 obtained from the data given by Kurat *et al.*, (1979). No other estimates of Ga mineral/mineral distribution coefficients could be found for comparison.

4.3.4 Comparison of Calculated and Measured Whole Rock Ga Abundances

Calculated and measured whole rock Ga abundances for the lherzolite xenoliths are compared in Table 24.

The Ga in the major mineral phases accounts, within experimental error, for all of the Ga present in the whole rock lherzolite samples. This suggests that minor intergranular mineral phases which host the bulk of the strongly siderophile elements in other lherzolite xenoliths (Mitchell and Keays, 1981), do not contain appreciable amounts of the moderately siderophile element Ga.

TABLE 24

Comparison of Calculated and Measured Whole Rock Ga Abundances for the Lherzolite Xenoliths (calculations based on data given in Tables 19 to 22, uncertainties (1σ) based on counting statistics of gamma ray spectrometry)

Sample	Calculated Contributions to Whole Rock Ga Content (ppm)			
Garnet Lherzolites	ol	opx	cpx	gnt
385	0.41±0.07	0.60±0.04	0.20±0.01	0.29±0.02
387	0.19±0.03	0.03±0.02	0.43±0.03	0.14±0.01
390	0.14±0.03	0.17±0.01	0.04±.004	0.18±0.01

	phl	Calculated Whole Rock Ga Content (ppm)	Measured Whole Rock Ga Content (ppm)
385	-	1.50 ± 0.08	1.44 ± 0.18
387	0.13±0.01	1.19 ± 0.05	1.12 ± 0.21
390	-	0.53 ± 0.03	0.52 ± 0.14

Spinel Lherzolites	ol	opx	cpx	sp
VSL-5	0.23±0.04	0.79±0.03	0.27±0.01	1.29±0.02
VSL-6	0.28±0.05	1.36±0.06	0.85±0.06	2.89±0.09
VSL-7	0.33±0.08	0.45±0.02	0.26±0.02	2.47±0.05

	Calculated Whole Rock Ga Content (ppm)	Measured Whole Rock Ga Content (ppm)
VSL-5	2.58 ± 0.05	2.78 ± 0.26
VSL-6	5.38 ± 0.13	5.23 ± 0.44
VSL-7	3.51 ± 0.10	3.78 ± 0.36

4.3.5 Estimated Abundances of Ga in the Upper Mantle and in Pyrolite

The abundance of Ga in upper mantle-derived xenoliths varies by at least a factor of ten from approximately 0.5 ppm to approximately 5.0 ppm. The dispersion of Ga abundances in ultramafic xenoliths and the limited number of analyses presently available for consideration may preclude calculation of a geochemically significant estimate for the abundance of Ga in the upper mantle.

Bearing the above in mind, maximum, minimum and average estimates for the abundance of Ga in the upper mantle based on the data obtained in the present study are given in Table 25.

TABLE 25

Estimates for the Abundance of Ga in the Upper Mantle

Assumed Upper Mantle Composition		Estimated Abundance of Ga in the Upper Mantle (ppm)		
Spinel Lherzolite	Garnet Lherzolite	Minimum	Maximum	Average
100%	0%	2.78	5.23	3.93
90	10	2.55	4.82	3.64
80	20	2.33	4.47	3.35
70	30	2.10	4.09	3.06
60	40	1.88	3.71	2.77
50	50	1.65	3.34	2.48
40	60	1.42	2.96	2.19
30	70	1.20	2.58	1.90
20	80	0.97	2.20	1.61
10	90	0.75	1.82	1.32
0	100	0.52	1.44	1.03

The estimate for the abundance of Ga in the upper mantle based solely on the averaged spinel lherzolite data of the present study (i.e., 3.93 ppm) is in good agreement with previous estimates based solely on spinel lherzolite data (i.e., from Table 18, 3 ppm to 5 ppm). The estimate for the abundance of Ga in the upper mantle based solely on the averaged garnet lherzolite data of the present study (i.e., 1.03 ppm) is significantly lower than all previous estimates based on spinel lherzolite or other rock data (i.e., from Table 18, 2.5 ppm to 5 ppm). The occurrence of significant numbers of garnet lherzolite xenoliths in kimberlites suggests an appreciable portion of the upper mantle is composed of garnet lherzolite. The results of the present study suggest that previous estimates of the abundance of Ga in the upper mantle may be too high by factors ranging from approximately 2 to 3. Previous estimates of the depletion of Ga in the upper mantle relative to C1 carbonaceous chondrite abundances (e.g., 0.28 (Jagoutz *et al.*, 1979) to 0.4 (Sun, 1981) may also be too high by factors ranging from approximately 2 to 3. The estimated depletion of Ga in the upper mantle relative to C1 carbonaceous chondrites calculated using the averaged upper mantle estimates of the present study and the chondrite data of Chou *et al.* (1975) and Kallemeyn and Wasson (1981) (i.e., 10.5 ppm Ga and 9.8 ppm Ga respectively) range from 0.1 to 0.4.

Reduction of the average abundance of Ga in the upper mantle necessitates revision of previous estimates of the

abundance of Ga in pyrolite (i.e., from Table 18, 5.5 ppm to 6 ppm). Estimates of the abundance of Ga in pyrolite based on Ringwood and Kesson's (1977) and De Argollo's (1974) MORB abundances and the average upper mantle estimates of the present study are given in Table 26.

TABLE 26

Estimates of the Abundance of Ga in Pyrolite

Assumed Upper Mantle Composition		Estimated Abundance of Ga in Pyrolite* (ppm)	
Spinel Lherzolite	Garnet Lherzolite	Ringwood & Kesson's (1977) average MORB (20 ppm Ga)	De Argollo's (1974) average MORB (19.4 ppm Ga)
100%	0%	7	6.6
90	10	6	6.3
80	20	6	6.1
70	30	6	5.8
60	40	6	5.6
50	50	5	5.4
40	60	5	5.1
30	70	5	4.9
20	80	5	4.6
10	90	4	4.4
0	100	4	4.2

* pyrolite = 17% MORB + 83% ultramafic xenolith

Previous estimates of the abundance of Ga in pyrolite may be too high by factors ranging from approximately 0.25 to 0.50.

4.3.6 Assessment of Core-Mantle Equilibria

The results of the present study suggest that previous estimates of the "overabundance" of Ga in the Earth's mantle (e.g., Ringwood, 1965; Ringwood and Kesson, 1977; Jagoutz *et al.*, 1979) may be too high.

An estimate of the distribution of Ga between the core and mantle of the Earth is given by Equation 2 (Brett, 1970).

$$D_{Ga}^{core/mantle} = \frac{100a - 69b}{31b} \qquad (2)$$

where: $D_{Ga}^{core/mantle}$: is the estimated Ga core/mantle distribution coefficient;

a: is the abundance of Ga in C1 carbonaceous chondrites;

b: is the abundance of Ga in pyrolite;

the constants 69 and 31 refer to the present ratio, by mass, of the mantle to core.

Estimates of $D_{Ga}^{core/mantle}$ calculated using Equation 2, the pyrolite data of the present study, and the chondrite data of Chou *et al.* (1975) and Kallemeyn and Wasson (1981) are given in Table 27.

TABLE 27

Estimates of $D_{Ga}^{core/mantle}$

Assumed Average Upper Mantle Composition		$D_{Ga}^{core/mantle}$	
Spinel Lherzolite	Garnet Lherzolite	10.5 ppm Ga in C1 chondrites (Chou *et al.*, 1975)	9.8 ppm Ga in C1 chrondites (Kallemeyn and Wasson, 1981)
100%	0%	2.94	2.59
90	10	3.14	2.78
80	20	3.35	2.97
70	30	3.57	3.19
60	40	3.82	3.42
50	50	4.09	3.57
40	60	4.39	3.95
30	70	4.71	4.25
20	80	5.09	4.60
10	90	5.49	4.98
0	100	5.94	5.39

The estimated values of $D_{Ga}^{core/mantle}$ vary from 2.59 to 5.94.

Drake *et al.* (1984) have experimentally determined that $D_{Ga}^{metal/silicate}$ varies from 1.0±0.1 to 3.8±0.7 for log fO_2 values ranging from −13.0 to −13.4 at 1190°C and 1 bar total pressure. The $D_{Ga}^{core/mantle}$ estimates of the present study are not significantly different from the experimentally determined values for $D_{Ga}^{metal/silicate}$ given by Drake *et al.* (1984). The similarity between the $D_{Ga}^{core/mantle}$ estimates of the present study and the $D_{Ga}^{metal/silicate}$ estimates of Drake *et al.* (1984) suggests that Ga is not significantly over-abundant in the Earth's mantle relative to the abundance predicted on the basis of low pressure partitioning experiments of Ga between metal and silicate phases.

The similarity between the $D_{Ga}^{core/mantle}$ estimates of the present study and the $D_{Ga}^{metal/silicate}$ estimates of Drake *et al.* (1984) provides no direct proof as to whether the core and mantle of the Earth are, or ever have been, in equilibrium or not. The $D_{Ga}^{core/mantle}$ estimates of the present study are only of geochemical significance if:

1. the abundance of Ga in C1 carbonaceous chondrites corresponds to the abundance of Ga in the bulk Earth;
2. the abundance of Ga in pyrolite correspond to the abundance of Ga in the Earth's mantle.

If the abundance of Ga in C1 carbonaceous chondrites and pyrolite do not correspond to the abundance of Ga in the bulk Earth and mantle respectively, then the $D_{Ga}^{core/mantle}$ estimates

of the present study will have no geochemical significance. In addition, if the $D_{Ga}^{metal/silicate}$ estimates of Drake *et al.* (1984) do not apply to core-mantle conditions of pressure, temperature and composition, then assessment of core-mantle equilibria using these estimates will be invalid.

Bearing the above in mind, it is presently impossible to state categorically whether or not the core and mantle of the Earth are, or ever have been, in equilibrium.

4.4 RELATIONSHIPS BETWEEN Ga MINERAL/MINERAL DISTRIBUTION COEFFICIENTS AND ESTIMATED EQUILIBRATION PRESSURES AND TEMPERATURES

Previous studies (e.g., Stosch, 1981; Kurat *et al.*, 1980 and Jagoutz *et al.*, 1979) indicate that the distribution of various trace elements (e.g., Co, Ni, and Sc between coexisting minerals in ultramafic xenoliths may serve as potential geothermometers. Stosch (1981), for example, presents empirical temperature calibrations for $D_{Sc}^{opx/cpx}$, $D_{Sc}^{ol/opx}$ and $D_{Cr}^{ol/cpx}$ which, in principle, might be used to estimate equilibration temperatures for spinel lherzolites, harzburgites and orthopyroxene-free peridotites. Data obtained in the present study (e.g., the consistency in the sequence of enrichment of Ga, in the lherzolite minerals and the minor variations of the Ga mineral/mineral distribution coefficients) suggest that the distribution of Ga between coexisting minerals in lherzolite xenoliths might also serve as potential geothermobarometers.

The most reliable estimates of equilibration temperatures and pressures for ultramafic xenoliths are presently obtained by using:

1. the Wells (1977) calibration of the pyroxene solvus to determine equilibration temperatures;
2. the Wood (1974) calibration of the solubility of Al_2O_3 in orthopyroxene to determine equilibration pressures (Carswell and Gibb, 1980; and Mitchell *et al.*, 1980).

Estimates of equilibration temperatures and pressures for the lherzolites of the present study are given in Table 28. The major element data used to calculate these equilibration conditions were obtained from multiple analyses of clean mineral grains using energy dispersive and wavelength dispersive electron microprobe techniques. The microprobe data are given in Appendix 2.

TABLE 28

Estimated Equilibration Conditions of Pressure and Temperature

Sample	Estimated Equilibration Conditions	
	Temperature °C (Wells, 1977)	Pressure Kb (Wood, 1974)
Garnet Lherzolites		
385	942.22	37.12
387	736.81	22.72
390	969.31	37.28
Spirel Lherzolites		
VSL-5	975	-
VSL-6	945	-
VSL-7	985	-

Correlation coefficients (r) for the relationships between estimated equilibration conditions of P & T and Ga mineral/mineral distribution coefficients are given in Table 29.

TABLE 29

Correlations Between Estimated Equilibration Conditions and Ga Mineral/Mineral Distribution Coefficients

Samples	Equilibration Conditions	Correlation Coefficients (r)				
		ol/opx	ol/cpx	ol/gnt	ol/sp	opx/cpx
Garnet lherzolites	Temperature	0.54	0.72	0.15	-	0.99
	Pressure	0.62	0.77	0.22	-	0.99
		opx/gnt	opx/sp	cpx/gnt	cpx/sp	
	Temperature	0.83	-	-0.96	-	
	Pressure	0.79	-	-0.80	-	
		ol/opx	ol/cpx	ol/gnt	ol/sp	opx/cpx
Spinel lherzolites	Temperature	0.48	0.48	-	0.05	0.85
		opx/gnt	opx/sp	cpx/gnt	cpx/sp	
	Temperature	-	-0.88	-	-0.97	

Although the data are very limited, it appears that significant correlations may exist between the estimated equilibration conditions of temperature and pressure and several of the Ga mineral/mineral distribution coefficients. The garnet lherzolite data yields the best correlations. For example:

1. for temperature vs. $D_{Ga}^{opx/cpx}$: $r = 0.99$,
2. for temperature vs. $D_{Ga}^{cpx/gnt}$: $r = -0.96$,
3. for pressure vs. $D_{Ga}^{opx/cpx}$: $r = 0.96$.

For the spinel lherzolite data:

1. for temperature vs. $D_{Ga}^{opx/cpx}$: $r = 0.85$,
2. for temperature vs. $D_{Ga}^{cpx/sp}$: $r = -0.97$,
3. for temperature vs. $D_{Ga}^{opx/sp}$: $r = -0.88$.

More data are required to assess the significance of the correlations observed in the present study. The preliminary results suggest that the distribution of Ga between certain mineral pairs (e.g., $D_{Ga}^{opx/cpx}$) is temperature dependent and might be profitably used as a geothermometer for garnet and spinel lherzolite xenoliths.

4.5 Ga/Al RATIOS

The abundance of Al in the lherzolites was determined by X-ray fluorescence spectrometry using a modification of the procedure described by Harvey *et al.*, (1973). The Al data are believed correct to ±5% of the weight of Al present in each sample.

The Ga/Al ratios for the lherzolites are given in Table 30. The Ga/Al x 10^4 ratios for the garnet lherzolites vary from 0.74 ± 0.20 to 1.40 ± 0.19 with a mean of 1.16 ± 0.38 and a standard deviation (1σ) of 25.86%. The Ga/Al x 10^4 ratios for the spinel lherzolites vary from 2.72 ± 0.27 to 3.38 ± 0.37 with a mean of 3.00 ± 0.46 and a standard deviation (1σ) of 2.29%. The mean Ga/Al x 10^4 ratio for the garnet lherzolites (1.16 ± 0.38) is significantly lower than the mean Ga/Al x 10^4 ratio for the spinel lherzolites (3.00 ± 0.46).

TABLE 30

Ga/Al Ratios for the Lherzolites

Sample	Ga (ppm)	Al (wt %)	Ga/Al x 10^4
Garnet Lherzolites			
385	1.44 ± 0.18	1.03 ± 0.05	1.40 ± 0.19
387	1.12 ± 0.21	0.83 ± 0.04	1.35 ± 0.26
390	0.52 ± 0.14	0.70 ± 0.04	0.74 ± 0.20
	Mean		1.16 ± 0.38
	Standard Deviation (1δ)		25.86%
Spinel Lherzolites			
VSL-5	2.78 ± 0.26	0.96 ± 0.05	2.90 ± 0.31
VSL-6	5.23 ± 0.44	1.92 ± 0.10	2.72 ± 0.27
VSL-7	3.78 ± 0.36	1.12 ± 0.06	3.38 ± 0.37
	Mean		3.00 ± 0.46
	Standard Deviation (1δ)		9.29%

4.6 ABUNDANCE AND DISTRIBUTION OF OTHER MODERATELY SIDEROPHILE ELEMENTS (Co AND Ni) AND Sc

4.6.1 Whole Rock Data

The abundances of Co, Ni, and Sc in the lherzolite xenoliths are given in Table 31.

Co and Sc abundances were determined by instrumental neutron activation analysis (INAA). A brief description of the INAA procedure used is given in Appendix 1, section A1.2 (REE data collected during the INAA procedure are given in Appendix 3).

Ni abundances were determined by atomic absorption spectroscopy. Replicate analysis of Ni in U.S.G.S. standard rock MRE-1 were accurate to ±5 weight percent of the Ni abundance given by Abbey (1983). The Ni abundances given in

TABLE 31

Abundances of Co, Ni, and Sc in the lherzolite Xenoliths (uncertainties (1σ) for Co and Sc based on counting statistics of gamma ray spectrometry)

Sample	Element Abundances (ppm)		
	Co	Ni	Sc
Garnet lherzolites			
385	102.32 ± 0.68	2130 ± 100	8.00 ± 0.05
387	106.79 ± 0.26	2298 ± 108	9.85 ± 0.05
390	108.51 ± 0.69	2100 ± 99	6.51 ± 0.04
Spinel lherzolites			
VSL-5	137.99 ± 0.79	2466 ± 116	9.53 ± 0.01
VSL-6	122.83 ± 0.70	1895 ± 89	15.36 ± 0.02
VSL-7	124.55 ± 2.15	2340 ± 110	10.60 ± 0.05

the present study are also believed correct to ±5 weight percent of the Ni present.

The spinel lherzolites contain slightly more Co (122.83 ± 0.70 ppm to 137.99 ± 0.79 ppm vs. 102.32 ± 0.68 ppm to 108.51 ± 0.69 ppm) and Ni (1895 ± 89 ppm to 2466 ± 116 ppm vs. 2100 ± 99 ppm to 2298 ± 108 ppm), and significantly more Sc (9.53 ± 0.01 ppm to 15.36 ± 0.02 ppm vs. 6.51 ± 0.04 ppm to 9.85 ± 0.05 ppm) than the garnet lherzolites. The abundances of Co and Ni in the lherzolites of the present study are similar to the abundances of Co and Ni in other spinel lherzolites analyzed in recent studies (e.g., Jagoutz *et al.*, 1979; Kurat *et al.*, 1980; Stosch, 1981). The abundance of Sc in the spinel lherzolites of the present study is similar to the abundance of Sc in other spinel lherzolites analyzed in recent studies (e.g., Jagoutz *et al.*, 1979; Kurat *et al.*, 1980; Stosch, 1981), but the abundance of Sc in the garnet lherzolites of the present study is significantly lower.

4.6.2 Mineral Data

The abundances of Co, Ni, and Sc in the major mineral phases comprising the lherzolites are given in Table 32.

TABLE 32

Co, Ni, and Sc Abundances for the Major Mineral Phases Comprising the Lherzolites (uncertainties (1σ) based on counting statistics of gamma ray spectrometry) (* = microprobe data; N.A. = not analyzed)

Sample		Abundances (ppm)		
		Co	Ni *	Sc
Garnet Lherzolites				
385	ol	141.39 ± 0.58	2671.78 ± 53.44	0.60 ± 0.02
	opx	59.66 ± 0.50	NA	1.55 ± 0.02
	cpx	23.11 ± 0.34	NA	13.56 ± 0.06
	gnt	43.22 ± 0.43	NA	108.89 ± 0.16
387	ol	139.48 ± 0.71	2593.19 ± 51.86	0.80 ± 0.02
	opx	54.32 ± 0.42	NA	2.44 ± 0.02
	cpx	16.65 ± 0.24	NA	46.74 ± 0.09
	gnt	40.33 ± 0.32	NA	101.19 ± 0.12
	phl	55.02 ± 0.50	1493.05 ± 29.86	1.63 ± 0.02
390	ol	147.62 ± 0.79	2750.36 ± 55.01	0.61 ± 0.02
	opx	60.45 ± 0.51	NA	1.44 ± 0.02
	cpx	22.44 ± 0.35	NA	12.34 ± 0.06
	gnt	43.28 ± 0.50	NA	109.19 ± 0.18
Spinel Lherzolites				
VSL-5	ol	146.76 ± 0.68	2677.18 ± 53.14	2.32 ± 0.03
	opx	62.81 ± 0.46	NA	15.78 ± 0.06
	cpx	22.60 ± 0.33	NA	69.34 ± 0.13
	sp	229.39 ± 0.96	1964.54 ± 39.29	1.12 ± 0.03
VSL-6	ol	150.09 ± 0.36	1965.45 ± 39.31	2.28 ± 0.02
	opx	60.39 ± 0.36	NA	16.70 ± 0.05
	cpx	23.38 ± 0.23	NA	61.90 ± 0.09
	sp	225.06 ± 1.06	2436.03 ± 48.72	0.67 ± 0.03
VSL-7	ol	143.48 ± 0.54	2278.87 ± 45.58	2.39 ± 0.02
	opx	63.03 ± 0.51	NA	18.62 ± 0.07
	cpx	23.97 ± 0.24	NA	60.63 ± 0.09
	sp	233.68 ± 1.01	2043.12 ± 40.86	1.36 ± 0.03

The mineral phases comprising the garnet lherzolites contain similar amounts of Co and Ni, but significantly less Sc than similar phases in the spinel lherzolites. The distributions of Co and Sc between the mineral phases of the lherzolites are illustrated in Figures 8 and 9. The sequences of enrichment of Co and Sc in the minerals of the garnet lherzolites are similar to the sequences of enrichment of Co and Sc in the minerals of the spinel lherzolites (Table 33).

TABLE 33

Sequences of Enrichment of Co and Sc in the Minerals Comprising the Lherzolites

Sequence of Enrichment	Minerals			
	Garnet Lherzolites		Spinel Lherzolites	
	Co	Sc	Co	Sc
Lowest Abundance	cpx	ol	cpx	sp
↓	gnt	phl *	opx	ol
↓	phl *	opx	ol	opx
↓	opx	cpx	sp	cpx
Highest Abundance	ol	gnt		

* if present

The sequences of enrichment of Co and Sc in the minerals of the lherzolites of the present study are similar to the sequences obtained for other lherzolites in recent studies (e.g., Kurat *et al.*, 1979; Mitchell, unpublished data given in Appendix 4). The consistency in the sequences of enrichment of Co and Sc suggests that there are crystallochemical controls for the distribution of these elements in these rocks.

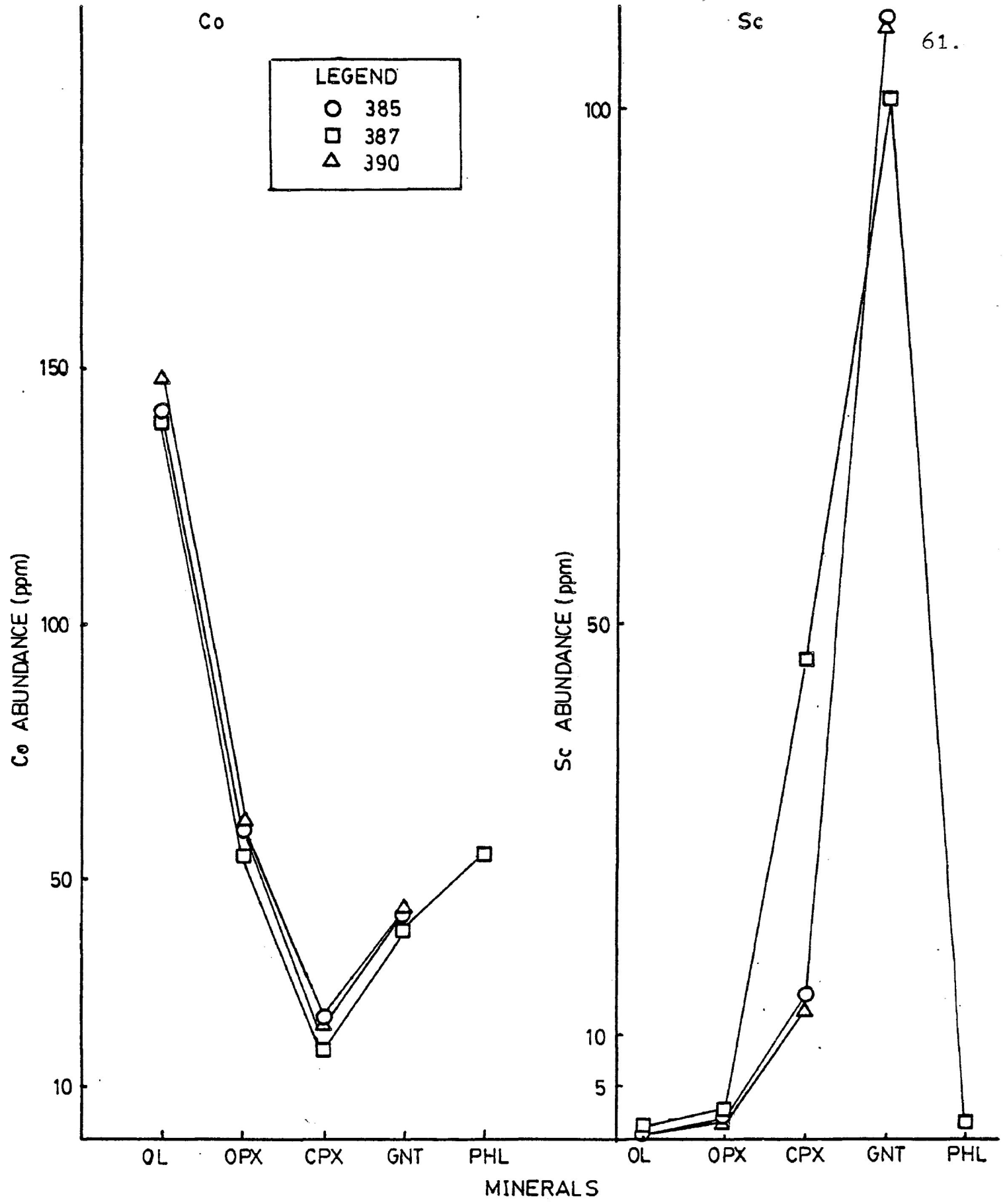

FIGURE 8. Distribution of Co and Sc between major constituent mineral phases of garnet lherzolites. Abbreviations: OL- olivine, OPX- orthopyroxene, CPX- clinopyroxene, GNT- garnet, PHL- phlogopite.

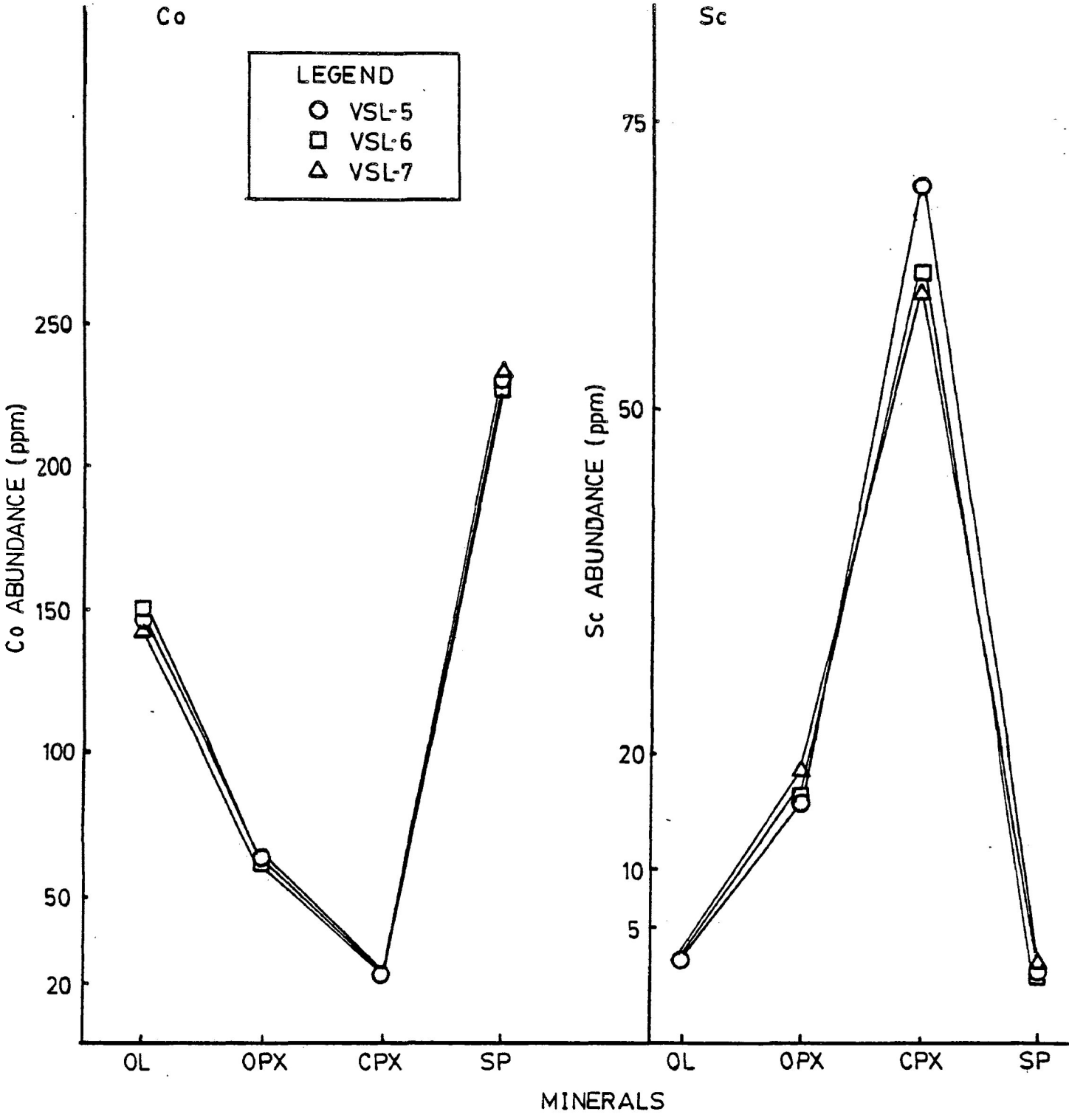

FIGURE 9. Distribution of Co and Sc between major constituent mineral phases of spinel lherzolites. Abbreviations: OL- olivine, OPX- orthopyroxene, CPX- clinopyroxene, SP- spinel.

4.6.3 Mineral/Mineral Distribution Coefficients

Calculated mineral/mineral distribution coefficients for Co and Sc in the lherzolites are given in Tables 34 and 35.

The mineral/mineral distribution coefficients for Co are more consistent than the mineral/mineral distribution coefficients for Sc. For the garnet lherzolites, $D_{Co}^{mnrl/mnrl}$ values vary by 5% ($D_{Co}^{gnt/opx}$) to 25% ($D_{Co}^{cpx/gnt}$) and $D_{Sc}^{mnrl/mnrl}$ values vary by 25% ($D_{Sc}^{ol/opx}$) to 75% ($D_{Sc}^{cpx/gnt}$). For the spinel lherzolites $D_{Co}^{mnrl/mnrl}$ values vary by 0% ($D_{Co}^{opx/sp}$) to 12% ($D_{Co}^{cpx/ol}$) and $D_{Sc}^{mnrl/mnrl}$ values vary by 15% ($D_{Sc}^{ol/cpx}$) to 50% ($D_{Sc}^{sp/cpx}$).

The values of $D_{Co}^{mineral/mineral}$ and $D_{Sc}^{mineral/mineral}$ for the spinel lherzolites of the present study are similar to the values reported for other spinel lherzolites in recent studies (e.g., Kurat *et al.*, 1979; Stosch, 1981).

4.6.4 Comparison of Calculated and Measured Whole Rock Co and Sc Abundances

Calculated and measured whole rock Co and Sc abundances for the lherzolite xenoliths are compared in Tables 36 and 37.

The minerals account for 85% to 110% of the measured whole rock Co and Sc abundances. In some of the samples (e.g., 387, VSL-7) the minerals account for nearly 100% of the measured whole rock Co and Sc abundances.

4.6.5 Estimated Abundances of Co, Ni, and Sc in the Upper Mantle

Maximum, minimum, and average estimates for the

TABLE 34

Calculated Mineral/Mineral Distribution Coefficients for Co and Sc in the Garnet Lherzolites (uncertainties (1σ) based on counting statistics of gamma ray spectrometry

Sample	Mineral/Mineral Distribution Coefficients for Co				
Garnet Lherzolites	cpx/gnt	cpx/phl	cpx/opx	cpx/ol	gnt/phl
385	0.53±0.01	-	0.39±0.01	0.16±0.01	-
387	0.41±0.01	0.30±0.01	0.31±0.01	0.12±0.01	0.73±0.01
390	0.52±0.01	-	0.37±0.01	0.15±0.01	-
	gnt/opx	gnt/ol	phl/ol	opx/phl	opx/ol
385	0.72±0.01	0.31±0.01	-	-	0.42±0.01
387	0.74±0.01	0.29±0.01	0.39±0.01	0.98±0.01	0.39±0.01
390	0.71±0.01	0.29±0.01	-	-	0.41±0.01

Sample	Mineral/Mineral Distribution Coefficients for Sc				
Garnet Lherzolites	ol/phl	ol/opx	ol/cpx	ol/gnt	phl/opx
385	-	0.39±0.01	.044±.001	.0005±.0002	-
387	0.49±0.01	0.32±0.01	.012±.001	.0079±.0002	0.67±0.01
390	-	0.42±0.01	0.49±0.01	.0056±.0002	-
	phl/cpx	phl/gnt	opx/cpx	opx/gnt	cpx/gnt
385	-	-	.114±.002	.014±.001	.125±.002
387	.035±.001	.016±.001	.052±.001	.024±.001	.462±.005
390	-	-	.117±.002	.013±.001	.113±.002

TABLE 35

Calculated Mineral/Mineral Distribution Coefficients for Co and Sc in the Spinel Lherzolites (uncertainties (1σ) based on counting statistics of gamma ray spectrometry

Sample	Mineral/Mineral Distribution Coefficients for Co				
Spinel Lherzolites	cpx/opx	cpx/ol	cpx/sp	opx/sp	opx/sp
VSL-5	0.36±0.01	0.15±0.01	.099±.002	0.43±0.01	0.27±0.01
VSL-6	0.38±0.01	0.16±0.01	.104±.002	0.40±0.01	0.67±0.01
VSL-7	0.38±0.01	0.17±0.01	.103±.002	0.44±0.01	0.27±0.01

	ol/sp
VSL-5	0.54±0.01
VSL-6	0.67±0.01
VSL-7	0.61±0.01

Sample	Mineral/Mineral Distribution Coefficients for Sc				
Spinel Lherzolites	sp/ol	sp/opx	sp/cpx	ol/opx	ol/cpx
VSL-5	0.48±0.01	.071±.002	.016±.002	.147±.002	.033±.002
VSL-6	0.29±0.01	.040±.002	.011±.002	.136±.002	.037±.002
VSL-7	0.57±0.01	.073±.002	.022±.002	.128±.002	.039±.002

	opx/cpx
VSL-5	0.23±0.01
VSL-6	0.27±0.01
VSL-7	0.31±0.01

TABLE 36

Comparison of Calculated and Measured Whole Rock Co and Sc Abundances for Garnet Lherzolites (calculations based on data given in Tables 19, 20, 31 and 32, uncertainties (1σ) based on counting statistics of gamma ray spectrometry

Garnet Lherzolites	Calculated Contributions to Whole Rock Co Content (ppm)				
	ol	opx	cpx	gnt	phl
385	79.74±0.30	18.96±0.16	1.61±0.02	2.09±0.02	-
387	88.63±0.45	10.53±0.08	2.04±0.02	1.26±0.02	0.91±0.01
390	102.92±0.55	13.68±0.12	0.61±0.01	2.13±0.02	-

	Calculated Whole Rock Co Content (ppm)	Measured Whole Rock Co Content (ppm)
385	102.40 ± 0.34	102.32 ± 0.68
387	103.39 ± 0.46	106.79 ± 0.26
390	119.34 ± 0.56	108.51 ± 0.69

Garnet Lherzolites	Calculated Contributions to Whole Rock Sc Content (ppm)				
	ol	opx	cpx	gnt	phl
385	0.34±0.01	0.49±0.01	0.95±0.01	5.27±0.01	-
387	0.51±0.01	0.47±0.01	5.73±0.01	3.16±0.01	0.03±.002
390	0.43±0.01	0.33±0.01	0.34±0.01	5.36±0.01	-

	Calculated Whole Rock Sc Content (ppm)	Measured Whole Rock Sc Content (ppm)
385	7.05 ± 0.02	8.00 ± 0.05
387	9.90 ± 0.02	9.85 ± 0.05
390	6.46 ± 0.02	6.51 ± 0.04

TABLE 37

Comparison of Calculated and Measured Whole Rock Co and Sc Abundances for Spinel Lherzolites (calculations based on data given in Tables 19, 20, 31 and 32, uncertainties (1δ) based on counting statistics of gamma ray spectrometry

Spinel Lherzolites	Calculated Contributions to Whole Rock Co Content (ppm)			
	ol	opx	cpx	sp
VSL-5	98.46±0.46	14.75±0.11	1.67±0.02	4.63±0.03
VSL-6	71.37±0.38	18.64±0.10	4.02±0.02	9.86±0.08
VSL-7	93.48±0.41	11.76±0.09	2.52±0.01	13.3±0.10
	Calculated Whole Rock Co Content (ppm)		Measured Whole Rock Co Content (ppm)	
VSL-5	119.51 ± 0.48		137.99 ± 0.79	
VSL-6	103.89 ± 0.40		122.83 ± 0.70	
VSL-7	121.06 ± 0.49		124.55 ± 2.15	

Spinel Lherzolites	Calculated Contributions to Whole Rock Sc Content (ppm)			
	ol	opx	cpx	sp
VSL-5	1.56±0.02	3.71±0.03	5.13±0.02	0.02±.002
VSL-6	1.08±0.01	4.87±0.03	10.65±.08	0.03±.002
VSL-7	1.56±0.02	3.47±0.03	6.37±0.07	0.08±.003
	Calculated Whole Rock Sc Content (ppm)		Measured Whole Rock So Content (ppm)	
VSL-5	10.42 ± 0.04		9.53 ± 0.01	
VSL-6	16.63 ± 0.10		15.36 ± 0.02	
VSL-7	11.48 ± 0.09		10.60 ± 0.05	

abundance of Co, Ni, and Sc in the upper mantle based on the data of the present study are given in Table 38. Average estimates for the abundance of Co and Ni in the upper mantle based on combinations of both the spinel and garnet lherzolite data of the present study (i.e., Co = 105.87 ppm to 128.45 ppm; Ni = 2176 ppm to 2237 ppm) are in good agreement with previous average estimates based on spinel lherzolite data (e.g., Jagoutz *et al.*, 1979, give Co = 105 ± 5 ppm and Ni = 2108 ± 105 ppm). Average estimates of the abundance of Sc in the upper mantle based on combinations of both the spinel and garnet lherzolite data of the present study (i.e., 8.12 ppm to 11.88 ppm) are significantly lower than previous average estimates based solely on spinel lherzolite data (e.g., Jagoutz *et al.*, 1979, give Sc = 17.0 ± 0.85 ppm).

The results of the present study suggest that previous estimates of the average abundance of Sc in the upper mantle may be too high by factors ranging from approximately 1.5 to 2.

4.6.6 Relationships Between Co and Sc Mineral/Mineral Distribution Coefficients and Estimated Equilibration Temperatures

Stosch (1981) has studied the partitioning of divalent (Co, Ni) and trivalent (Sc, Cr) trace elements in spinel peridotite xenoliths. Stosch (1981) concluded that the Sc and Cr mineral/mineral distribution coefficients displayed high but systematic variations which could be assigned to dependencies upon equilibration temperature. The Sc mineral/

TABLE 38

Maximum, Minimum, and Average Estimates for the Abundance of Co, Ni, and Sc in the Upper Mantle

Assumed Upper Mantle Compositions		Estimated Abundances in the Upper Mantle		
		Co		
Spinel Lherzolite	Garnet Lherzolite	Minimum	Maximum	Average
100%	0%	122.83	137.99	128.45
90	10	120.78	135.04	126.20
80	20	118.73	132.09	123.94
70	30	116.68	129.15	121.68
60	40	114.63	126.20	119.42
50	50	112.58	123.25	117.16
40	60	110.52	120.30	114.90
30	70	108.47	117.35	112.65
20	80	106.42	114.41	110.39
10	90	104.37	111.46	108.13
0	100	102.32	108.51	105.51
		Ni		
100%	0%	1895	2466	2237
90	10	1916	2449	2228
80	20	1935	2432	2222
70	30	1957	2416	2216
60	40	1977	2399	2211
50	50	1998	2382	2205
40	60	2018	2365	2199
30	70	2039	2348	2193
20	80	2059	2332	2188
10	90	2080	2315	2182
0	100	2100	2298	2176
		Sc		
100%	0%	9.53	15.36	11.83
90	10	9.23	14.81	11.46
80	20	8.93	14.26	11.09
70	30	8.62	13.71	10.72
60	40	8.32	13.16	10.35
50	50	8.02	12.61	9.98
40	60	7.72	12.05	9.60
30	70	7.42	11.50	9.23
20	80	7.11	10.95	8.86
10	90	6.81	10.40	8.49
0	100	6.51	9.85	8.12

mineral distribution coefficients, and to a lesser degree the Co mineral/mineral distribution coefficients, for the lherzolite xenoliths of the present study also display variations which may be attributable to differences in equilibration temperature.

Correlation coefficients (r) for the relationships between the Co and Sc mineral/mineral distribution coefficients and the estimated equilibration temperatures for the lherzolites of the present study are given in Table 39.

TABLE 39

Correlations Between Estimated Equilibration Temperatures and Co and Sc Mineral/Mineral Distribution Coefficients (temperature data from Table 28, mineral/mineral distribution coefficients from Tables 34 and 35)

Element	Samples	Correlation Coefficients (r)				
		ol/opx	ol/cpx	ol/gnt	ol/sp	opx/cpx
Co	Garnet Lherzolites	0.90	0.94	0.41	–	0.94
		opx/gnt	opx/sp	cpx/gnt	cpx/sp	
		0.97	–	0.98	–	
		ol/opx	ol/cpx	ol/gnt	ol/sp	opx/cpx
	Spinel Lherzolites	1.00	0.24	–	0.96	0.28
		opx/gnt	opx/sp	cpx/gnt	cpx/sp	
		–	–	–	0.45	
Sc		ol/opx	ol/cpx	ol/gnt	ol/sp	opx/cpx
	Garnet Lherzolites	0.98	0.99	0.99	–	0.99
		opx/gnt	opx/sp	cpx/gnt	cpx/sp	
		0.99	–	0.99	–	
		ol/opx	ol/cpx	ol/gnt	ol/sp	opx/cpx
	Spinel Lherzolites	0.15	0.05	–	0.99	0.24
		opx/gnt	opx/sp	cpx/gnt	cpx/sp	
		–	0.98	–	0.94	

Although the data are very limited, it appears that significant correlations may exist between the estimated equilibration temperatures and several of the Co and Sc mineral/mineral distribution coefficients (e.g., for the garnet lherzolites: $D_{Co}^{cpx/gnt}$, $D_{Co}^{opx/gnt}$, $D_{Sc}^{opx/cpx}$, $D_{Sc}^{opx/gnt}$; for the spinel lherzolites: $D_{Co}^{ol/opx}$, $D_{Co}^{ol/sp}$, $D_{Sc}^{ol/sp}$, $D_{Sc}^{opx/sp}$). The Sc mineral/mineral distribution coefficients are more variable than the Co mineral/mineral distribution coefficients. As a result, geothermometers based on the distribution of Sc might be more temperature sensitive, as suggested by Stosch (1981), than those based on the distribution of Co.

Stosch (1981) presents empirical temperature calibrations for geothermometers based on $D_{Sc}^{opx/cpx}$ and $D_{Sc}^{ol/cpx}$. A comparison of estimated equilibration temperatures for the lherzolites of the present study based on the Stosch (1981) calibrations of the $D_{Sc}^{opx/cpx}$ and $D_{Sc}^{ol/cpx}$ geothermometers and the Wells (1977) calibration of the pyroxene solvus is given in Table 40.

The estimated equilibration temperatures based on the Stosch (1981) calibrations of the $D_{Sc}^{opx/cpx}$ and $D_{Sc}^{ol/cpx}$ geothermometers are generally not in good agreement with one another or with the temperature estimates based on the Wells (1977) calibration of the pyroxene solvus.

The estimated equilibration temperatures for the garnet lherzolites based on the Stosch (1981) calibrations of the $D_{Sc}^{opx/cpx}$ and $D_{Sc}^{ol/cpx}$ geothermometers are 66°C to 156°C lower

TABLE 40

Comparison of Estimated Equilibration Temperatures

Samples	Estimated Equilibration Temperatures (°C)		
	Wells (1977)	Stosch (1981)	
		$D_{Sc}^{opx/cpx}$	$D_{Sc}^{ol/cpx}$
Garnet Lherzolite			
385	942	807	1046
387	737	671	877
390	969	813	1068
Spinel Lherzolite			
VSL-5	975	968	990
VSL-6	945	1012	1012
VSL-7	985	1052	1022

and 99°C to 140°C higher, respectively, than the temperature estimates based on the Wells (1977) calibration of the pyroxene solvus.

The estimated equilibration temperatures for the spinel lherzolites based on the Stosch (1981) calibrations of the $D_{Sc}^{cpx/opx}$ and $D_{Sc}^{ol/cpx}$ geothermometers are 13°C lower to 67°C higher and 15°C to 67°C higher, respectively, than the temperature estimates based on the Wells (1977) calibration of the pyroxene solvus.

More data, from both natural and experimental systems, are required to assess the significance of the correlations observed in the present study. The results suggest that the distribution of Sc between certain mineral pairs (e.g. $D_{Sc}^{opx/cpx}$) is temperature dependent and might be profitably used as a geothermometer for garnet and spinel lherzolite

xenoliths. The Stosch (1981) calibrations of the $D_{Sc}^{opx/cpx}$ and $D_{Sc}^{ol/cpx}$ geothermometers do not yield estimates of equilibration temperatures for the lherzolites of the present study that are consistent with those based on the Wells (1977) calibration of the pyroxene solvus.

4.7 CONCLUSIONS

1. The abundance of Ga in the lherzolite xenoliths studied varies by a factor of approximately 10 from 0.52 ± 0.14 ppm (sample 390) to 5.23 ± 0.44 ppm (sample VSL-6). The spinel lherzolites contain more Ga (2.78 ± 0.26 ppm to 5.23 ± 0.44 ppm than the garnet lherzolites (0.52 ± 0.14 ppm to 1.44 ± 0.18 ppm).
2. If the lherzolite xenoliths studied are residua from melting of the upper mantle, then the fact that they contain appreciable amounts of Ga (i.e., 0.52 ± 0.14 ppm to 5.23 ± 0.44 ppm) suggests that the Ga bulk-solid melt distribution coefficient during the genesis of these rocks must have been considerably greater than zero (i.e. Ga did not behave as a highly incompatible trace element during the genesis of these lherzolites).
3. Estimates of the abundance of Ga in the upper mantle based on the averaged lherzolite data of the present study range from 1.03 ppm (100% garnet lherzolite based upper mantle composition) to 3.93 ppm (100% spinel lherzolite based upper mantle composition). The latter estimate (i.e., 3.93 ppm Ga) is in good agreement with previous estimates for the abundance of Ga in the upper

mantle (i.e., 3 ppm to 5 ppm). The estimate based solely on the averaged garnet lherzolite data (i.e., 1.03 ppm Ga) is substantially lower than all previous estimates. The occurrence of significant numbers of garnet lherzolite xenoliths in kimberlites suggests an appreciable portion of the upper mantle is composed of garnet lherzolite. As a consequence, previous estimates of the abundance of Ga in the upper mantle and in pyrolite may be too high by factors ranging from 2 to 3 and from 0.25 to 0.50 respectively.

4. Estimates of the distribution of Ga between the core and mantle of the Earth based on the lherzolite data of the present study vary from 2.59 (100% spinel lherzolite based upper mantle composition) to 5.94 (100% garnet lherzolite based upper mantle composition). These estimates are in good agreement with experimentally determined values for the distribution of Ga between equilibrated metal and silicate phases (i.e. 1.0 ± 0.2 to 3.8 ± 0.7 (Drake *et al.*, 1984)). As a consequence, Ga may not be significantly overabundant in the Earth's mantle relative to the abundance predicted on the basis of low pressure partitioning experiments of Ga between metal and silicate phases.

5. The abundance of Ga in the major mineral phases comprising the lherzolites of the present study varies from 0.20 ± 0.04 ppm (an olivine from sample 390) to 65.91 ± 2.10 ppm (a spinel from sample VSL-6). The

sequence of enrichment of Ga in the minerals of the garnet and spinel lherzolites are similar. The sequence of enrichment, from lowest to highest Ga content, is olivine, orthopyroxene, clinopyroxene, garnet (if present), phlogopite (if present), and spinel (if present). The consistency in the sequence of enrichment of Ga in the minerals comprising the lherzolites suggests there is a crystallochemical control for the distribution of Ga in these rocks.

6. The Ga in the major mineral phases of the lherzolites can account, within experimental error, for all of the Ga present in the whole rock lherzolite samples. This suggests that minor intergranular mineral phases, which host the bulk of the strongly siderophile elements in other lherzolite samples, do not contain appreciable amounts of the moderately siderophile element Ga.

7. Although the data are very limited, preliminary results suggest that the distribution of Ga between certain mineral pairs (e.g., $D_{Ga}^{opx/cpx}$) is temperature dependent and might be profitably utilized as a geothermometer for garnet and spinel lherzolite xenoliths.

8. The Ga/Al x 10^4 weight ratios for the garnet lherzolites of the present study vary from 0.74 ± 0.20 to 1.40 ± 0.19 (mean 1.16 ± 0.38). The Ga/Al x 10^4 weight ratios for the spinel lherzolites of the present study vary from 2.72 ± 0.27 to 3.38 ± 0.37 (mean 3.00 ± 0.46). The mean Ga/Al x 10^4 weight ratio for the garnet lherzolites

(1.16 ± 0.38) is significantly lower than the mean Ga/Al x 10^4 weight ratio for the spinel lherzolites (3.00 ± 0.46).

9. The abundances of the moderately siderophile elements Co and Ni in the lherzolites of the present study (i.e., for the garnet lherzolites: 102.32 ± 0.68 ppm Co to 108.51 ± 108 ppm Ni; for the spinel lherzolites: 122.83 ± 0.70 ppm Co to 137.99 ± 0.79 ppm Co and 1895 ± 89 ppm Ni to 2466 ± 116 ppm Ni) are similar to the abundances of Co and Ni in other spinel lherzolites analyzed in previous studies. As a consequence, estimates of the abundances of these elements in the Earth's upper mantle based on the averaged lherzolite data of the present study (i.e., Co = 105.87 ppm to 128.45 ppm, Ni = 2175 ppm to 2237 ppm) are in good agreement with previous estimates based solely on spinel lherzolite data.

10. The abundance of Sc in the garnet lherzolites of the present study (i.e., 6.51 ± 0.04 ppm to 9.85 ± 0.85 ppm) is significantly lower than the abundance of Sc in spinel lherzolites analyzed in recent studies. As a consequence, estimates of the abundance of Sc in the Earth's upper mantle based solely on the spinel lherzolite data of previous studies may be too high by factors ranging from approximately 1.5 to 2.

11. The sequences of enrichment of Co and Sc in the minerals of the garnet and spinel lherzolites are similar. The sequences of enrichment, from lowest to highest Co and

Sc contents, are, for Co, clinopyroxene, garnet (if present), phlogopite (if present), orthopyroxene, and spinel (if present) and, for Sc, spinel (if present), olivine, phlogopite (if present), orthopyroxene, clinopyroxene, and garnet (if present). The consistency in the sequences of enrichment of Co and Sc in the minerals comprising the lherzolites suggests there are crystallochemical controls for the distribution of these elements in these rocks.

12. Although the data are very limited, preliminary results suggest that the distribution of Sc between certain mineral pairs (e.g., $D_{Sc}^{opx/cpx}$) is temperature dependent and might be profitably utilized as a geothermometer for garnet and spinel lherzolite xenoliths. The Stosch (1981) calibrations of the $D_{Sc}^{opx/cpx}$ and $D_{Sc}^{ol/cpx}$ geothermometers do not yield estimates of equilibration temperatures for the lherzolites of the present study that are consistent with those based on the Wells (1977) calibration of the pyroxene solvus.

CHAPTER FIVE

ASPECTS OF GALLIUM GEOCHEMISTRY IN CONTINENTAL ALKALINE VOLCANIC ROCKS

5.1 INTRODUCTION

Very few accurate Ga data for volcanic rocks have been published. Most recent studies of the abundance of Ga in volcanic rocks have been undertaken on various types of oceanic basalts (e.g., Wasson and Baedecker, 1970; De Argollo, 1974; De Argollo and Schilling, 1978 (a,b); Saunders and Tarney, 1979). No accurate Ga data for continental alkaline volcanic rocks could be found in the available literature (i.e., Chemical Abstracts, Mineralogical Abstracts, Geochimica et Cosmochimica Acta, Contributions to Mineralogy and Petrology, Journal of Petrology).

The abundances of Ga, Al, and various compatible and incompatible trace elements in rocks from 4 continental alkaline volcanic suites (Freemans Cove, Balcones, Hegau, and Urach) are presented below and compared with the abundances of Ga in, and the Ga/Al ratios of, mid-oceanic ridge basalts from the Reykjanes Ridge (De Argollo, 1971), back-arc basalts from the East Scotia Sea (Saunders and Tarney, 1979), and oceanic island basalts from Hawaii and Iceland (De Argollo, 1974; De Argollo and Schilling, 1978 (a,b)).

5.2 PETROLOGY OF THE CONTINENTAL ALKALINE VOLCANIC ROCKS STUDIED

5.2.1 Freemans Cove Suite

5.1.1.1 Geologic Setting

The Freemans Cove Eocene Volcanic Suite (Temple, 1965; Kerr, 1974; Mitchell and Platt, 1983, 1984) is located in the Freemans Cove area of southeastern Bathurst Island in the Canadian Arctic Archipelago. The suite is composed of numerous dikes, sills, small plugs, and agglomeratic vents. Magmatism in the region is bimodal consisting predominantly of nephelinite or larnite-normative nephelinites and basanites with subordinate amounts of olivine-melilite nephelinites, phonolites and tholeiitic and alkali basalts (Mitchell and Platt, 1984). Present levels of erosion are such that the lavas are preserved only as clasts within the agglomeratic vents.

Xenoliths of spinel and garnet lherzolite do not occur in this suite of rocks (Mitchell and Platt, 1984). The Freemans Cove volcanic suite possesses the petrological characteristics of intraplate continental magmatism of the type associated with rifting and doming (Bailey, 1974), and is believed to have been emplaced during uplift and compression of the region during the Eurekan rifting episode (Mitchell and Platt, 1984).

5.2.1.2 Petrography

One melilite olivine nephelinite (BI-268), 5 olivine nephelinites (BI-49, BI-84, BI-104, BI-245, BI-247) and 4

basanites (BI-4, BI-63, BI-75, N2-13) were studied. Petrographic descriptions and representative chemical compositions of the rocks are given by Mitchell and Platt (1984).

Briefly, the nephelinites are fine-grained, porphyritic rocks containing phenocrysts of forsteritic olivine and augitic clinopyroxene. The groundmass consists of nepheline, glass and accessory phlogopite and apatite.

The basanites are fine-grained porphyritic rocks containing phenocrysts of forsteritic olivine and augitic clinopyroxene. The groundmass consists of plagioclase, nepheline, glass, and accessory apatite, zeolite, and calcite. A complete gradation to nephelinite appears to exist with decreasing amounts of modal plagioclase (Mitchell and Platt. 1984).

5.2.1.3 Petrogenesis

Many of the nephelinites and basanites have the geochemical characteristics of primary magmas (i.e., Mg-numbers between 65 and 75 and Ni contents greater than 250 ppm; Brey, 1978; Frey *et al.*, 1978; Wass, 1980) and it has been proposed by Mitchell and Platt (1983, 1984) that these members of the suite represent an integrated series of primary melts erupted in an essentially unmodified state from the upper mantle. The sequence olivine melilite nephelinite-olivine nephelinite - basanite is believed to represent increasing degrees of fusion of a common mantle source (Mitchell and Platt, 1984; Barker *et al.*, 1985).

5.2.2 Balcones Suite

5.2.2.1 Geologic Setting

The Balcones Magmatic Province (Lonsdale, 1927; Spencer, 1969; Barker and Young, 1979; Barker *et al.*, 1985) consists of intrusive, extrusive, and pyroclastic silica undersaturated rocks that occur in a belt over 400 km long stretching from southwest and west of Uvalde to northeast of Austin, Texas. More than 100 sills, laccoliths and plugs are exposed on the surface. Many more are unexposed but have been detected by means of gravity and magnetic surveys. Magmatism in the region is bimodal consisting of olivine melilite nephelinite, olivine nephelinite and minor amounts of alkali basalt, phonolite and nepheline basanite (Spencer, 1969).

Xenoliths of spinel lherzolites, dunite, and harzburgite occur in the mafic rocks of the suite (Barker *et al.*, 1985).

Volcanic rocks in the region are believed to have been deposited on the floor of a shallow epicontinental sea (Ewing and Caran; 1982) during Cretaceous time, approximately 100 to 66 Ma ago (Barker *et al.*, 1985). The Balcones Province coincides with a part of the buried Ouachita structural belt and lies along the major Balcones Fault Zone (Spencer, 1969).

The Balcones Province differs from the Freemans Cove in being exposed at a relatively higher level and in being, on average, more undersaturated (Mitchell and Platt, 1984).

5.2.2.2 Petrography

Five olivine melilite nephelinites (6-1, 6-3, U2-1, V2-5, V3-3), 2 olivine nephelinites (7-4, V1-2) and 3 phonolites

(7-7, V4-2, V5-1) were studied. Petrographic descriptions and representative chemical compositions of the rocks are given by Lonsdale (1927), Spencer (1969), McKay (1984), and Barker *et al.* (1985). Petrographically many of the mafic rocks are identical to those of Freemans Cove (Mitchell and Platt, 1984).

Briefly, the nephelinites are fine-grained porphyritic rocks containing phenocrysts of forsteritic olivine and augitic clinopyroxene. The groundmass consists of nepheline, clinopyroxene, apatite, and titanomagnetite. Melilite and locally perovskite are additional groundmass phases in the olivine melilite nephelinites.

The phonolites are fine-grained porphyritic rocks containing phenocrysts of olivine, clinopyroxene, sphene, kaersutitic amphibole, nepheline, and alkali feldspar. The groundmass consists of nepheline, clinopyroxene, apatite, titanomagnetite, alkali feldspar, and analcime.

5.2.2.3 Petrogenesis

Many of the nephelinites, basanites, and alkali basalts of the Balcones Province have the geochemical characteristics of primary magmas and may have formed by varying (but small) degrees of fusion of a common upper mantle source (Barker *et al.*, 1985). The sequence olivine melilite nephelinite-olivine nephelinite-basanite-alkali basalt is believed to represent increasing degrees of fusion.

The phonolites probably formed from olivine nephelinite magma by fractionation of kaersutitic amphibole, olivine, and

clinopyroxene at high pressure (McKay, 1984; Barker *et al.*, 1985).

5.2.3 Hegau and Urach Suites

5.2.3.1 Geologic Setting

The Hegau and Urach Miocene Volcanic Provinces (Wimmenauer, 1970; Sick, 1970; Brey, 1978; Brey and Keller, 1982) are located in Germany approximately 70 km east of the eastern shoulder of the Rhine graben. The provinces are composed of numerous plugs, dikes, lavas, tuffs, and diatremes and are considered to be tectonically related to the Rhine graben (Brey and Keller, 1982). Magmatism in the region consists primarily of olivine melilitites, melilititic tuffs, and phonolites (Brey, 1978). Xenoliths of spinel lherzolite occur in the melilititic tuffs of the Hegau Province (Brey and Keller, 1982).

5.2.3.2 Petrography

Eight olivine melilitites, 4 from the Hegau Province (HEG-3, HEG-4, HEG-6, HEG-7), and 4 from the Urach Province (U-1, U-4, U-7, U-16) were studied. Petrographic descriptions and representative chemical compositions of the rocks are given by Sick (1970) and Brey and Keller (1982).

Briefly, the olivine melilitites are fine-grained porphyritic rocks containing phenocrysts of forsteritic olivine and augitic clinopyroxene. Microphenocrysts of melilite are also present. The groundmass consists of nepheline, melilite, magnetite, glass, cpx, mica, perovskite and cr-spinel. Amygdules of zeolite are present in some of

the samples.

The Hegau rocks are petrographically and geochemically similar to the mafic rocks of the Balcones and Freemans Cove Suites. The Urach rocks are petrographically similar to the mafic rocks of the Balcones and Freemans Cove Suites but contain more CaO and MgO and less Na_2O, Al_2O_3, and SiO_2 (Brey, 1978).

5.2.3.3 Petrogenesis

The olivine melilitites of the Hegau and Urach Volcanic Provinces have the geochemical characteristics of primary magmas and are considered to have been produced from a common upper mantle source (Brey, 1978). The Urach rocks are believed to have formed by smaller degrees of partial melting (and/or higher CO_2 contents) than the Hegau rocks (Brey, 1978).

5.3 Ga ABUNDANCES

5.3.1 Freemans Cove Suite

The Ga contents of the Freemans Cove volcanic rocks are given in Table 41.

The Ga contents of the rocks vary from 15.85 ± 0.45 ppm (BI-4) to 18.22 ± 0.49 ppm (BI-75). Considerable overlap exists between the Ga contents of the different rock types. For example, BI-268 (an olivine melilite nephelinite contains 17.23 ± 0.44 ppm Ga, BI-84 (an olivine nephelinite) contains 17.06 ± 0.48 ppm Ga, and N2-13 (a basanite) contains 17.31 ± 0.48 ppm Ga. As a result it is not possible to differentiate

TABLE 41

Ga Contents of the Freemans Cove Volcanic Rocks (uncertainties (1σ) due to counting statistics of gamma ray spectrometry)

Sample	Rock Type	Ga Content (ppm)
BI-268	OMN	17.23 ± 0.44
BI-49	ON	16.54 ± 0.48
BI-84	ON	17.06 ± 0.48
BI-104	ON	16.53 ± 0.45
BI-245	ON	18.19 ± 0.46
BI-247	ON	16.46 ± 0.49
BI-4	B	15.85 ± 0.45
BI-63	B	16.07 ± 0.47
BI-75	B	18.22 ± 0.49
N2-13	B	17.31 ± 0.48

Abbreviations: OMN - olivine melilite nephelinite
ON - olivine nephelinite
B - basanite

categorically the rock types on the basis of their Ga contents.

5.3.2 Balcones Suite

The Ga contents of the Balcones volcanic rocks are given in Table 42.

The Ga contents of the rocks vary from 16.97 ± 0.48 ppm (V1-2) to 41.97 ± 1.20 ppm (V4-2). The Ga contents of the olivine melilite nephelinites and the olivine nephelinites overlap. For example, V3-3 (an olivine melilite nephelinite) contains 17.58 ± 0.47 ppm Ga, and V1-2 (an olivine nephelinite) contains 16.97 ± 0.48 ppm Ga. The Ga contents of the phonolites vary from 31.07 ± 0.91 ppm (7-7) to 41.97 ±

TABLE 42

Ga Contents of the Balcones Volcanic Rocks (uncertainties (1σ) due to counting statistics of gamma ray spectrometry)

Sample	Rock Type	Ga Content (ppm)
V2-5	OMN	22.02 ± 0.62
U2-1	OMN	20.29 ± 0.57
6-1	OMN	20.62 ± 0.60
V3-3	OMN	17.58 ± 0.47
6-3	OMN	19.40 ± 0.47
7-4	ON	26.26 ± 0.72
V1-2	ON	16.97 ± 0.48
VA-2	P	41.97 ± 1.20
7-7	P	31.07 ± 0.91
V5-1	P	32.52 ± 0.91

Abbreviations: OMN - olivine melilite nephelinite
ON - olivine nephelinite
P - phonolite

1.20 ppm (V4-2) and are significantly higher than the Ga contents of the mafic rocks.

The Ga contents of the Balcones olivine melilite nephelinite and olivine nephelinites are similar to, although slightly higher than, the Ga contents of the corresponding mafic rocks of the Freemans Cove Suite.

5.3.3 Hegau and Urach Suites

The Ga contents of the Hegau and Urach volcanic rocks are given in Table 43.

The Ga contents of the Hegau rocks vary from 12.14 ± 0.32 ppm (HEG-3) to 14.82 ± 0.44 ppm (HEG-6) and are generally lower than the Ga contents of similar rocks from

TABLE 43

Ga Contents of the Hegau and Urach Volcanic Rocks (uncertainties (1σ) due to counting statistics of gamma ray spectrometry)

Sample	Rock Type	Ga Content (ppm)
Hegau Rocks		
HEG-3	OM	12.14 ± 0.32
HEG-4	OM	12.43 ± 0.35
HEG-6	OM	14.82 ± 0.44
HEG-7	OM	12.73 ± 0.33
Urach Rocks		
U-1	OM	17.00 ± 0.49
U-4	OM	15.73 ± 0.45
U-7	OM	17.33 ± 0.51
U-16	OM	14.20 ± 0.42

Abbreviation: OM - olivine melilitite

the Freemans Cove and Balcones volcanic provinces.

The Ga contents of the Urach rocks vary from 14.20 ± 0.42 ppm (U-16) to 17.33 ± 0.51 ppm (U-7) and overlap with the Ga contents of similar rocks from the other volcanic provinces studied.

5.4 OTHER TRACE ELEMENT ABUNDANCES

Sc, Cr, Co, La, Eu, Hf, Ta, and Th abundances were determined by instrumental neutron activation analysis (Appendix 1, section A1.3). Ni abundances were determined by atomic absorption spectroscopy.

5.4.1 Freemans Cove Suite

The trace element contents of the Freemans Cove volcanic

rocks are given in Table 44. Systematic variations exist in the trace element contents of the different rock types (e.g., see Figures 10, 11, and 12). These variations suggest the rocks are genetically related.

Mitchell and Platt (1984) have proposed that the different rock types were formed by varying degrees of partial melting of a common upper-mantle source. The trace element data for these rocks are consistent with this proposal and reflect not only the effects of increasing degrees of fusion but also, for some of the rocks (BI-49, BI-84, BI-245, BI-4, and N2-13), the effects of subsequent crystal fractionation.

Samples BI-268 (an olivine melilite nephelinite), BI-104 (an olivine nephelinite), BI-247 (an olivine nephelinite), and BI-63 (a basinite) possess the geochemical characteristics of primary magmas. Sample BI-268, which is believed to have formed by the least degree of partial melting, is enriched in incompatible trace elements (Figure 12) and depleted in compatible trace elements (Figure 11) relative to the other primary melts.

Samples BI-49, BI-84, BI-245, BI-4, and N2-13, which are believed to be related to the primary melts by fractionation of olivine and clinopyroxene, are enriched in incompatible trace elements (Figure 12) and depleted in compatible trace elements (Figure 11) relative to the primary melts.

TABLE 44

Trace Element Contents of the Freemans Cove Volcanic Rocks (uncertainties, 1σ, due to counting statistics of gamma ray spectrometry)

Sample	Rock Type	Trace Element Abundances (ppm)				
		Sc	Co	Ni	La	Cr
BI-268	OMN	31.80±0.64	68.62±0.35	263±13	103.49±1.55	314.37± 9.42
BI-49	ON	22.41±0.51	64.12±0.34	218±11	93.68±1.68	281.58± 8.15
BI-84	ON	29.79±0.59	75.51±0.39	233±12	67.40±1.08	283.80± 8.10
BI-104	ON	34.34±0.66	69.70±0.37	335±17	60.60±1.05	419.30±11.73
BI-245	ON	26.02±0.50	52.77±0.26	155± 8	178.75±3.20	182.41± 5.11
BI-247	ON	29.80±0.59	70.36±0.38	330±12	56.31±1.01	591.78±17.73
BI-4	B	26.86±0.51	59.99±0.30	210±10	82.32±1.65	388.14±10.51
BI-63	B	28.36±0.55	68.81±0.36	260±13	61.71±1.05	542.93±17.01
BI-75	B	22.33±0.45	61.34±0.32	143± 7	99.29±1.50	257.58± 8.05
N2-13	B	26.61±0.51	65.44±0.34	245±12	69.44±1.10	387.44±10.84

Sample	Rock Type	Trace Element Abundances (ppm)			
		Eu	Hf	Ta	Th
BI-268	OMN	3.03±0.68	2.80±0.17	7.63±0.10	12.68±0.63
BI-49	ON	2.65±0.15	3.76±0.23	6.95±0.09	12.32±0.61
BI-84	ON	2.63±0.15	3.98±0.28	6.14±0.08	8.33±0.42
BI-104	ON	2.93±0.17	3.85±0.75	5.54±0.05	7.22±0.33
BI-245	ON	4.13±0.24	3.87±0.25	5.97±0.06	22.63±1.13
BI-247	ON	2.17±0.13	3.67±0.22	4.35±0.04	6.39±0.31
BI-4	B	2.34±0.14	3.33±0.21	4.36±0.04	9.99±0.51
BI-63	B	2.25±0.14	3.29±0.21	3.89±0.04	6.87±0.34
BI-75	B	2.69±0.15	3.47±0.22	6.09±0.06	12.48±0.62
N2-13	B	1.91±0.11	3.52±0.21	3.81±0.04	7.93±0.39

Abbreviations: OMN - olivine melitite nephelinite
ON - olivine nephelinite
B - basanite

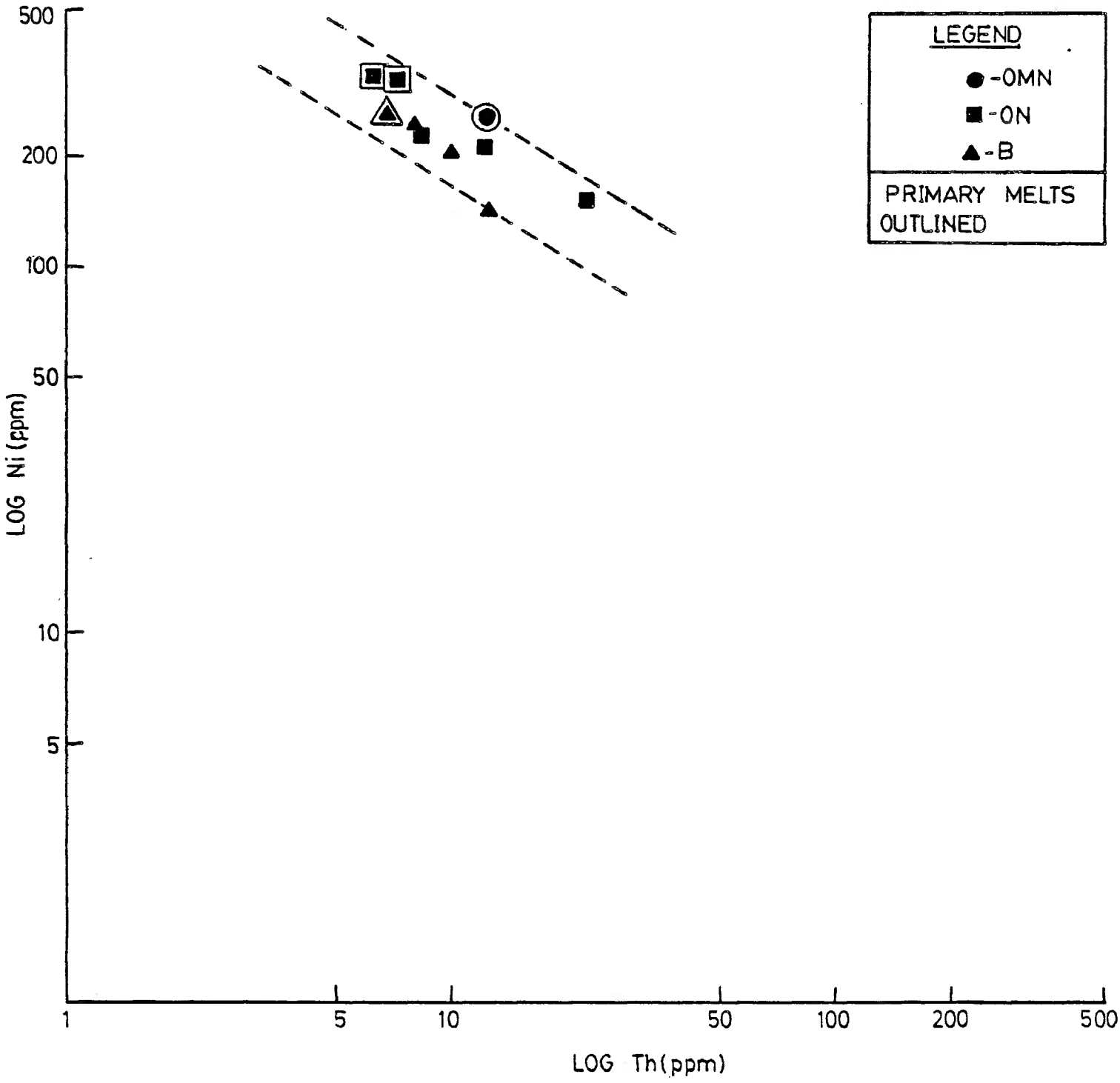

FIGURE 10 Log Ni vs. Log Th plot for Freemans Cove volcanic rocks (abbreviations: OMN- olivine melilite nephelinite, ON- olivine nephelinite, B- basanite).

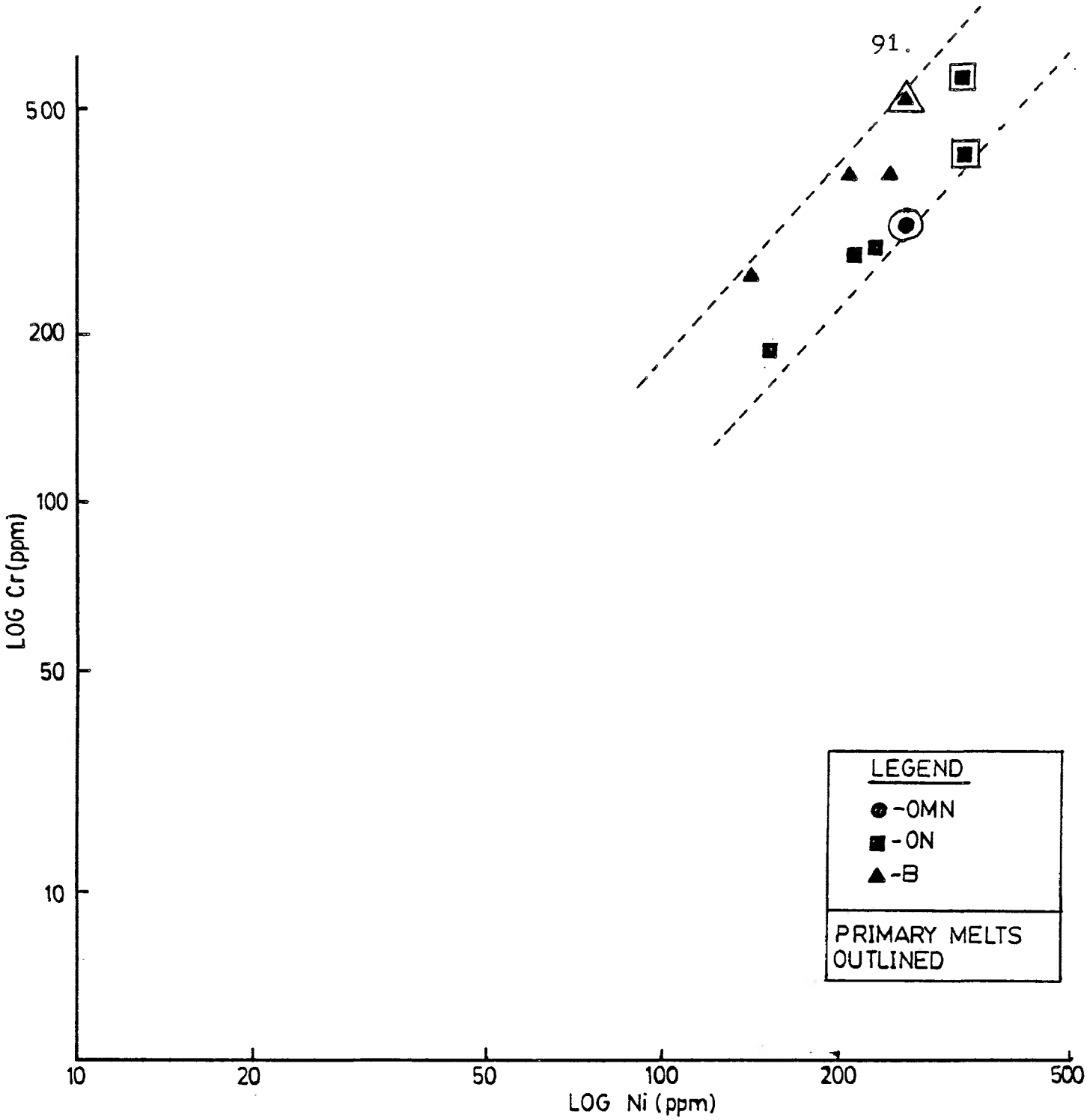

FIGURE 11 Log Cr vs. Log Ni plot for Freemans Cove volcanic rocks (abbreviations: OMN- olivine melilite nephelinite, ON- olivine nephelinite, B- basanite).

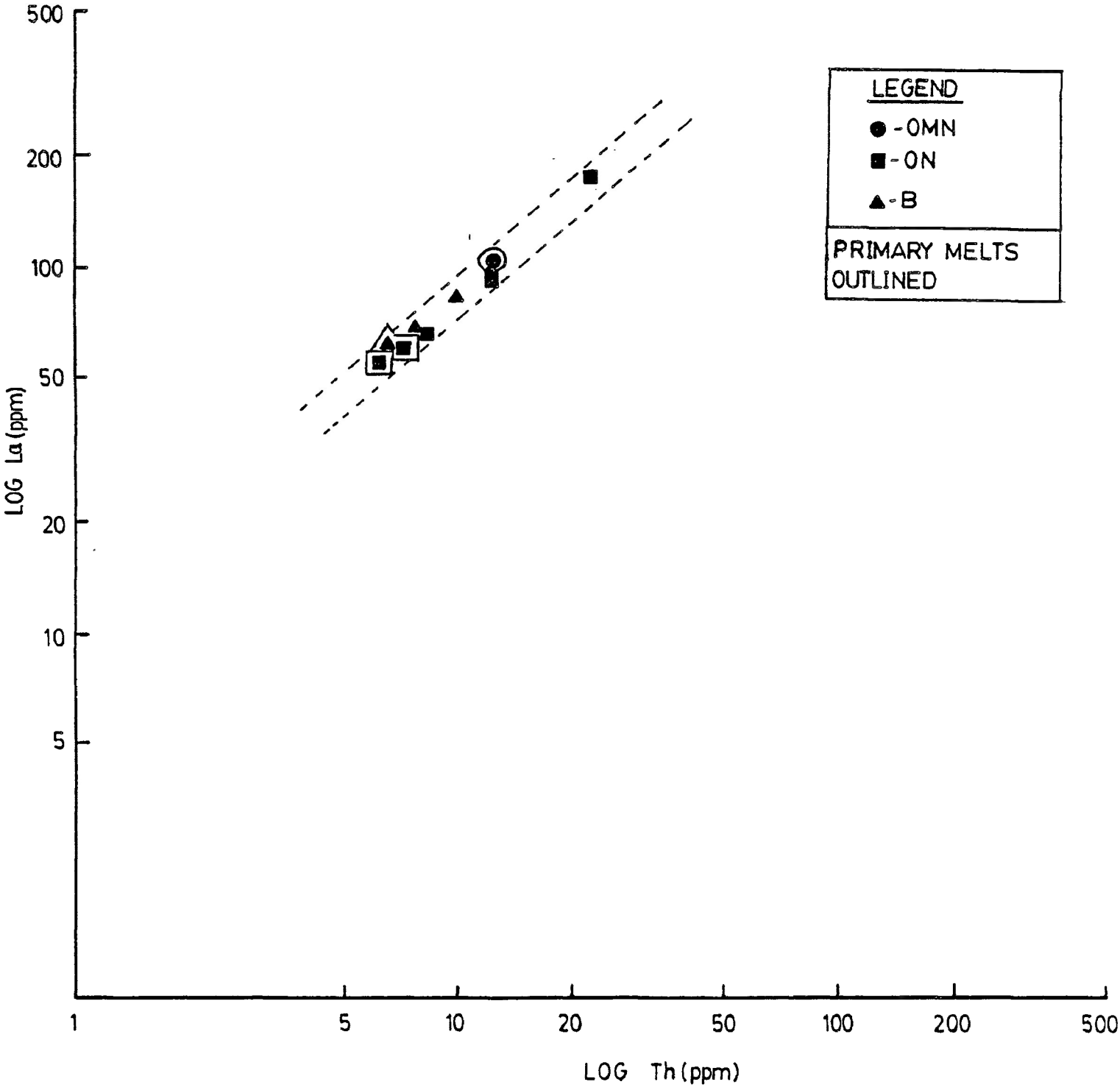

FIGURE 12 Log La vs. Log Th plot for Freemans Cove volcanic rocks (abbreviations: OMN- olivine melilite nephelinite, ON- olivine nephelinite, B- basanite).

5.4.2 Balcones Suite

The trace element contents of the Balcones volcanic rocks are given in Table 45. Systematic variations exist in the trace element contents of the different rock types (e.g., see Figures 13, 14, and 15). These variations suggest the rocks are genetically related.

Barker *et al.*, (1985) have proposed that the different rock types were formed by varying degrees of partial melting of a common upper-mantle source. The trace element data for these rocks are consistent with this proposal and reflect not only the effects of increasing degrees of fusion but also, for some of the rocks (6-1, 7-4, V4-2, 7-7, and V5-1), the effects of subsequent crystal fractionation.

Samples V2-5, U2-1, V3-3, 6-3 (all olivine melilite nephelinites), and V1-2 (an olivine nephelinite) possess the geochemical characteristics of primary magmas. Sample V2-5, which is believed to have formed by the least degree of partial melting, is enriched in incompatible trace elements (Figure 15) and depleted in compatible trace elements (Figure 14) relative to the other primary melts. Sample V1-2, which is believed to have formed by the greatest degree of partial melting is depleted in incompatible trace elements (Figure 15) and enriched in compatible trace elements (Figure 14) relative to the other primary melts.

The phonolite samples (V4-2, 7-7, V5-1), which are believed related to the primary melts by fractionation of amphibole, olivine and clinopyroxene, are enriched in incom-

TABLE 45

Trace Element Contents of the Balcones Volcanic Rocks (uncertainties, 1σ, due to counting statistics of gamma ray spectrometry)

Sample	Rock Type	Trace Element Abundances (ppm)				
		Sc	Co	Ni	La	Cr
V2-5	OMN	22.28±0.45	69.74±0.63	338±17	68.83±1.36	384.26±11.84
U2-1	OMN	24.75±0.48	69.03±0.55	400±20	60.63±1.21	510.62±14.81
6-1	OMN	22.19±0.46	61.26±0.51	235±12	59.41±1.18	350.76±10.87
V3-3	OMN	21.88±0.42	63.64±0.52	515±26	53.47±1.01	445.46±13.36
6-3	OMN	26.29±0.55	69.70±0.59	340±17	46.55±0.95	532.14±16.50
7-4	ON	15.83±0.31	48.91±0.45	184±10	52.42±1.00	252.68± 7.83
V1-2	ON	25.56±0.51	91.85±0.85	630±32	44.26±0.95	688.49±19.97
V4-2	P	0.57±0.02	28.46±0.33	30± 2	101.01±2.05	8.35± 0.27
7-7	P	2.38±0.05	22.38±0.30	30± 2	88.86±1.78	21.13± 0.61
V5-1	P	8.11±0.15	27.58±0.29	45± 3	76.61±1.46	53.02± 1.59

Sample	Rock Type	Trace Element Abundances (ppm)			
		Eu	Hf	Ta	Th
V2-5	OMN	3.77±0.18	6.70±0.41	6.00±0.08	7.85±0.40
U2-2	OMN	3.51±0.17	6.93±0.42	5.42±0.07	7.77±0.40
6-1	OMN	3.45±0.17	6.08±0.17	6.06±0.08	6.65±0.33
V3-3	OMN	2.96±0.14	5.37±0.33	4.80±0.06	5.94±0.30
6-3	OMN	2.63±0.13	5.21±0.31	5.83±0.07	5.66±0.28
7-4	ON	2.86±0.14	7.06±0.44	6.41±0.08	5.62±0.28
V1-2	ON	2.35±0.12	2.39±0.16	4.43±0.05	4.99±0.25
V4-2	P	1.77±0.09	13.60±0.81	9.78±0.13	24.10±1.20
7-7	P	2.52±0.13	12.20±0.76	9.90±0.14	13.60±0.68
V5-1	P	2.71±0.14	7.90±0.47	7.12±0.09	10.60±0.52

Abbreviations: OMN - olivine melitite nephelinite
ON - olivine nephelinite
P - phonolite

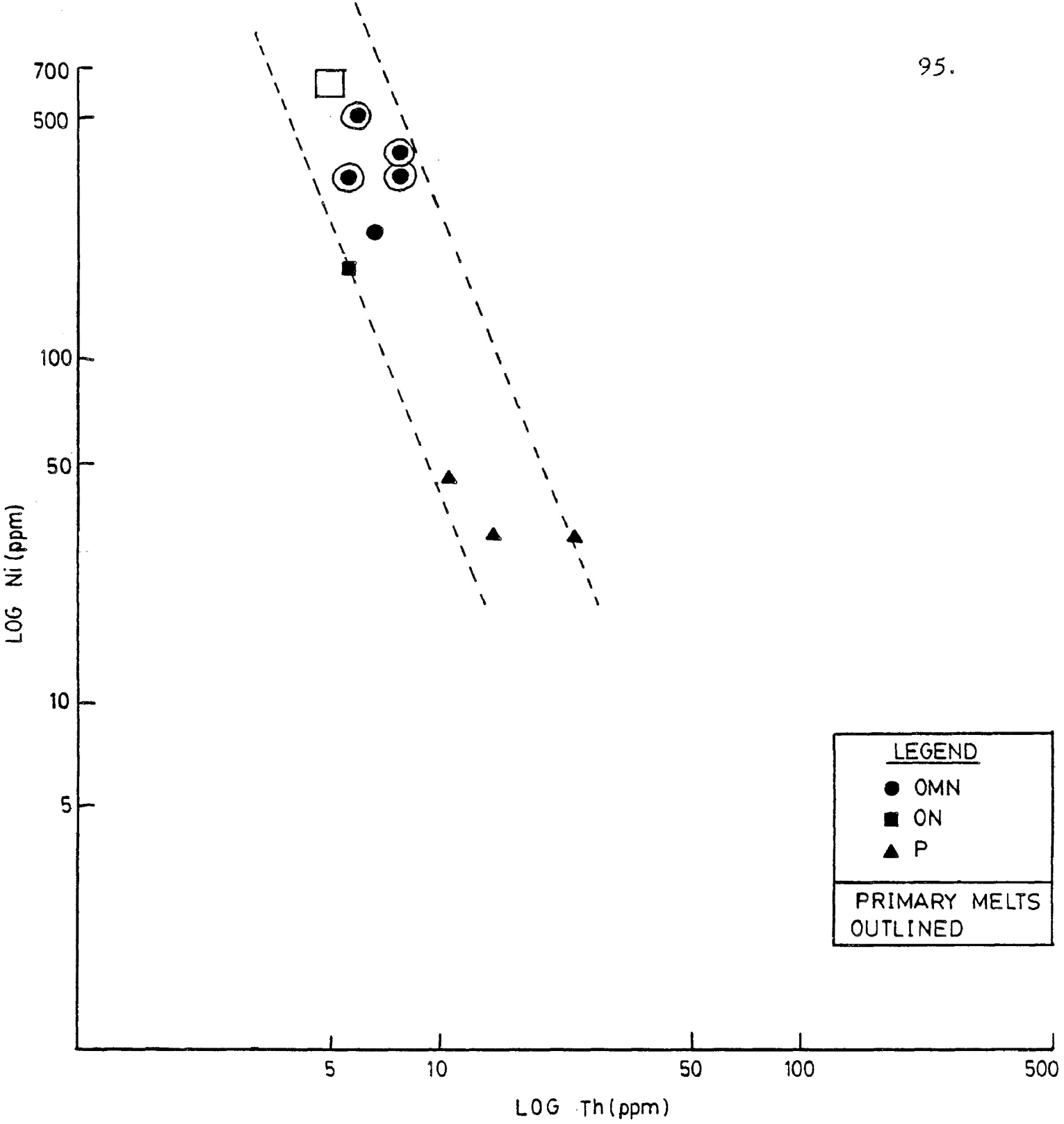

FIGURE 13 Log Ni vs. Log Th plot for Balcones volcanic rocks (abbreviations: OMN- olivine melilite nephelinite, ON- olivine nephelinite, P- phonolite).

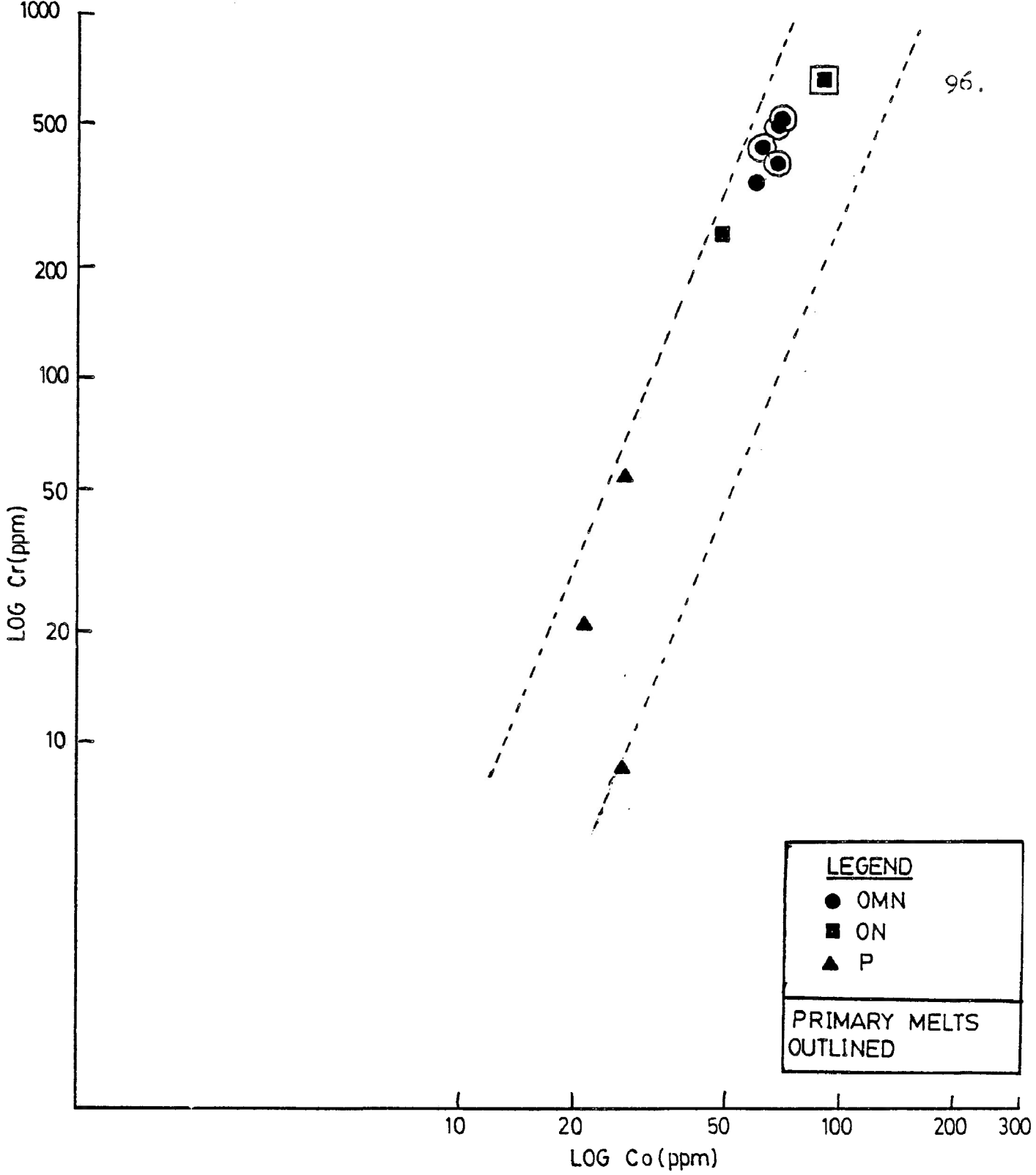

FIGURE 14 Log Cr vs. Log Co plot for Balcones volcanic rocks (abbreviations: OMN- olivine melilite nephelinite, ON- olivine nephelinite, P- phonolite).

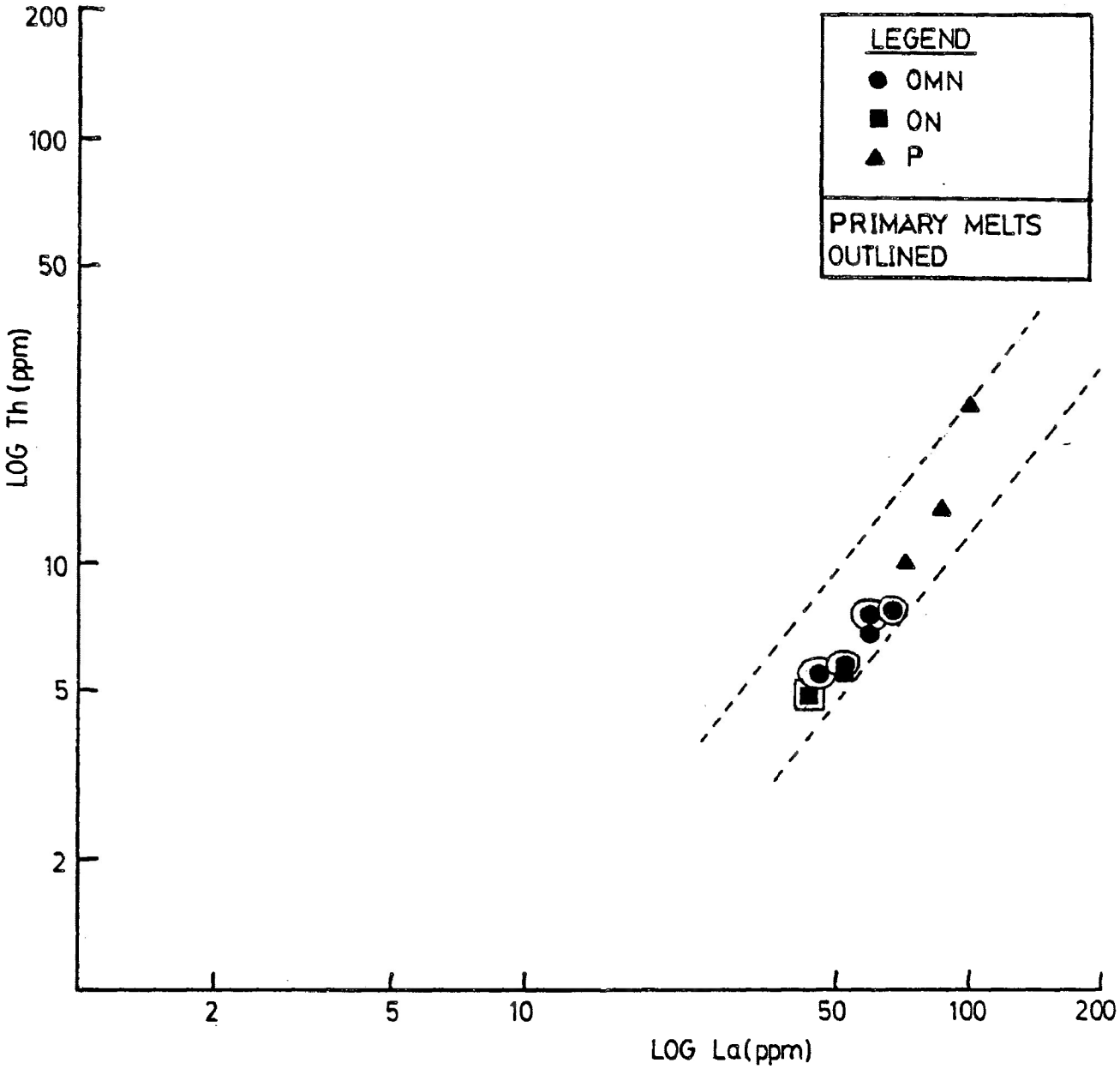

FIGURE 15 Log Th vs. Log La plot for Balcones volcanic rocks (abbreviations: OMN- olivine melilite nephelinite, ON- olivine nephelinite, P- phonolites).

patible trace elements (Figure 15) and depleted in compatible trace elements (Figure 14) relative to the primary melts.

5.4.3 Hegau and Urach Suites

The trace element contents of the Hegau and Urach volcanic rocks are given in Table 46. Systematic variations exist in the trace element contents of the different rock types (e.g., see Figures 16, 17 and 18). These variations suggest the rocks are genetically related.

Brey (1978) has proposed that the Hegau and Urach rocks were produced by varying degrees of partial melting of a common upper-mantle source. The Urach rocks are believed to have been produced by the least degrees of partial melting (Brey, 1978). The trace element data for these rocks are consistent with these proposals. The Urach rocks (U-1, U-4, U-7, U-16), for example, are enriched in incompatible trace elements (Figure 18) and depleted in compatible trace elements (Figures 16 and 17) relative to the Hegau rocks.

All of the samples possess the geochemical characteristics of primary magmas.

5.5 RELATIONSHIPS BETWEEN Ga ABUNDANCES AND OTHER TRACE ELEMENT ABUNDANCES

The results of comparisons between the abundances of Ga and the abundances of other trace elements in the rocks of the present study are given in Table 47.

In all cases the data points define broad linear trends (e.g., see Figures 19 to 24). Positive linear correlations

TABLE 46

Trace Element Contents of the Hegau and Urach Volcanic Rocks (uncertainties, 1σ, due to counting statistics of gamma ray spectrometry)

Sample	Rock Type	Trace Element Abundances (ppm)				
		Sc	Co	Ni	La	Cr
Hegau						
HEG-3	OM	41.48±0.83	96.35±0.34	350±18	55.82±0.88	1074.02±32.22
HEG-4	OM	33.46±0.65	86.48±0.44	340±17	84.86±1.36	902.29±27.10
HEG-6	OM	33.86±0.65	70.39±0.36	268±14	89.43±1.39	752.72±22.52
HEG-7	OM	35.08±0.70	65.63±0.33	315±16	83.26±1.29	908.60±22.25
Urach						
U-1	OM	34.87±0.68	62.65±0.32	330±17	108.88±1.72	842.68±25.20
U-4	OM	32.57±0.64	74.73±0.38	519±26	93.96±1.50	1308.96±33.24
U-7	OM	32.80±0.63	65.96±0.33	380±19	113.95±1.82	931.62±27.99
U-16	OM	37.09±0.74	66.99±0.34	350±18	88.99±1.38	900.14±27.15

Sample	Rock Type	Trace Element Abundances (ppm)			
		Eu	Hf	Ta	Th
Hegau					
HEG-3	OM	1.81±0.11	4.68±0.28	5.71±0.07	6.35±0.31
HEG-4	OM	3.08±0.18	6.36±0.39	9.51±0.12	8.83±0.43
HEG-6	OM	3.05±0.18	5.78±0.35	9.07±0.11	10.83±0.53
HEG-7	OM	3.01±0.18	5.24±0.32	8.18±0.11	9.60±0.47
Urach					
U-1	OM	2.80±0.17	6.52±0.40	9.36±0.12	13.18±0.65
U-4	OM	3.36±0.20	4.73±0.29	7.95±0.10	11.31±0.56
U-7	OM	3.35±0.20	5.46±0.33	9.35±0.11	13.10±0.65
U-16	OM	2.90±0.17	5.77±0.35	9.39±0.11	10.70±0.53

Abbreviation: OM - olivine melitite

TABLE 47

Relationships Between the Abundances of Ga and the Abundances of Other Trace Elements

Trace Element Abundances Compared	Correlation Coefficients (r)	Equations of Lines of Best Fit (y=mx+b)
Freemans Cove Suite		
Ga vs. Sc	-0.46	y = -0.52 x +31.92
Ga vs. Cr	-0.70	y = -0.01 x +20.23
Ga vs. Co	-0.41	y = -0.30 x +36.91
Ga vs. Ni	-0.61	y = -0.02 x +22.01
Ga vs. La	+0.66	y = +0.04 x +13.99
Ga vs. Hf	+0.12	y = +18.46 x -48.66
Ga vs. Ta	+0.42	y = +1.48 x +8.84
Ga vs. Th	+0.66	y = +0.25 x +14.24
Balcones Suite		
Ga vs. Sc	-0.94	y = -0.88 x +40.28
Ga vs. Cr	-0.91	y = -0.04 x +37.12
Ga vs. Co	-0.87	y = -0.41 x +47.25
Ga vs. Ni	-0.87	y = -0.04 x +37.13
Ga vs. La	+0.90	y = +0.48 x -6.42
Ga vs. Hf	+0.90	y = +2.71 x +4.95
Ga vs. Ta	+0.90	y = +4.77 x -6.49
Ga vs. Th	+0.91	y = +1.52 x +10.81
Hegau and Urach Suites		
Ga vs. Sc	-0.54	y = -1.27 x +59.10
Ga vs. Cr	-0.02	y = -0.55 x +542.36
Ga vs. Co	-0.67	y = -0.26 x +33.41
Ga vs. Ni	+0.13	y = 0.10 x -20.38
Ga vs. La	+0.89	y = +0.13 x +2.90
Ga vs. Hf	+0.22	y = +13.79 x -62.24
Ga vs. Ta	+0.48	y = +3.27 x -13.48
Ga vs. Th	+0.93	y = +0.96 x +4.42

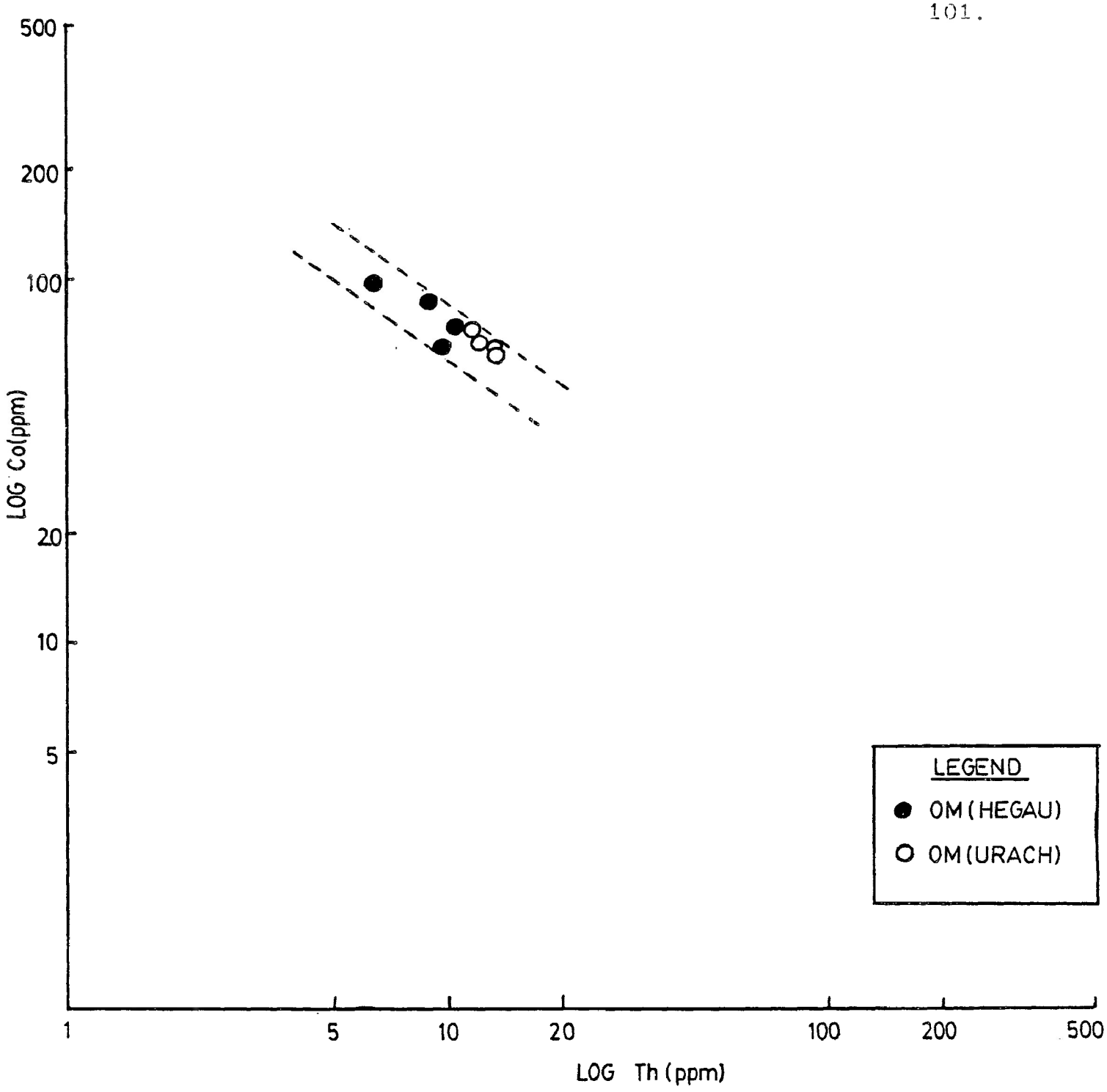

FIGURE 16 Log Co vs. Log Th plot for Hegau and Urach volcanic rocks (abbreviation: OM- olivine melilitite).

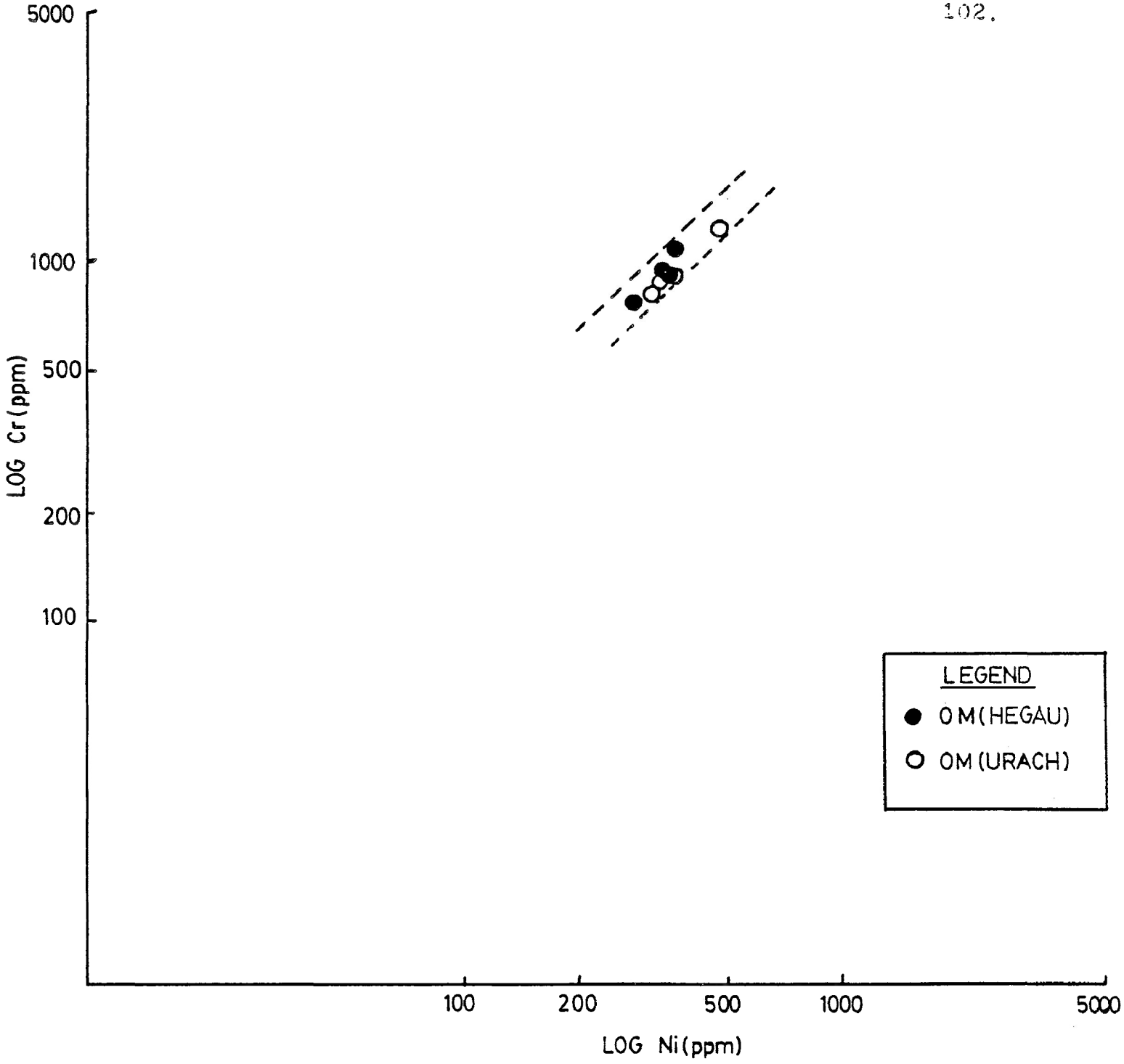

FIGURE 17 Log Cr vs. Log Ni plot for Hegau and Urach volcanic rocks (abbreviation: OM- olivine melilitite).

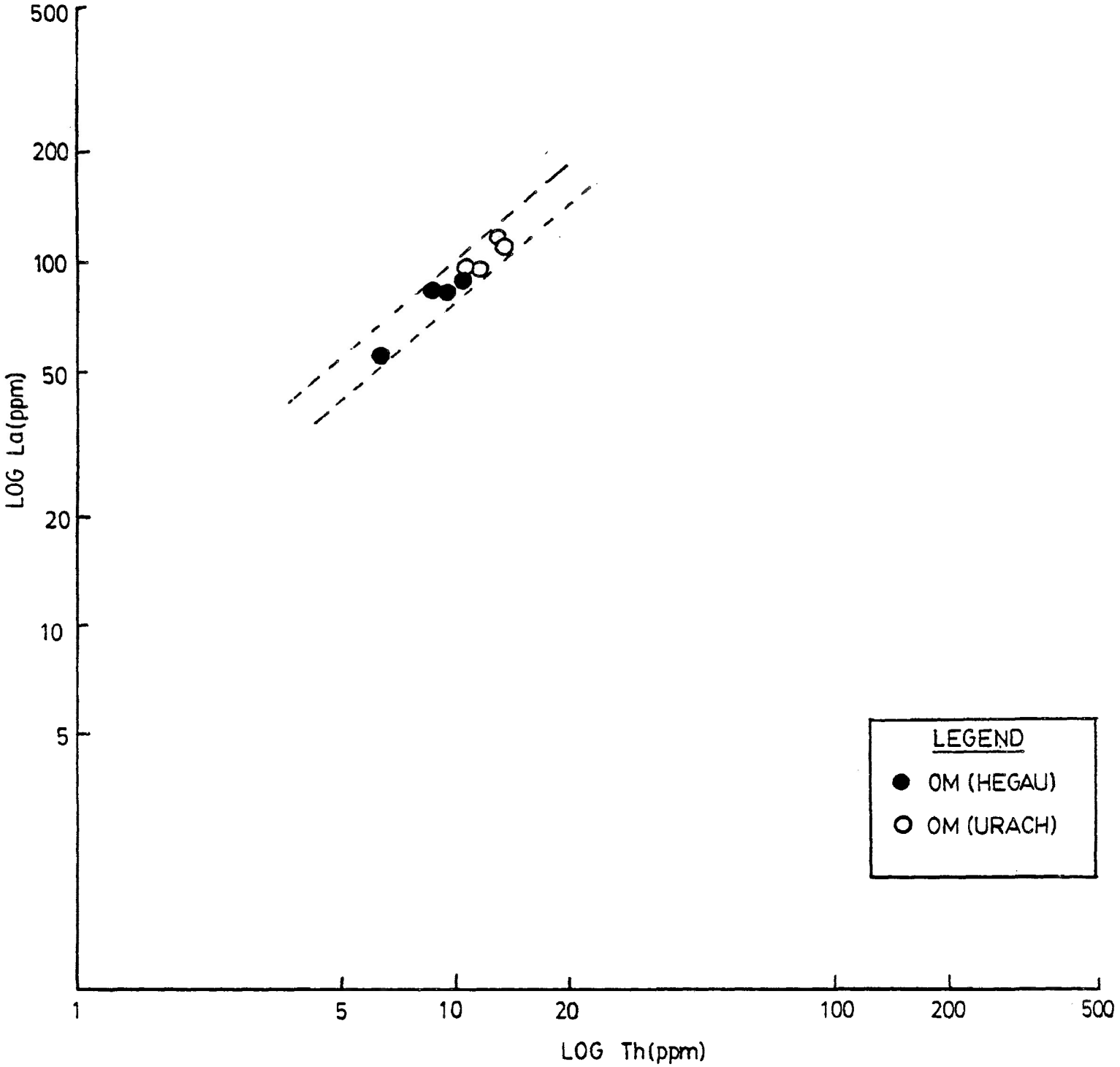

FIGURE 13 Log La vs. Log Th plot for Hegau and Urach volcanic rocks (abbreviation: OM- olivine melilitite).

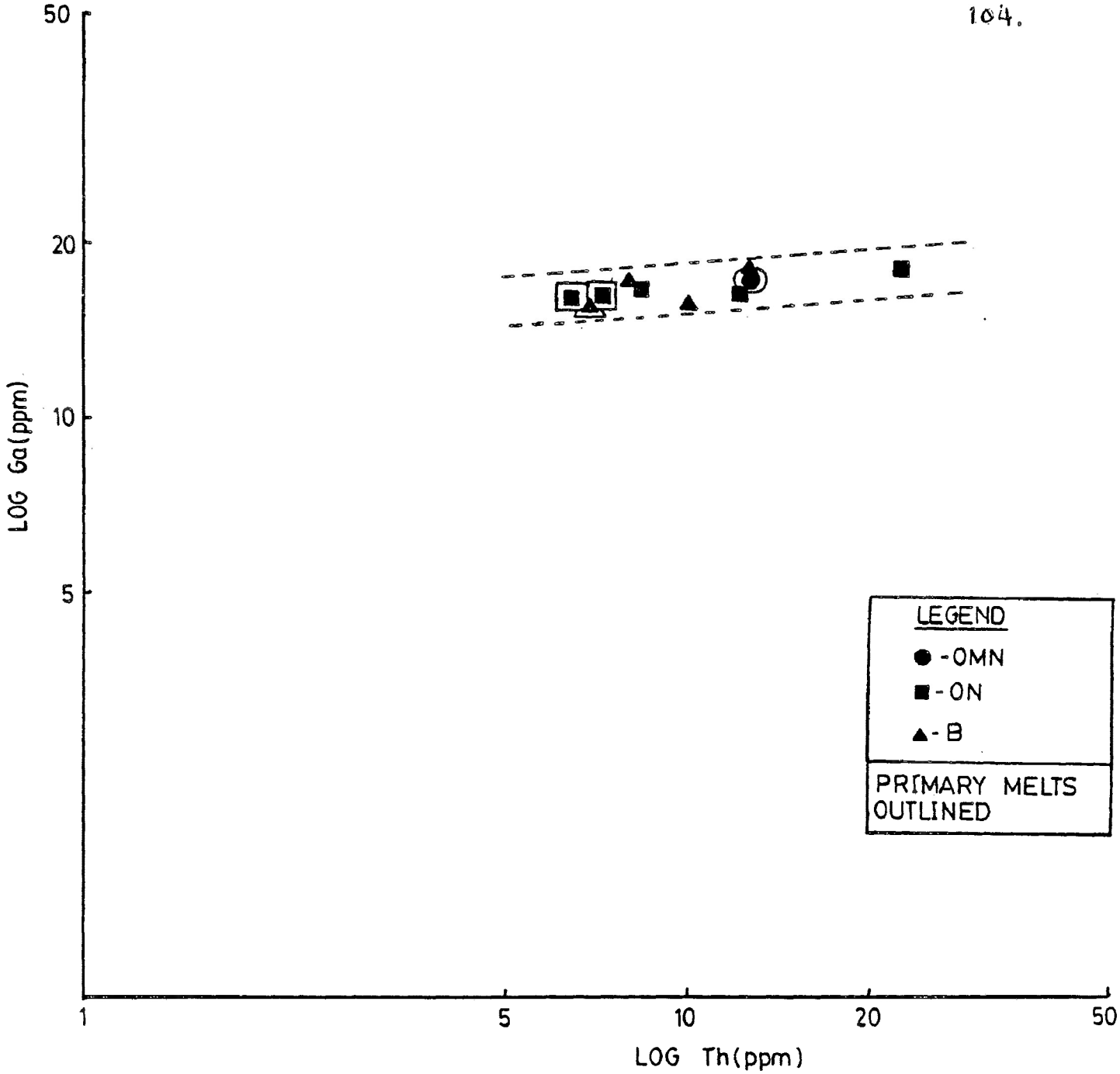

FIGURE 19 Log Ga vs. Log Th plot for Freemans Cove volcanic rocks (abbreviations: OMN- olivine melilite nephelinite, ON- olivine nephelinite, B- basanite).

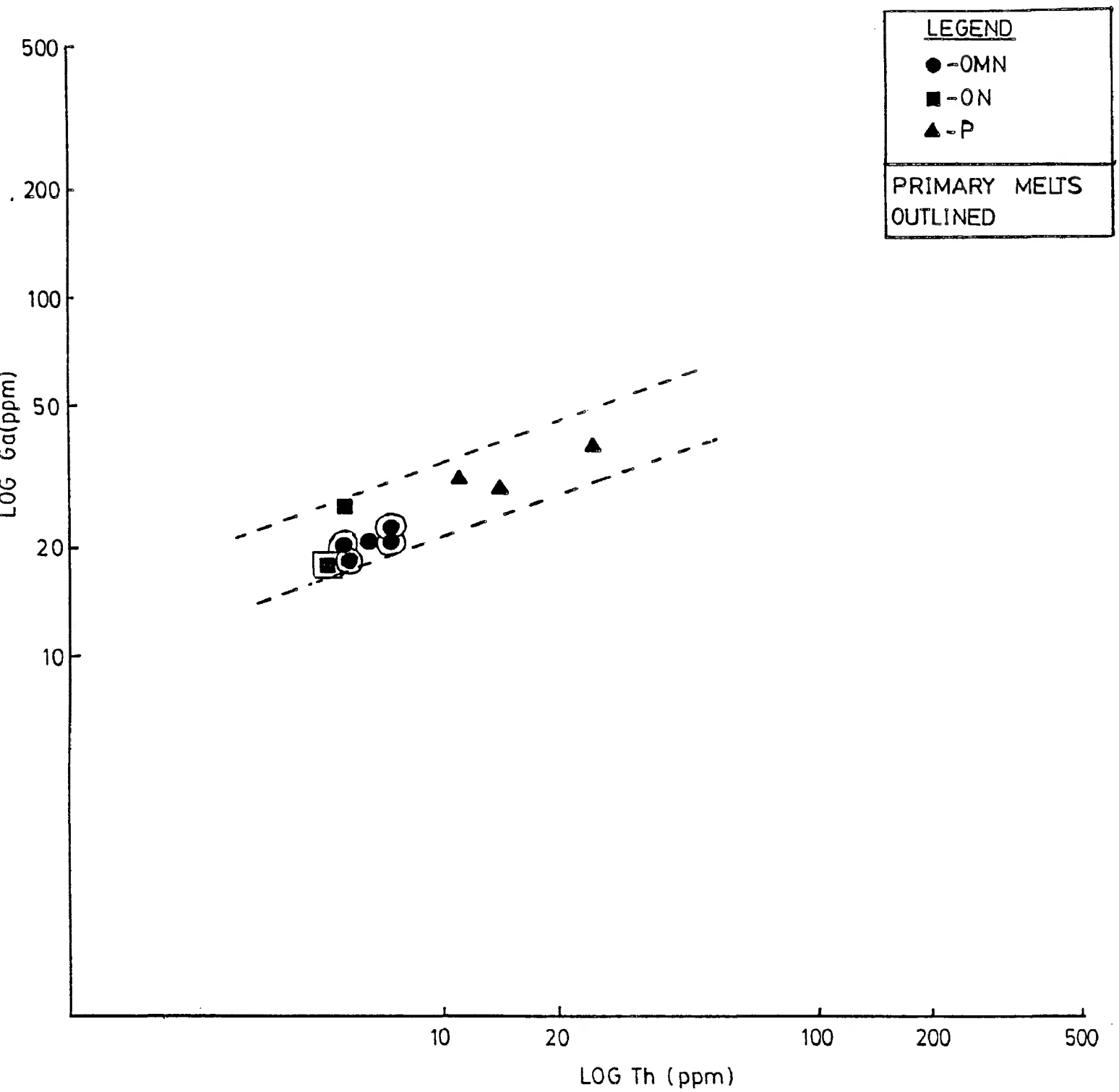

FIGURE 20 Log Ga vs. Log Th plot for Balcones volcanic rocks (abbreviations: OMN- olivine melilite nephelinite, ON- olivine nephelinite, P- phonolite).

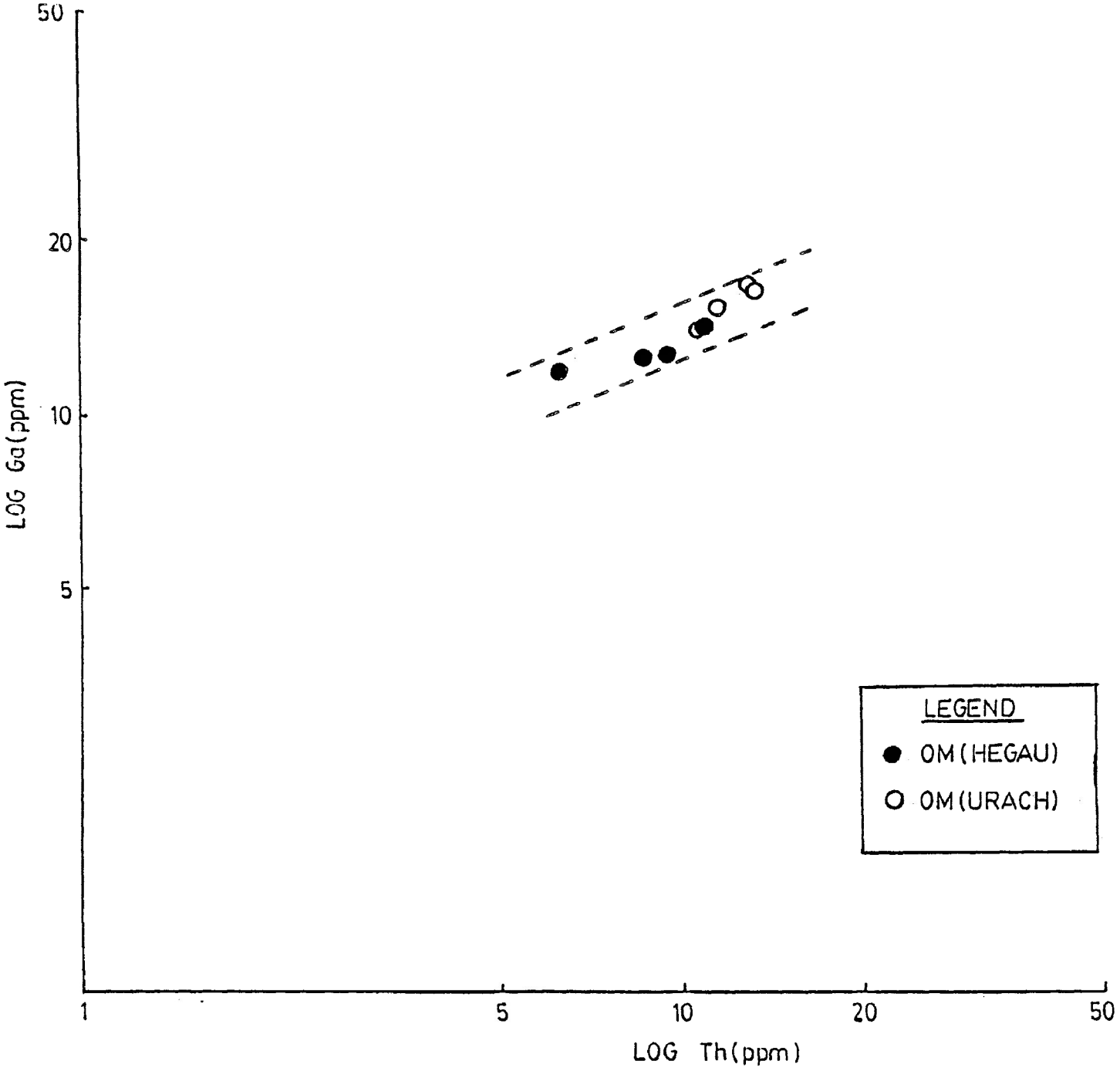

FIGURE 21 Log Ga vs. Log Th plot for Hegau and Urach volcanic rocks (abbreviation: OM- olivine melilitite).

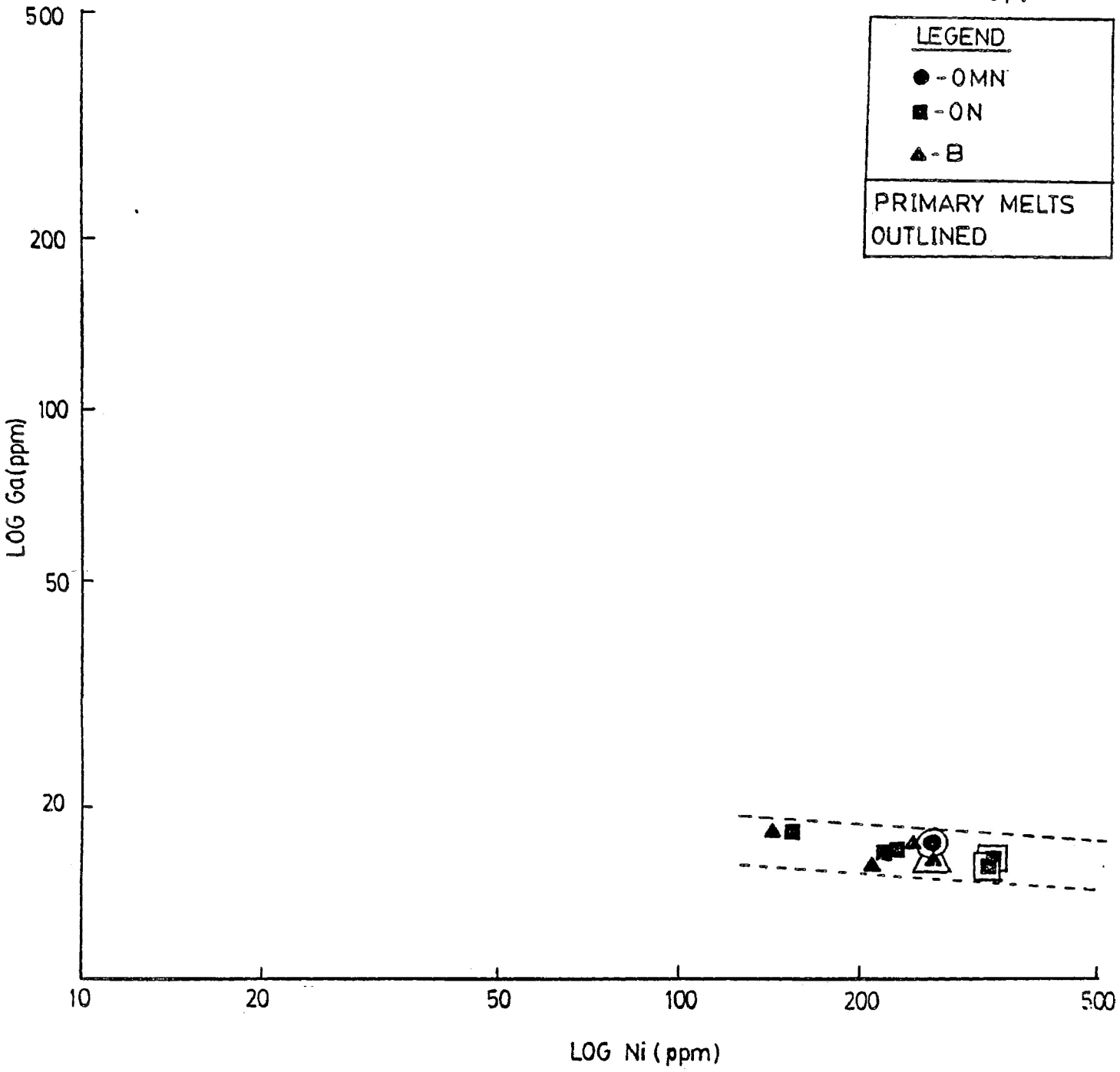

FIGURE 22 Log Ga vs. Log Ni plot for Freemans Cove volcanic rocks (abbreviations: OMN- olivine melilite nephelinite, ON- olivine nephelinite, B- basanite).

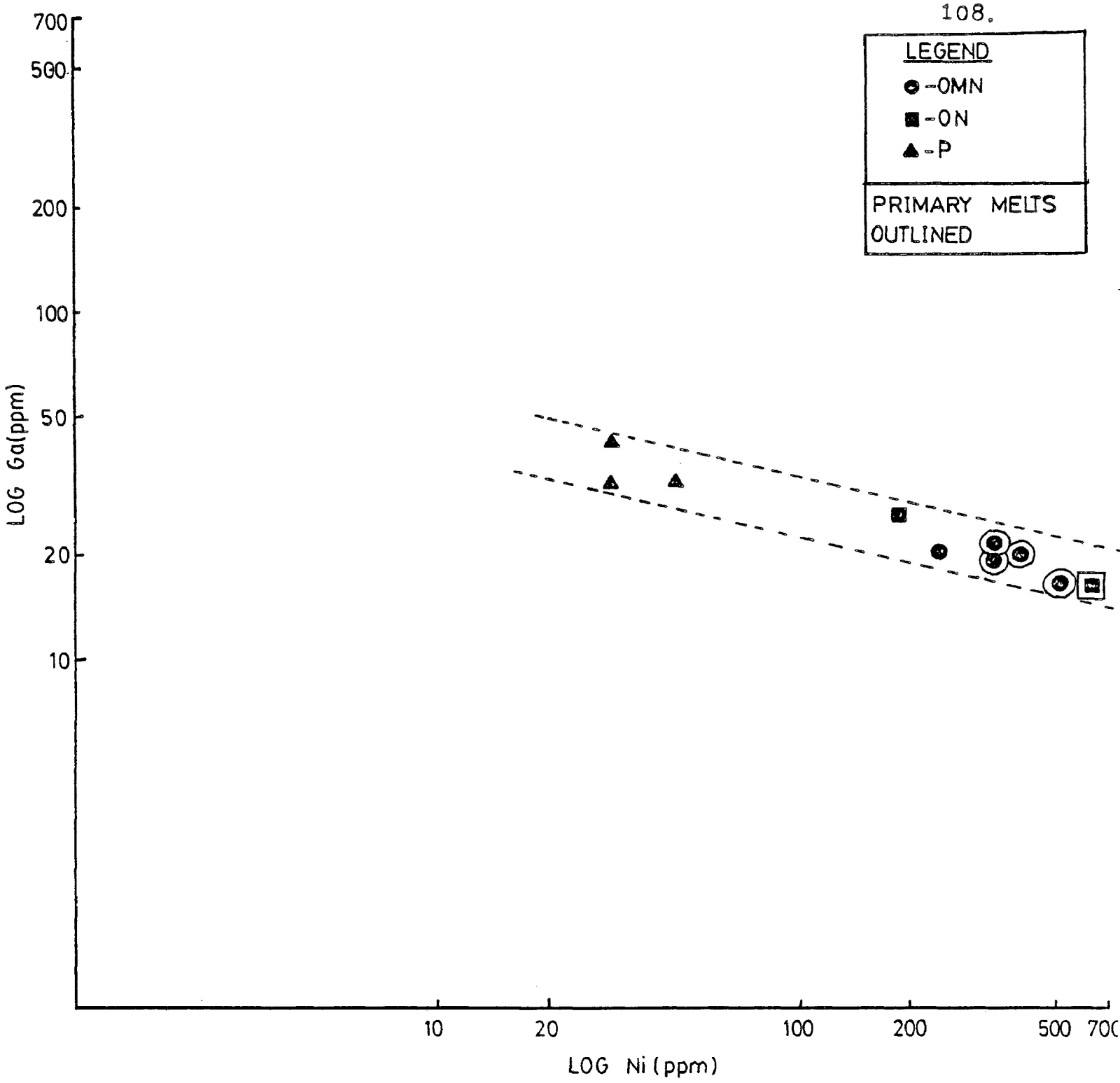

FIGURE 23 Log Ga vs. Log Ni for Balcones volcanic rocks (abbreviations: OMN- olivine melilite nephelinite, ON- olivine nephelinite, P- phonolite).

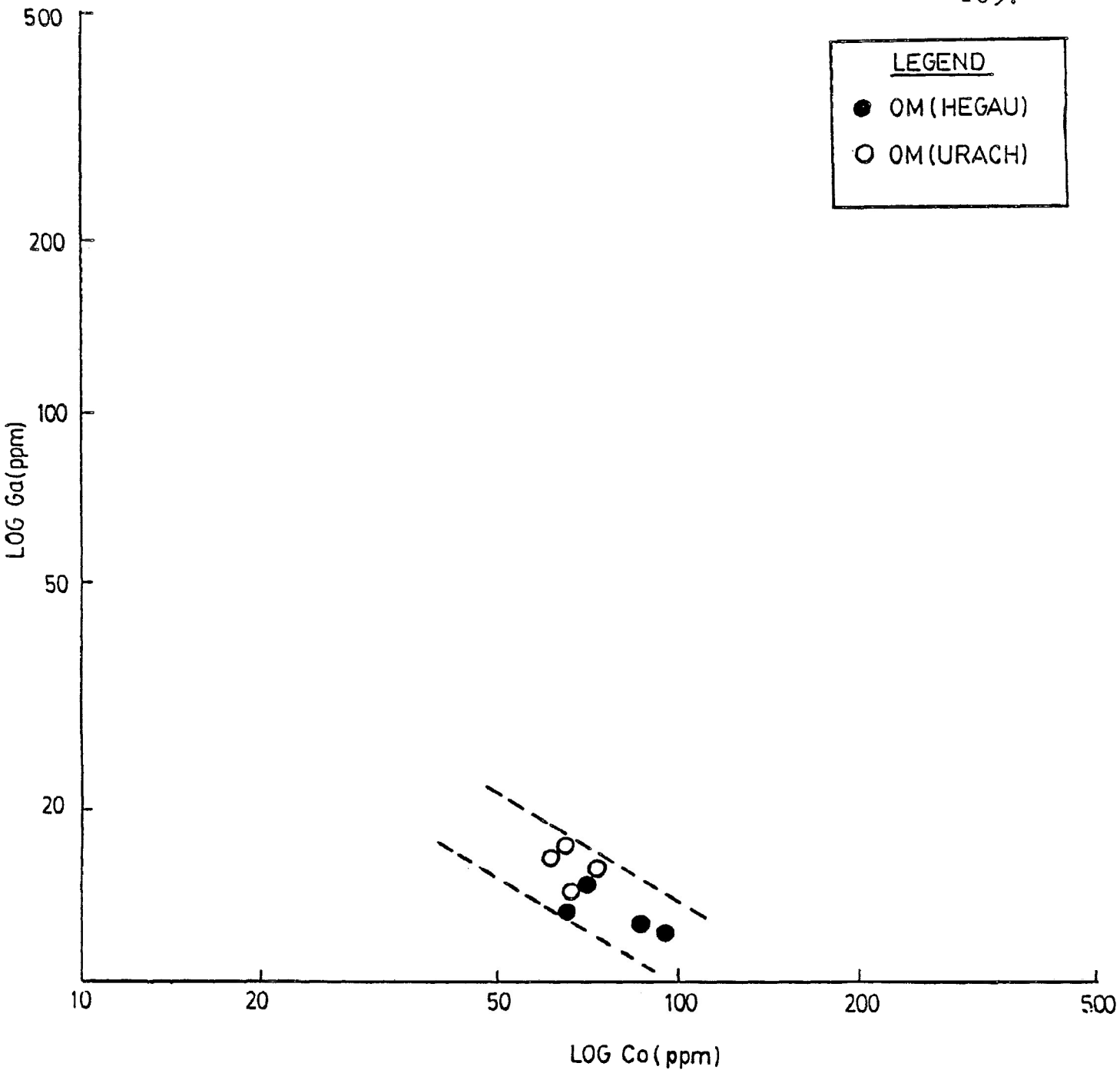

FIGURE 24 Log Ga vs. Log Co for Hegau and Urach volcanic rocks (abbreviation: OM- olivine melilitite).

exist between the abundances of Ga and the abundances of the incompatible (La, Th, Hf, Ta) trace elements (e.g., see Figures 19, 20, 21). Negative linear correlations exist between the abundances of Ga and the abundances of the compatible (Sc, Cr, Co, Ni) trace elements (e.g., see Figures 22, 23, 24) except for Ni in the Hegau and Urach rocks, for which a poorly defined positive correlation exists.

The data suggest Ga behaved as an incompatible trace element during the genesis of the rocks of the present study. The slopes of the lines of best fit defining the correlations between the abundances of Ga and the abundances of the other incompatible trace elements suggest that the bulk solid/liquid distribution coefficients for Ga during the genesis of these rocks were greater than those for La and Th (except for the Balcones Suite in which $D_{Ga}^{S/L} < D_{Th}^{S/L}$) and less than those for Hf and Ta.

5.6 Ga/Al RATIOS

5.6.1 Introduction

The geochemical coherence of Ga and Al during partial melting and fractional crystallization has been noted by many geochemists (e.g., Goldschmidt, 1937; Ringwood, 1955; Ahrens, 1965; De Argollo, 1974; De Argollo and Schilling, 1978) and can be attributed to the similarity of the ionic radii, valency and ionization potentials of the two elements.

De Argollo (1974) and De Argollo and Schilling (1978) have studied the Ga/Al ratios of different types of Hawaiian

basalts (alkalic, nephelinitic, and tholeiitic) and found that no systematic variations of the Ga/Al ratios could be assigned to distinct pressure regimes, or degrees of partial melting. As a result, they proposed (De Argollo and Schilling, 1978) that Ga/Al ratios in basalts might be used to infer mantle source Ga/Al ratios, to differentiate basalts derived from different mantle sources, and to map mantle heterogenities. In order to assess the validity of these proposals, the Ga/Al ratios of the mafic continental alkaline volcanic rocks of the present study were determined.

The Al contents of the rocks were determined by X-ray fluorescence spectrometry using a modification of the procedure described by Harvey *et al.* (1973). The Al data are believed correct to ±5% of the weight of Al present in each sample.

5.6.2 Freemans Cove Suite

The aluminum abundances and the Ga/Al ratios of the Freemans Cove volcanic rocks are given in Table 48.

Although considerable variation exists, the Al abundances of the Freemans Cove rocks correlate positively with the Ga abundances of the Freemans Cove rocks (Figure 25). The Ga x 10^4/Al weight ratios of the Freemans Cove rocks vary by approximately 20% from 2.28 ± 0.13 (sample BI-63, a basanite) to 2.86 ± 0.16 (sample BI-268, an olivine melilite nephelinite). The mean Ga x 10^4/Al weight ratio of the Freemans Cove rocks is 2.51 ± 0.14.

TABLE 48

Al Abundances and Ga/Al Ratios of the Freemans Cove Volcanic Rocks

Sample	Rock Type	Ga (ppm)	Al (wt.%)	Ga/Al x 10^4
BI-268	OMN	17.23 ± 0.44	6.02 ± 0.30	2.86 ± 0.16
BI-49	ON	16.54 ± 0.45	6.81 ± 0.34	2.43 ± 0.14
BI-84	ON	17.06 ± 0.48	6.93 ± 0.35	2.46 ± 0.14
BI-104	ON	16.53 ± 0.45	6.19 ± 0.31	2.67 ± 0.15
BI-245	ON	18.19 ± 0.46	6.57 ± 0.33	2.76 ± 0.15
BI-247	ON	16.46 ± 0.49	6.62 ± 0.33	2.49 ± 0.14
BI-4	B	15.85 ± 0.45	6.71 ± 0.34	2.36 ± 0.14
BI-63	B	16.07 ± 0.47	7.03 ± 0.35	2.28 ± 0.13
BI-75	B	18.22 ± 0.49	7.98 ± 0.40	2.29 ± 0.13
N2-13	B	17.31 ± 0.48	7.00 ± 0.35	2.47 ± 0.14
		Mean		2.51 ± 0.14
		Standard Deviation (1σ)		0.19

Abbreviations: OMN - olivine melilite nephelinite
ON - olivine nephelinite
B - basanite

Although considerable overlap exists in the Ga/Al ratios of the different rock types, the data for the primary melts (BI-268, BI-103, BI-247, BI-63) suggest the Ga/Al ratios of the Freemans Cove volcanic rocks decrease slightly with increasing degrees of partial melting.

5.6.3 Balcones Suite

The abundances and the Ga/Al ratios of the Balcones volcanic rocks are given in Table 49.

The Al abundances of the Balcones rocks positively correlate with the Ga abundances of the Balcones rocks (Fig.26).

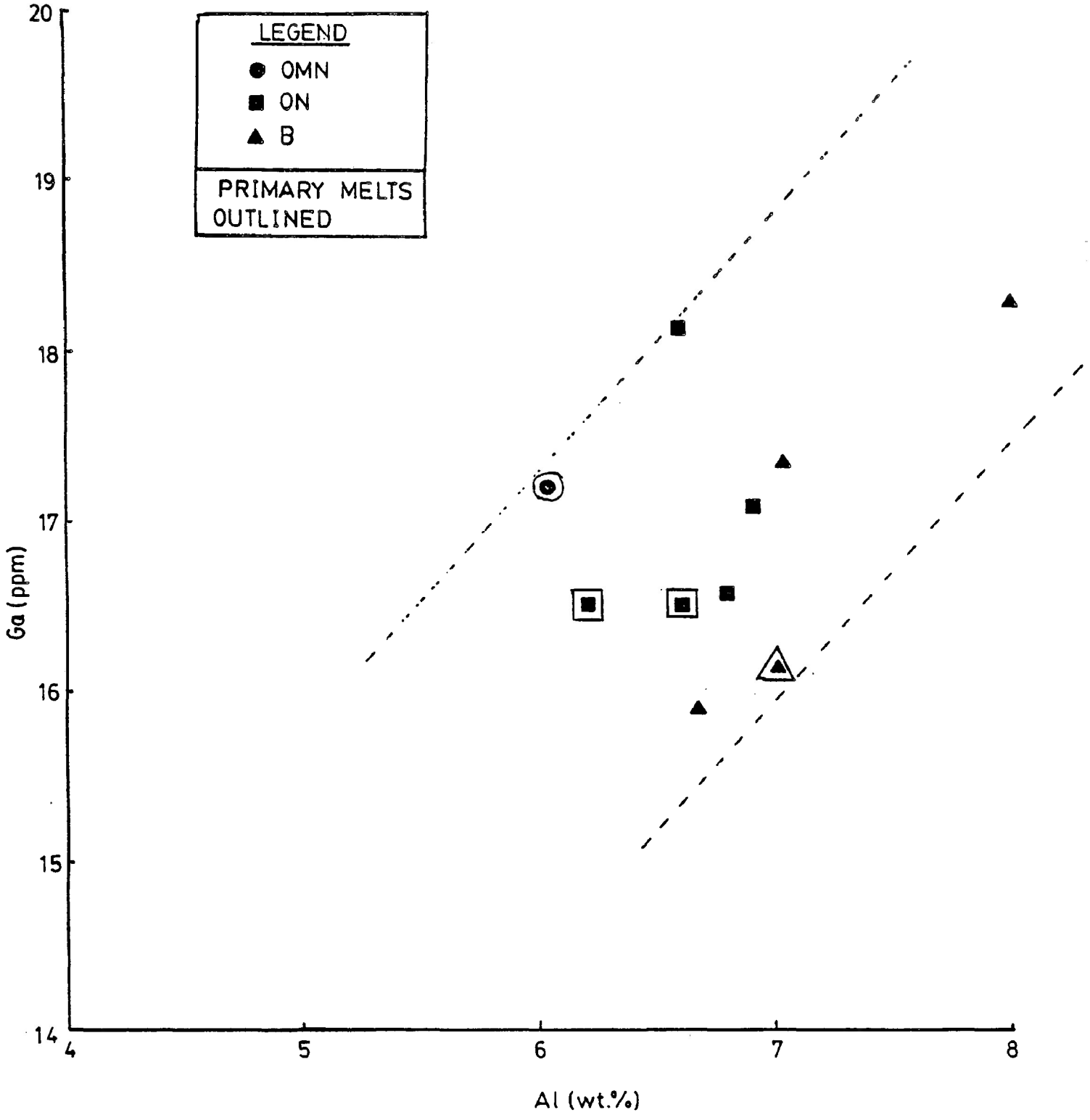

FIGURE 25. Ga vs. Al plot for the Freemans Cove volcanic rocks (abbreviations: OMN- olivine melilite nephelinite, ON- olivine nephelinite, B- basanite).

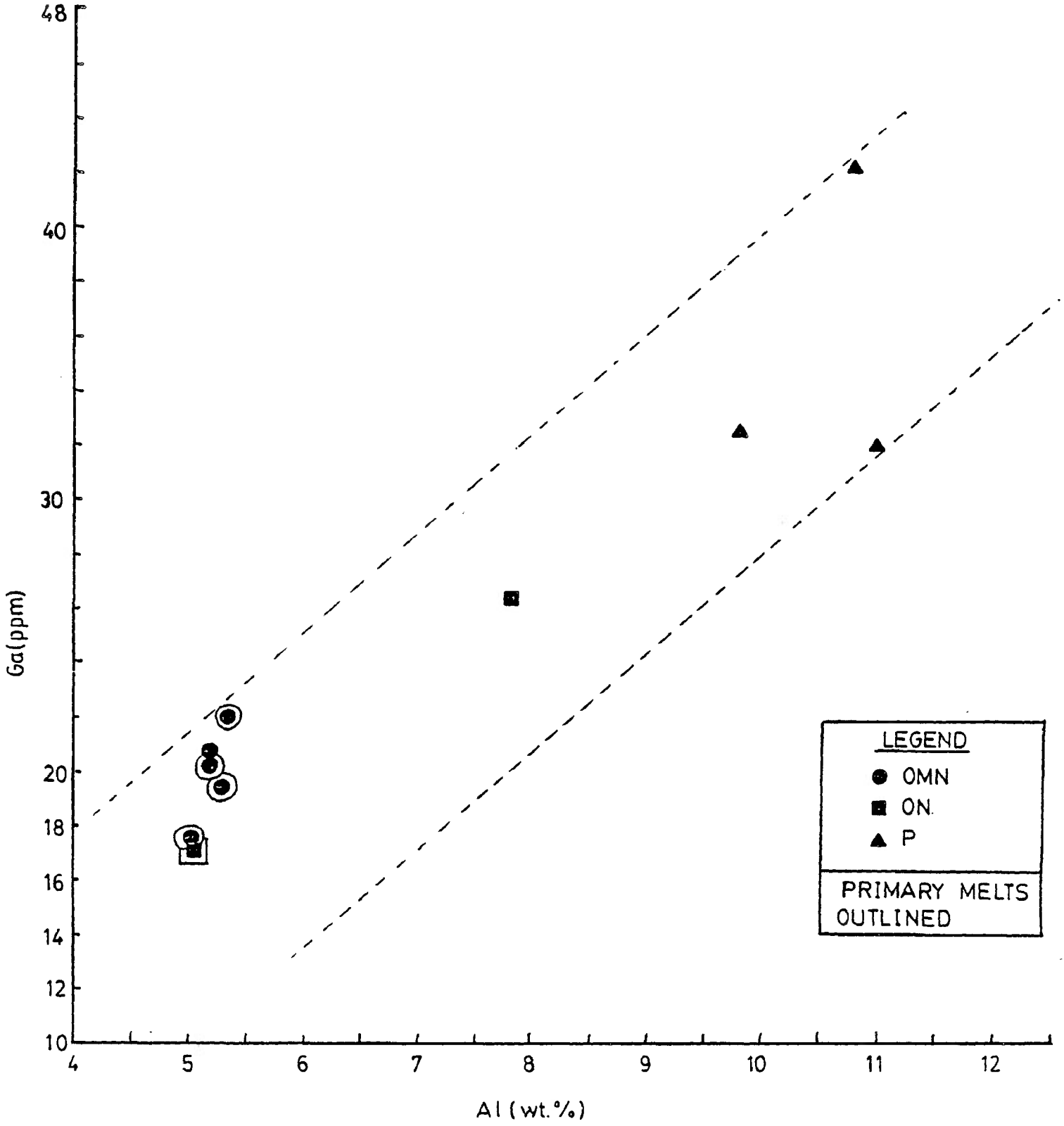

FIGURE 26. Ga vs. Al plot for the Balcones volcanic rocks (abbreviations: OMN- olivine melilite nephelinite, ON- olivine nephelinite, P- phonolite).

TABLE 49

Al Abundances and Ga/Al Ratios of the Balcones Volcanic Rocks

Sample	Rock Type	Ga (ppm)	Al (wt.%)	Ga/Al x 10^4
V2-5	OMN	22.02 ± 0.62	5.35 ± 0.27	4.12 ± 0.24
U2-1	OMN	20.29 ± 0.57	5.21 ± 0.26	3.89 ± 0.22
6-1	OMN	20.62 ± 0.60	5.21 ± 0.26	3.96 ± 0.22
V3-3	OMN	17.58 ± 0.47	5.03 ± 0.25	3.50 ± 0.20
6-3	OMN	19.40 ± 0.54	5.32 ± 0.27	3.65 ± 0.20
7-4	ON	26.26 ± 0.72	7.81 ± 0.39	3.36 ± 0.19
V1-2	ON	16.97 ± 0.48	5.06 ± 0.25	3.35 ± 0.19
V4-2	P	41.97 ± 1.20	10.84 ± 0.54	3.87 ± 0.22
7-7	P	31.07 ± 0.91	11.00 ± 0.55	2.82 ± 0.16
V5-1	P	35.52 ± 0.91	9.80 ± 0.49	3.32 ± 0.19
		Mean (all rocks)		3.58 ± 0.20
		Mean (mafic rocks only)		3.69 ± 0.21
Standard Deviation (1σ)		(all rocks)		0.19
		(mafic rocks only)		0.31

Abbreviations: OMN - olivine melilite nephelinite
ON - olivine nephelinite
P - phonolite

The Ga x 10^4 /Al weight ratios of the Balcones rocks vary by approximately 32% from 2.82 ± 0.16 (sample 7-7, a phonolite) to 4.12 ± 0.24 (sample V2-5, an olivine melilite nephelinite). The mean Ga x 10^4 /Al weight ratio of the Balcones rocks is 3.58 ± 0.20. The Ga x 10^4 /Al weight ratios of the Balcones rocks, excluding the phonolites, vary by approximately 19% from 3.35 ± 0.19 (sample V1-2, an olivine nephelinite) to 4.12 ± 0.24 (sample V2-5, an olivine melilite nephelinite). The mean Ga x 10^4 /Al weight ratio of the mafic

Balcones rocks, excluding the phonolites, is 3.69 ± 0.21. This value is significantly greater than the Ga x 10^4 /Al weight ratio of the Freemans Cove volcanic rocks (2.51 ± 0.14).

Although considerable overlap exists in the Ga x 10^4 /Al weight ratios of the different rock types, the data for the primary melts (V2-5, U2-1, V3-3, 6-3, V1-2) suggest that the Ga/Al ratios of these Balcones volcanic rocks decrease slightly with increasing degrees of partial melting.

5.6.4 Hegau and Urach Suites

The Al abundances and the Ga/Al ratios of the Hegau and Urach volcanic rocks are given in Table 50.

TABLE 50

Al Abundances and Ga/Al Ratios of the Hegau and Urach Rocks

Sample	Rock Type	Ga (ppm)	Al (wt.%)	Ga/Al x 10^4
Hegau				
HEG-3	OM	12.14 ± 0.32	5.51 ± 0.28	2.20 ± 0.11
HEG-4	OM	12.43 ± 0.35	5.63 ± 0.28	2.21 ± 0.12
HEG-6	OM	14.82 ± 0.44	5.76 ± 0.29	2.57 ± 0.15
HEG-7	OM	12.73 ± 0.33	5.66 ± 0.28	2.25 ± 0.13
		Mean		2.31 ± 0.13
		Standard Deviation (1σ)		0.15
Urach				
U-1	OM	17.00 ± 0.49	4.54 ± 0.23	3.74 ± 0.22
U-4	OM	15.72 ± 0.45	4.45 ± 0.22	3.53 ± 0.20
U-7	OM	17.33 ± 0.51	4.29 ± 0.21	4.04 ± 0.23
U-16	OM	14.20 ± 0.42	4.10 ± 0.21	3.46 ± 0.20
		Mean		3.69 ± 0.22
		Standard Deviation (1σ)		0.23

Abbreviation: OM - olivine melilitite

The Ga and Al data for the Hegau and Urach rocks define two separate trends on a Ga vs. Al plot (Figure 27). The Al abundances of the Hegau rocks correlate positively with the Ga abundances of the Hegau rocks (Figure 27). The Ga x 10^4 /Al weight ratios of the Hegau rocks vary by approximately 14% from 2.20 ± 0.12 (sample HEG-3) to 2.57 ± 0.14 (sample HEG-6). The mean Ga x 10^4/Al weight ratio of the Hegau rocks is 2.31 ± 0.13. This value is similar to the mean Ga x 10^4 /Al weight ratio of the Freemans Cove rocks (2.51 ± 0.14) but is significantly lower than the mean Ga x 10^4/Al weight ratio of the Balcones rocks (3.58 ± 0.20).

The Al abundances of the Urach rocks correlate positively with the Ga abundances of the Urach rocks (Figure 27). The Ga x 10^4 /Al weight ratios of the Urach rocks vary by approximately 14% from 3.46 ± 0.20 (sample U-16) to 4.04 ± 0.23 (sample U-7). The mean Ga x 10^4 /Al weight ratio of the Urach rocks is 3.69 ± 0.22. This value is similar to the mean Ga x 10^4 /Al weight ratio of the Balcones rocks (3.58 ± 0.20) but is significantly higher than the mean Ga x 10^4 /Al weight ratios of the Freemans Cove rocks (2.51 ± 0.14) and the Hegau rocks (2.31 ± 0.13).

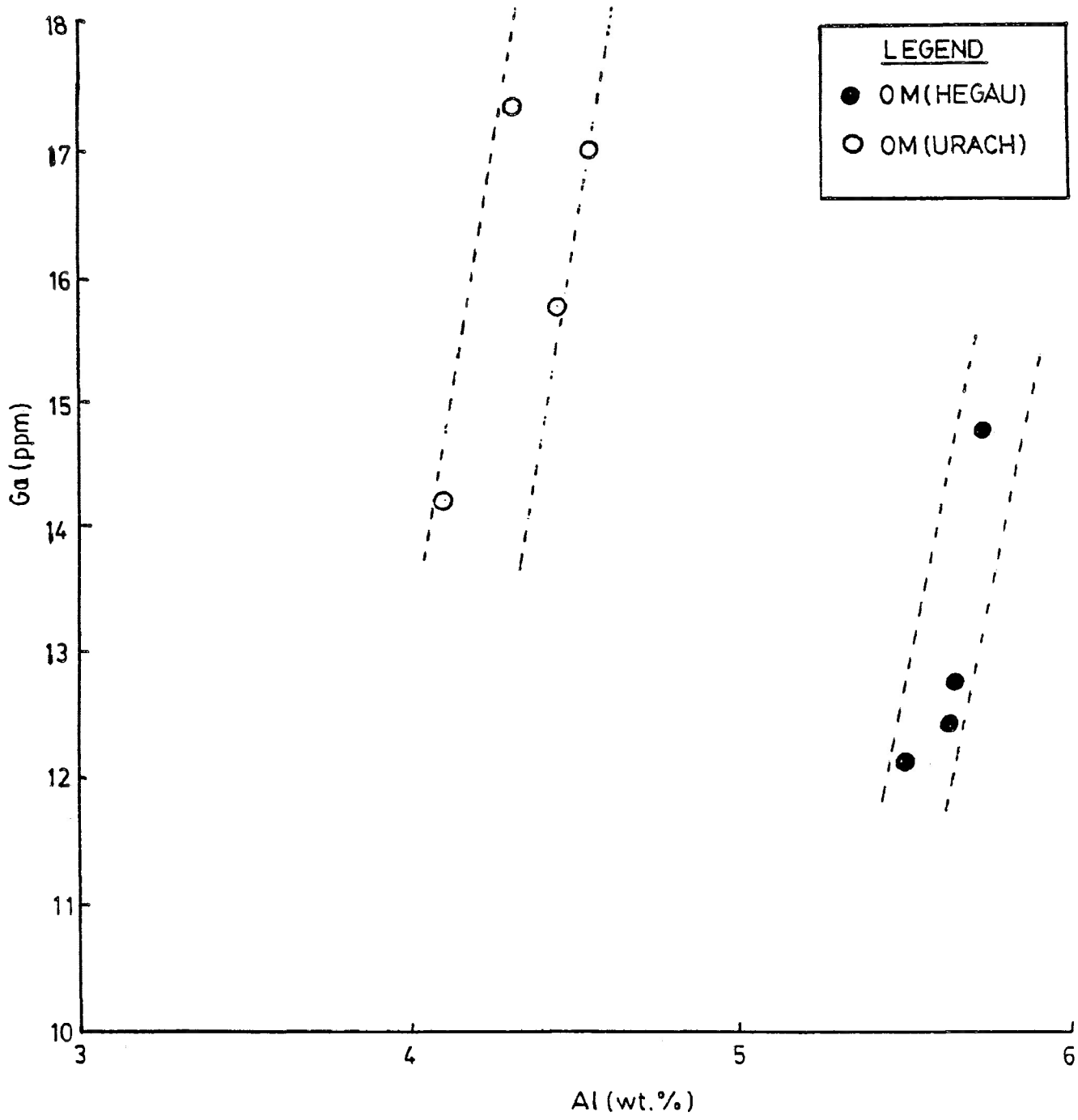

FIGURE 27. Ga vs. Al plot for Hegau and Urach volcanic rocks (abbreviation: OM- olivine melilitite).

5.7 COMPARISONS WITH Ga ABUNDANCES AND Ga/Al RATIOS OF MAFIC OCEANIC VOLCANIC SUITES

5.7.1 Results of Previous Studies of Mafic Oceanic Volcanic Suites

5.7.1.1 Mid-oceanic Ridge Basalts

De Argollo (1974) has studied the abundances of Ga in mid-oceanic ridge basalts (MORBs) from the Reykjanes Ridge south of Iceland. The abundance of Ga in the MORBs studied varies from 16.4 ppm to 18.5 ppm and average 17.5 ppm (De Argollo, 1974). The Ga x 10^4 /Al weight ratio of the MORB samples varies by approximately 15% from 1.97 ± 0.12 to 2.33 ± 0.14 (mean 2.16 ± 0.13).

5.7.1.2 Back-Arc Basalts

Saunders and Tarney (1979) have determined the abundance of Ga in basalts from a back-arc spreading center in the East Scotia Sea. The abundance of Ga in these basalts varies from 12 ppm to 19 ppm and average 16 ppm. The Ga x 10^4 /Al weight ratio of the back-arc basalts (BAB) varies by approximately 41% from 1.37 to 2.32 (mean 1.80).

5.7.1.3 Oceanic Island Basalts

5.7.1.3.1 Iceland

De Argollo (1974) has studied the abundance of Ga in tholeiitic basalts from Iceland. The abundance of Ga in these oceanic island basalts (OIBs) varies from 19.1 ppm to 23.6 ppm and averages 21.3 ppm (De Argollo, 1974). The Ga x 10^4/Al weight ratio of these OIBs varies by approximately 24%

from 2.17 ± 0.13 to 2.85 ± 0.17 (mean 2.59 ± 0.16).

5.7.1.2.2 Hawaii

De Argollo (1974) and De Argollo and Schilling (1978 (a,b)) have studied the abundance of Ga in nephelinitic, alkalic, and tholeiitic basalts from Hawaii. The abundance of Ga in these Hawaiian OIBs varies from 18.2 ppm to 27.1 ppm and averages 22.2 ppm. The Ga x 10^4 /Al weight ratio of the Hawaiian OIBs varies by approximately 61% from 2.54 ± 0.15 to 4.08 ± 0.24 (mean 3.02 ± 0.18).

5.7.2 Comparisons of Ga Abundances and Ga/Al Ratios

The Ga abundances and Ga/Al ratios of the mafic continental alkaline volcanic suites of the present study are compared to the Ga abundances and Ga/Al ratios of the mafic oceanic volcanic suites studied by De Argollo (1974) and Saunders and Tarney (1979) in Table 51.

The ranges in the abundances of Ga and Al in these volcanic suites are illustrated in Figure 28.

The abundance of Ga in the rocks comprising the different mafic volcanic suites varies by a factor of approximately 2 from 12.14 ± 0.32 ppm (an olivine melilitite from Hegau) to 25.0 ± 1.5 ppm (a melilite nepheline basalt from Hawaii). Considerable overlap exists between the ranges in Ga abundances for the different suites (Figure 28) despite the fact that the suites were formed under very different conditions in very different tectonic settings. The Hegau suite is slightly depleted in Ga (mean abundance of 13.03 ± 0.40 ppm), and the Hawaiian and Icelandic suites are slightly

TABLE 51

Comparisons of Ga Abundances and Ga/Al Ratios

Rock Type	Locality	Data Source	Ga Abundances	
			Range	Mean
CAV	Freemans Cove	Present Study	15.85±0.45–18.22±0.49	16.95±0.47
CAV	Balcones	" "	16.97±0.48–26.26±0.72	20.45±0.58
CAV	Hegau	" "	12.14±0.32–14.82±0.44	13.03±0.40
CAV	Urach	" "	14.2010.42–17.33±0.51	16.06±0.48
MORB	Reykjanes Ridge	De Argollo (1974)	16.4±0.8 – 18.5±0.9	12.5±0.9
BAB	East Scotia Sea	Saunders and Tarney (1979)	12±0.7 – 19±1.5	16±1.3
OIB	Iceland	De Argollo (1974)	19.1±1.1 – 23.6±1.4	21.3±1.3
OIB	Hawaii	DeArgollo and Schilling(1978)	18.2±1.1 – 25.0±1.5	21.1±1.3
			Ga/Al x 10^4	
CAV	Freemans Cove	Present Study	2.28±0.13 – 2.86±0.16	2.51±0.14
CAV	Balcones	" "	3.35±0.19 – 4.12±0.24	3.69±0.21
CAV	Hegau	" "	2.20±0.12 – 2.57±0.13	2.31±0.13
CAV	Urach	" "	3.46±0.20 – 4.04±0.23	3.69±0.22
MORB	Reykjanes Ridge	De Argollo (1974)	1.97±0.12 – 2.33±0.14	2.16±0.13
BAB	East Scotia Sea	Saunders and Tarney (1979)	1.37±0.14 – 2.32±0.23	1.80±1.18
OIB	Iceland	De Argollo (1974)	2.17±0.13 – 2.85±0.17	2.59±0.16
OIB	Hawaii	De Argollo and Schilling(1978)	2.54±0.15 – 4.08±0.24	3.20±0.18

Abbreviations: CAV – continental alkaline volcanics
MORB – mid-oceanic ridge basalts
BAB – back-arc basalts
OIB – oceanic island basalts

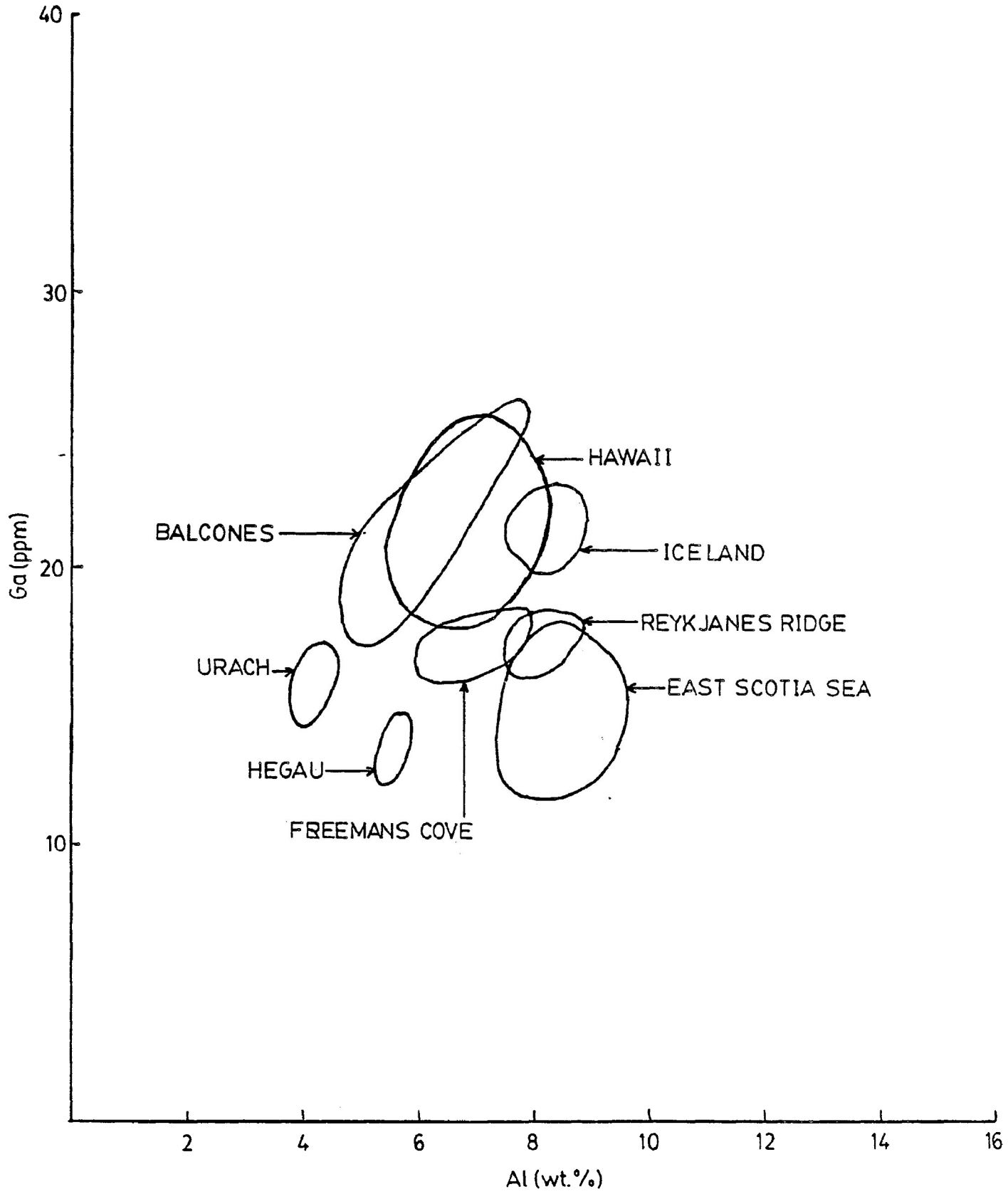

FIGURE 28. Ga vs. Al plot for different mafic volcanic suites. Data for Hawaii, Iceland, and Reykjanes Ridge from DeArgollo(1974); data for the East Scotia Sea from Saunders and Tarney(1979).

enriched in Ga (mean abundances of 21.1 ± 1.3 ppm and 21.3 ± 1.3 ppm respectively) relative to the other suites.

The Ga x 10^4 /Al weight ratios of the rocks comprising the different suites vary by a factor of approximately 3.0 from 1.37 ± 0.14 (a basalt from the East Scotia Sea) to 4.12 ± 0.24 (an olivine melilite nephelinite from Balcones). Considerable overlap exists between the ranges in Ga x 10^4 /Al weight ratios for some of the suites, for example, the Freemans Cove and Iceland suites (mean Ga x 10^4 /Al weight ratios of 2.51 ± 0.14 and 2.59 ± 0.16 respectively), the Balcones and Urach suites (mean Ga x 10^4 /Al weight ratios of 3.69 ± 0.21 and 3.69 ± 0.22 respectively), and the Hegau and Reykjanes Ridge suites (2.31 ± 0.13 and 2.16 ± 0.13 respectively).

If Ga/Al ratios in basalts can be used to infer the composition of their mantle sources (as proposed by De Argollo and Schilling (1974, 1978) and supported by the results of the present study), then the similarities in the mean Ga x 10^4 /Al weight ratios of the suites compared above may reflect compositional similarities in the mantle sources of these suites, at least with respect to Ga and Al.

5.8 CONCLUSIONS

1. Ga positively correlates with Al in the continental alkaline volcanic rocks studied.
2. The abundance of Ga in the continental alkaline volcanic rocks studied varies by a factor of approximately 3.5

from 12.14 ± 0.32 ppm (an olivine melilitite of the Hegau suite) to 41.97 ± 1.20 ppm (a phonolite of the Balcones suite). The abundance of Ga in the mafic alkaline volcanic rocks studied (excluding the Balcones phonolites) varies by a factor of approximately 2.2 from 12.14 ± 0.32 ppm (an olivine melilitite of the Hegau suite) to 26.26 ± 0.72 ppm (an olivine nephelinite of the Balcones suite).

3. Intrasuite variations in the abundance of Ga in the mafic continental alkaline volcanic suites studied range from approximately 15% (Freemans Cove suite) to approximately 54% (Balcones suite).

4. Ga behaved as an incompatible trace element during the genesis of the continental alkaline volcanic suites studied. Comparisons between Ga abundances and other incompatible trace element abundances suggest the bulk solid/liquid distribution coefficients for Ga during the genesis of these suites were greater than those for La and Th and less than those for Hf and Ta.

5. Considerable overlap exists between the abundance of Ga in the different mafic continental alkaline volcanic suites studied. The Hegau suite is slightly depleted in Ga relative to the other suites.

6. Ga/Al ratios of primary melts from the Freemans Cove and Balcones suites decrease slightly (from 2.86 ± 0.16 to 2.28 ± 0.13, and from 4.12 ± 0.24 to 3.35 ± 0.19 respectively) with increasing degrees of partial melting.

7. Ga/Al ratios of the Balcones rocks decrease slightly with increasing degrees of differentiation (e.g., the mean Ga x 10^4 /Al weight ratio of the mafic Balcones rocks is 3.69 ± 0.21 and the mean Ga x 10^4 /Al weight ratio of the felsic Balcones rocks is 3.34 ± 0.19).

8. Intrasuite variations in the Ga/Al ratios of the mafic continental alkaline volcanic rocks studied range from 14% (Hegau and Urach suites) to 20% (Freemans Cove suite). These small intrasuite variations support De Argollo and Schilling's (1978) proposals that Ga/Al ratios of basalts might be used to infer the Ga/Al ratios of the mantle sources of the basalts, and to map mantle heterogeneities.

9. The mean Ga x 10^4 /Al weight ratios of the following mafic continental and oceanic volcanic suites are similar:

   a) Freemans Cove (2.51 ± 0.14) and Iceland (2.59 ± 0.16);

   b) Balcones (3.69 ± 0.21) and Urach (3.69 ± 0.22);

   c) Hegau (2.31 ± 0.13) and Reykjanes Ridge (2.16 ± 0.13.

   If Ga/Al ratios in basalts reflect mantle source Ga/Al ratios, then the similarities in the mean Ga x 10^4 /Al weight ratios of the pairs of suites above may reflect compositional similarities in the mantle sources of these suites, at least with respect to Ga and Al.

10. The mean Ga x 10^4 /Al weight ratios of the Hegau and

Urach suites (2.31 ± 0.13 and 3.69 ± 0.22 respectively) are significantly different even though Hegau and Urach are geographically close. If Ga/Al ratios in basalts reflect mantle source Ga/Al ratios, then this difference may reflect compositional differences in the mantle sources to these suites, at least with respect to Ga and Al.

11. Considerable overlap exists between the abundances of Ga in the different types of basalts (alkalic, nephelinite, and tholeiitic) compared in the present study despite the fact that these basalts were formed under different conditions in very different tectonic settings.

CHAPTER SIX

APPLICATION OF GALLIUM DATA TO TRACE ELEMENT MELTING MODELS

6.1 INTRODUCTION

Trace element behaviour during partial melting is not fully understood. Attempts to explain and predict trace element behaviour during partial melting have resulted in the development of numerous mathematical models (e.g., Gast, 1968; Shaw, 1970; Hertogen and Gijbels, 1976; Shaw, 1977; Langmuir *et al.*, 1978). All of these models incorporate trace element distribution coefficients (the theory of trace element distribution coefficients and their application to geology are discussed by McIntire, 1963, and Arth, 1976) and are based on equations developed by Rayleigh (1896), Schilling and Winchester (1967), and Gast (1968). Examples of how trace element melting models may be used to help solve problems of petrology are given by Allegre and Minster (1978), Minster and Allegre (1978), and Clague and Frey (1982).

Although considerable progress has been made in recent years concerning the development of trace element melting models and their application to solving problems of petrology, many difficulties still exist. For example, our present knowledge of distribution coefficients is imperfect (Shaw, 1977). In general, the numerical values presently available for distribution coefficients are of questionable

validity. At best they are thought only to approximate true values (Allegre and Minster, 1978). In addition, it is presently not possible to adjust quantitatively distribution coefficients for variations in temperature, pressure, and composition. As a result, distribution coefficients determined for one system are probably not applicable to other systems unless the conditions of temperature, pressure, and composition are identical in each. This is unlikely and would probably be impossible to prove. Another difficulty arises from the fact that the phase petrology of melting is actually much more complex than depicted by the simplified mathematical models (Shaw, 1977).

At best, trace element melting models can only be used, in conjunction with other geological information, to determine a) the *possibility* of a genetic relationship between the members of an igneous rock suite, b) the *possible* magmatic processes which may have acted to produce the rock suite, and c) estimates of *possible* constraints for the parameters (i.e. source geochemistry, bulk distribution coefficients, degrees of melting, etc.) associated with the genesis of the suite. Many combinations of models and parameter values may satisfy the available trace element data. In general, it is usually impossible to determine which models or parameter values are true.

6.2 PREVIOUS ESTIMATES OF Ga DISTRIBUTION COEFFICIENTS

Very few estimates of Ga distribution coefficients (i.e., mineral/melt distribution coefficients and bulk-solid/melt distribution coefficients) have been published. All available estimates (e.g., Goodman, 1972; De Argollo and Schilling, 1978 (a,b); Frey *et al.*, 1985) are based on studies of natural systems. Estimates based on analyses of artificial samples created under controlled experimental conditions could not be found in the available literature (i.e., Chemical Abstracts, Mineralogical Abstracts, Geochimica et Cosmochimica Acta, Contributions to Mineralogy and Petrology, Journal of Petrology).

6.2.1 Ga Mineral/Melt Distribution Coefficients

Goodman (1972) measured Ga phenocryst/melt distribution coefficients ($D_{Ga}^{phenocryst/melt}$) in a large variety of mafic volcanic rocks from Hawaii, Iceland, Azores, and Jaun Fernandez Islands. Goodman (1972) found that $D_{Ga}^{plagioclase/melt}$ values in these rocks vary from 0.84 to 1.27 (mean 0.98), $D_{Ga}^{cpx/melt}$ values vary from 0.30 to 0.58 (mean 0.41), and $D_{Ga}^{olivine/melt}$ values vary from 0.04 t 0.05 (mean 0.04).

De Argollo and Schilling (1978(b)) used the abundance of Ga in garnet and clinopyroxene from a Roberts Victor Mine eclogite to estimate $D_{Ga}^{garnet/melt}$ to be 0.39 and $D_{Ga}^{cpx/melt}$ to 0.41 during high pressure fractional crystallization of this type of eclogite.

6.2.2 Ga Bulk-Solid/Melt Distribution Coefficients

De Argollo and Schilling (1978(a)) used a variety of mathematical models in attempts to estimate the Ga bulk-solid /melt distribution coefficient during the genesis of a suite of Hawaiian alkaline volcanic rocks. De Argollo and Schilling (1978(a)) found that their estimates of the Ga bulk-solid/melt distribution coefficient for this suite varied from 0.27 to 0.95 depending on the mathematical model used. The lower estimates (i.e., 0.27 to 0.59) were obtained using equations which incorporated the Ga mineral/melt distribution coefficients given by Goodman (1972). The higher estimates (i.e., 0.75 to 0.95) were obtained using equations which did not incorporate Goodman's (1972) Ga mineral/melt distribution coefficients. De Argollo and Schilling (1978(a)) state that the discrepancies between the different estimates emphasize the need for Ga mineral/melt distribution coefficient determinations under various temperature, pressure, and melt compositions. De Argollo and Schilling (1978(a)) emphasize that actual observations of the abundance of Ga in the Hawaiian rocks indicate that the abundance of Ga changes only slightly during shallow depth fractional crystallization of the olivine gabbro type, and that the Ga bulk-solid/melt distribution coefficient during the genesis of these rocks was indeed less than, but close to, unity. Accordingly, De Argollo and Schilling (1978(b)) give an average estimate for the Ga bulk-solid/melt distribution coefficient during the genesis of the Hawaiian alkaline volcanic rocks of 0.75.

Frey *et al.* (1985) used two methods, one incorporating Goodman's (1972) Ga mineral/melt distribution coefficients, to estimate the Ga bulk-solid/melt distribution coefficient during the genesis of the Rhonda peridotite. The estimates obtained using each technique were identical yielding a value of 0.12.

Clague and Frey (1982) measured (by X-ray fluorescence) the abundance of Ga in a limited number of mafic volcanic rocks from Honolulu and concluded that the Ga bulk-solid/melt distribution coefficient during the genesis of these rocks was greater than unity (i.e., Ga behaved as a compatible trace element). Clague and Frey (1982) did not try to calculate a numerical value for this Ga bulk-solid/melt distribution coefficient.

6.3 TRACE ELEMENT MODELLING APPROACH

Interpretation of the Ga data obtained in the present study is based on equilibrium mass-balance equations for simple single stage modal batch melting. During modal batch melting, the solid and liquid phases remain in constant equilibrium as melting proceeds and the minerals melt in the proportions in which they occur in the original solid. This model was chosen for use, not because it is believed that there is no variation in the modal composition of the residual solid, but mainly to reduce the number of variable parameters because neither the $D_{Ga}^{mineral/melt}$ values (e.g., $D_{Ga}^{phlogopite/melt}$) nor the modal compositions of the residual

solids are precisely known.

The basic equation used to describe trace element behaviour during modal batch melting was developed by Shaw (1970):

$$C_L/C_o = 1/(D_o+F(1-D_o)) \quad \text{(Shaw, 1970, equation (11))} \quad (3)$$

where: C_L = the concentration of a trace element in the derived liquid;

C_o = the initial concentration of a trace element in the solid, i.e. the source rock, before partial melting;

F = the degree of partial melting;

D_o = the initial bulk-solid/liquid partition coefficient, given by $X_o^{\alpha} D^{\alpha/l} + X_o^{\beta} D^{\beta/l} + ...$, where X_o^{α}, X_o^{β} ...., are the weight fractions of phases α, β. .., in the initial solid and the individual-mineral/liquid distribution coefficients, i.e. $\frac{\text{concentration of element in mineral}}{\text{concentration of element in liquid}}$.

Possible constraints for the initial Ga bulk-solid/melt distribution coefficients ($D_{Ga}^{\text{bulk-solid/melt}}$) and the degrees of melting (F) associated with the genesis of the primary melts of the present study will be developed by assigning values to C_o (i.e., C_o = 4.2 ppm Ga and 6.6 ppm Ga, corresponding to 100% garnet lherzolite based pyrolite and 100% spinel lherzolite based pyrolite source compositions respectively) and comparing the ranges in model-derived C_L values to the measured ranges in the abundance of Ga in the primary melts. Since Sun and Hansen (1975) determined that the range

of melting associated with the genesis of Antarctic nephelinites was 3% to 7%, F will be restricted to the range 1% to 10% in the model calculations.

6.4 POSSIBLE CONSTRAINTS FOR Ga BULK-SOLID/MELT DISTRIBUTION COEFFICIENTS

The ranges in the abundance of Ga in the primary melts of the present study are compared to model-derived C_L values in Figures 29 to 36. The ranges in $D_{Ga}^{bulk-solid/melt}$ and F that correspond to ranges in C_L comparable to the observed ranges in the abundance of Ga in the primary melts are given in Table 52.

TABLE 52

Possible Constraints for $D_{Ga}^{bulk-solid/melt}$ and F

Primary Melts	C_o = 4.2 ppm Ga		C_o = 6.6 ppm Ga	
	$D_{Ga}^{bulk-solid/melt}$	F(%)	$D_{Ga}^{bulk-solid/melt}$	F(%)
Freemans Cove	0.18-0.24	8-10, 1-3	0.35 - 0.38	5-10, 1-5
Balcones	0.16-0.18	3.5-10, 1-8	0.29*- 0.32*	1-10*,1-10*
Hegau	0.27-0.28	1-10, 1-10	0.43*- 0.49*	1-10*,1-10*
Urach	0.21-0.23	4-10, 1-9	0.37*- 0.41*	1-10*,1-10*

* Model-derived C_L values do not duplicate the entire range of observed Ga abundances.

The measured ranges for the abundance of Ga in the primary melts can all be duplicated by ranges in model-derived C_L values calculated using the garnet lherzolite based pyrolite source composition estimate (i.e., C_o = 4.2 ppm

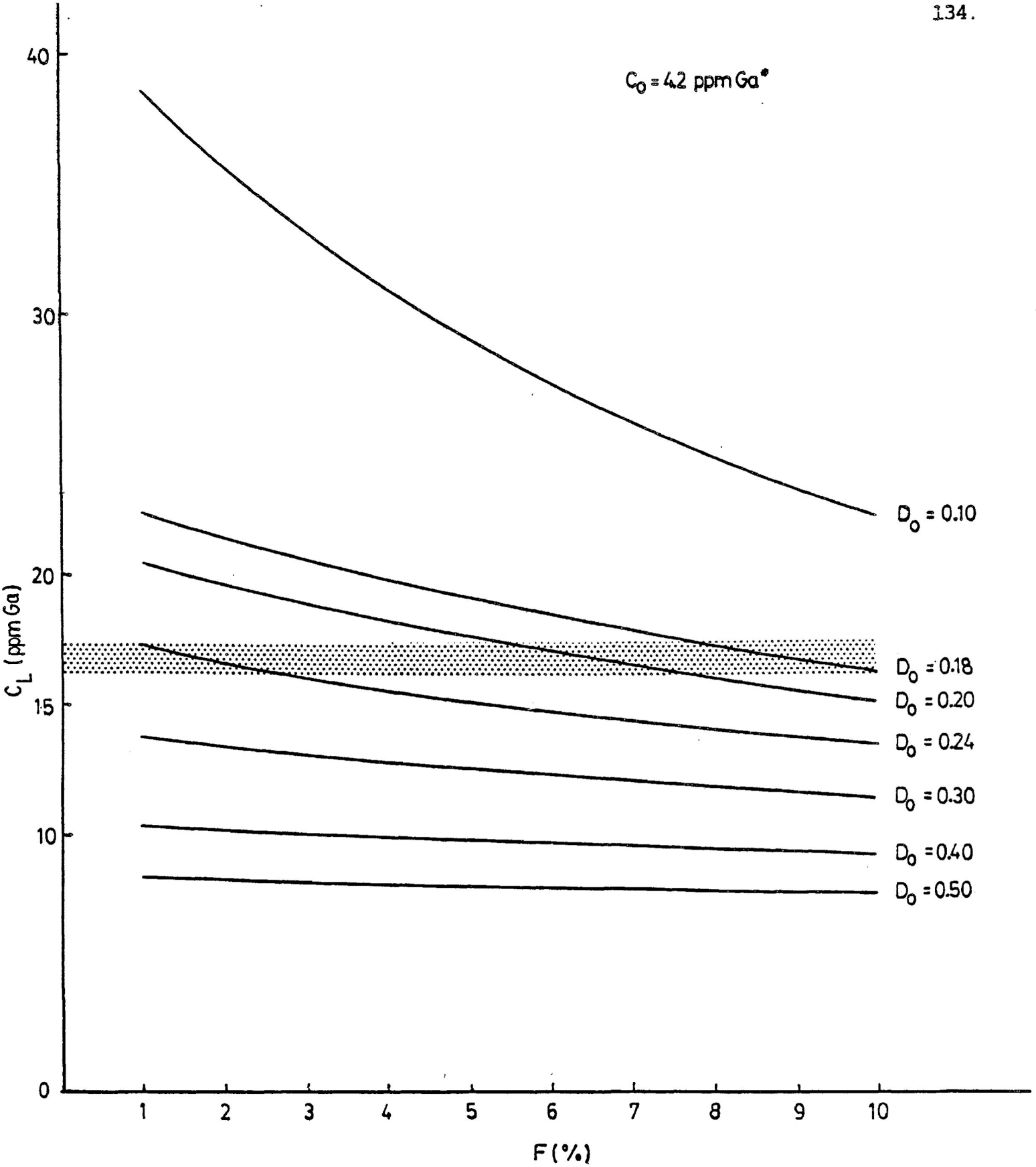

Figure 29. C_L vs. F plot for modal batch melting model. Stippled region defines the range in the abundance of Ga in the Freemans Cove primary melts (i.e., 16.07 to 17.23 ppm). * garnet lherzolite based pyrolite estimate of the present study.

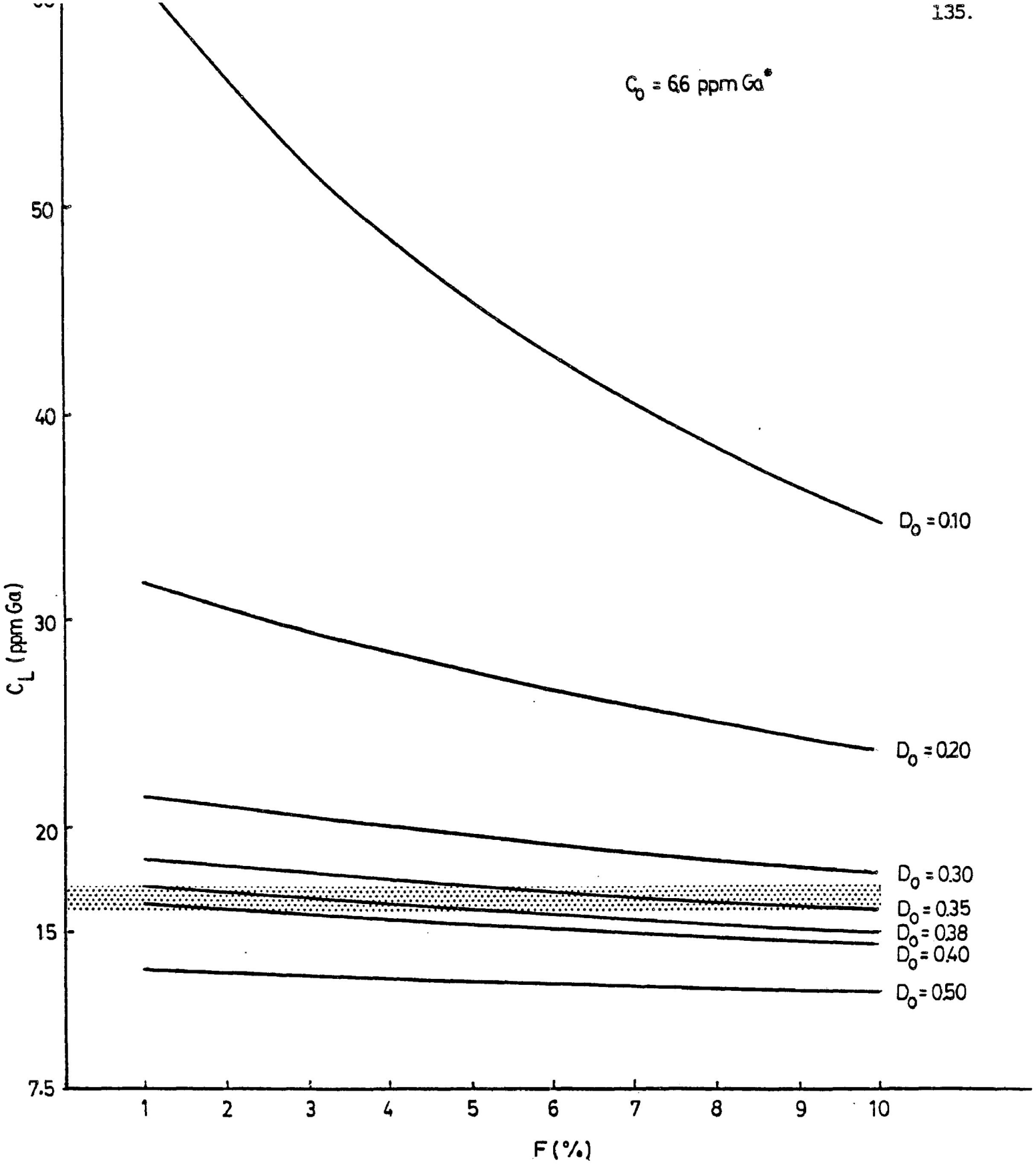

Figure 30. C_L vs. F plot for modal batch melting model. Stippled region defines the range in the abundance of Ga in the Freemans Cove primary melts (i.e., 16.07 to 17.23 ppm). * spinel lherzolite based pyrolite estimate of the present study.

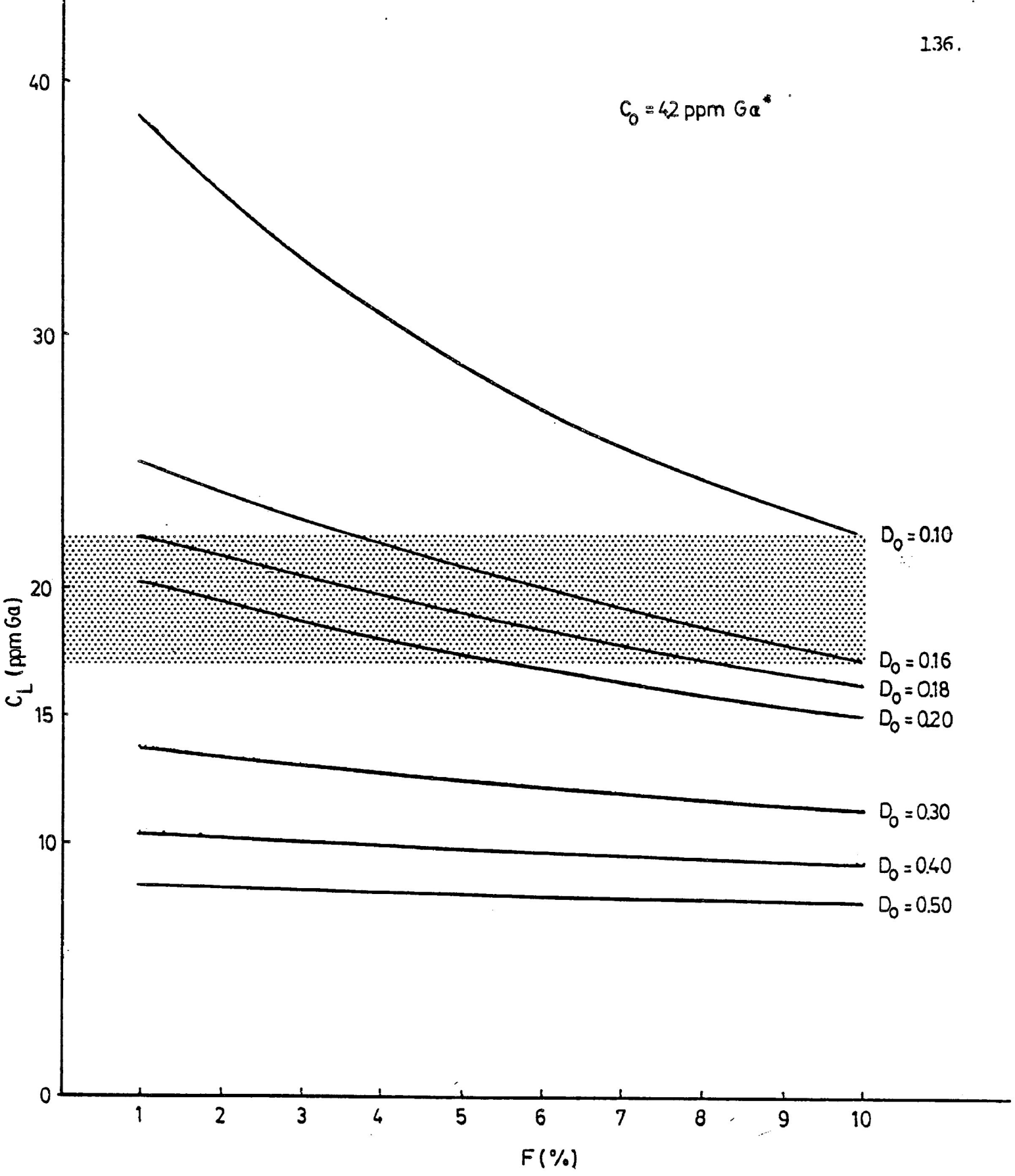

Figure 31. C_L vs. F plot for modal batch melting model. Stippled region defines the range in the abundance of Ga in the Balcones primary melts (i.e., 16.97 to 22.02 ppm). * garnet lherzolite based pyrolite estimate of the present study.

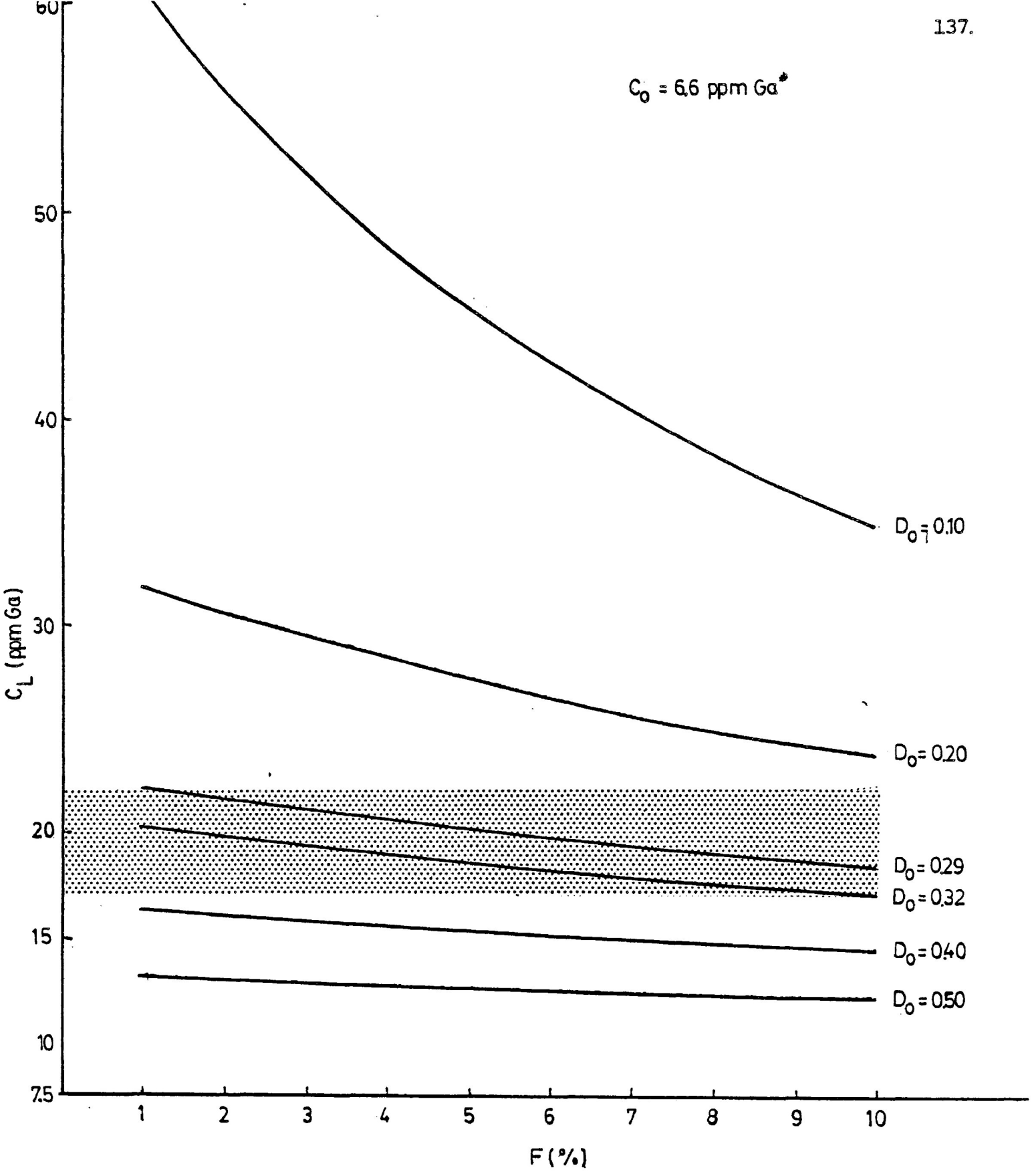

Figure 32. C_L vs. F plot for modal batch melting model. Stippled region defines the range in the abundance of Ga in the Balcones primary melts (i.e., 16.97 to 22.02 ppm). * spinel lherzolite based pyrolite estimate of the present study.

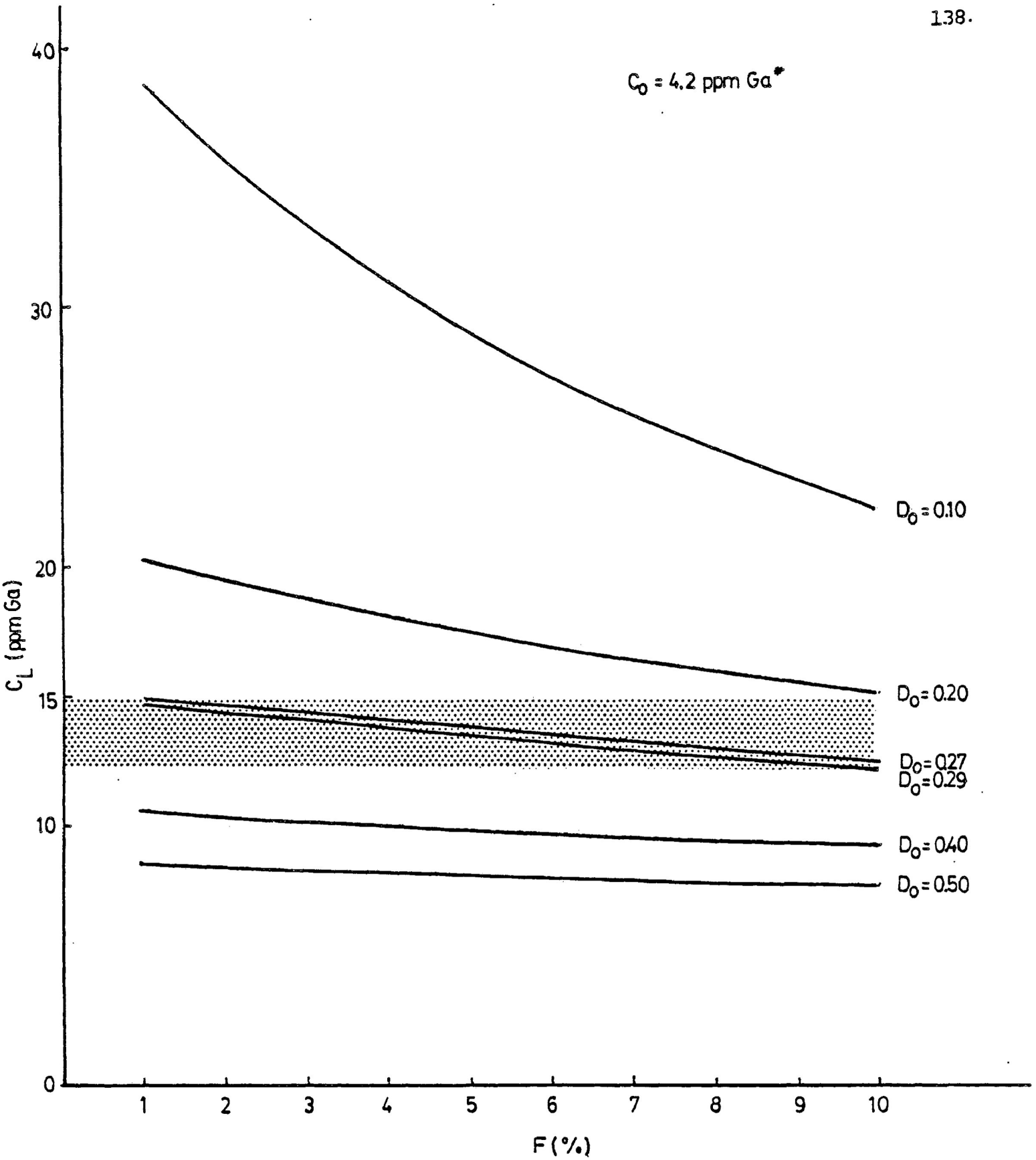

Figure 33. C_L vs. F plot for modal batch melting model. Stippled region defines the range in the abundance of Ga in the Hegau primary melts (i.e., 12.14 to 14.82 ppm). * garnet lherzolite based pyrolite estimate of the present study.

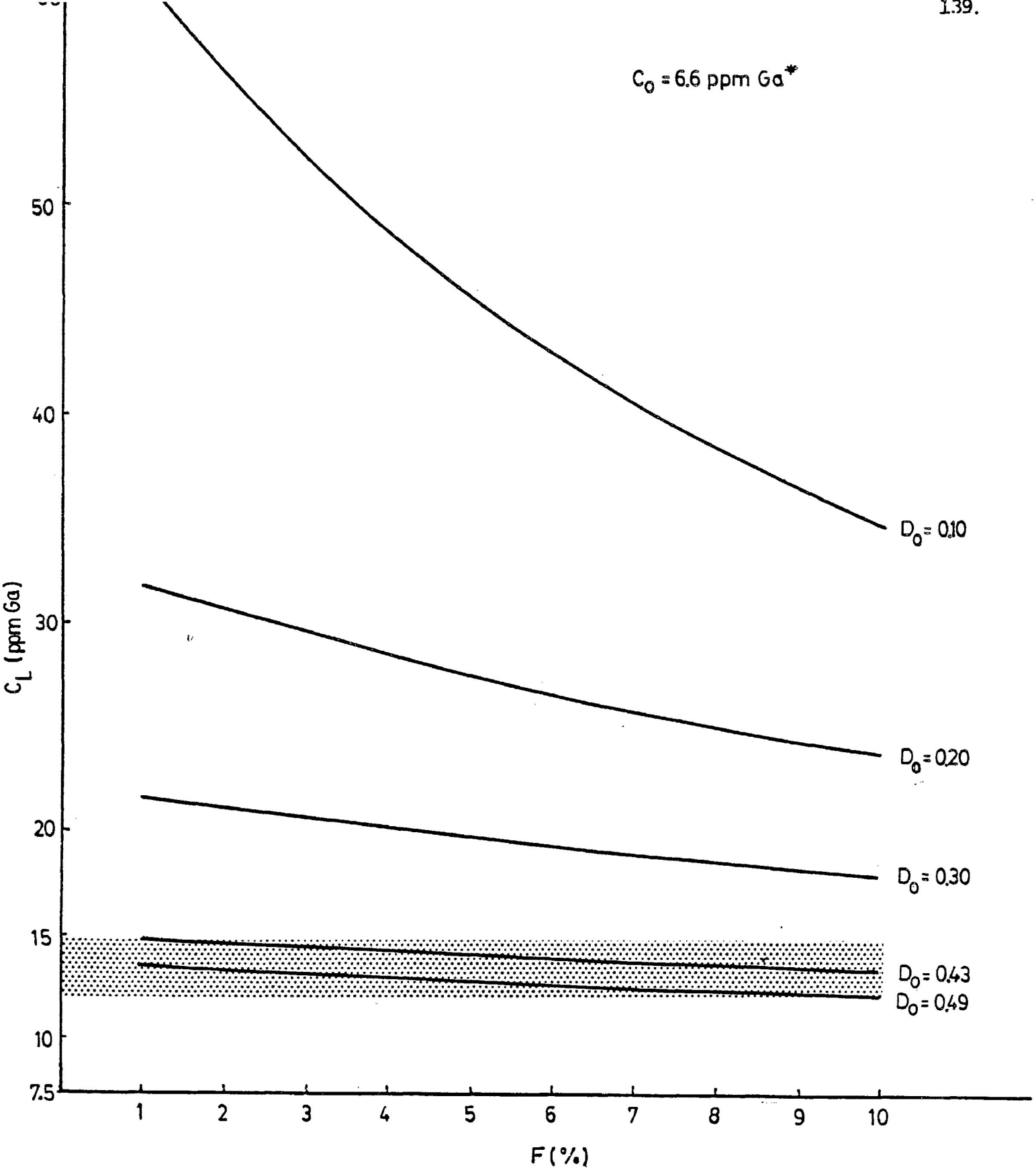

Figure 34. C_L vs. F plot for modal batch melting model. Stippled region defines the range in the abundance of Ga in the Hegau primary melts (i.e., 12.14 to 14.82 ppm). * spinel lherzolite based pyrolite estimate of the present study.

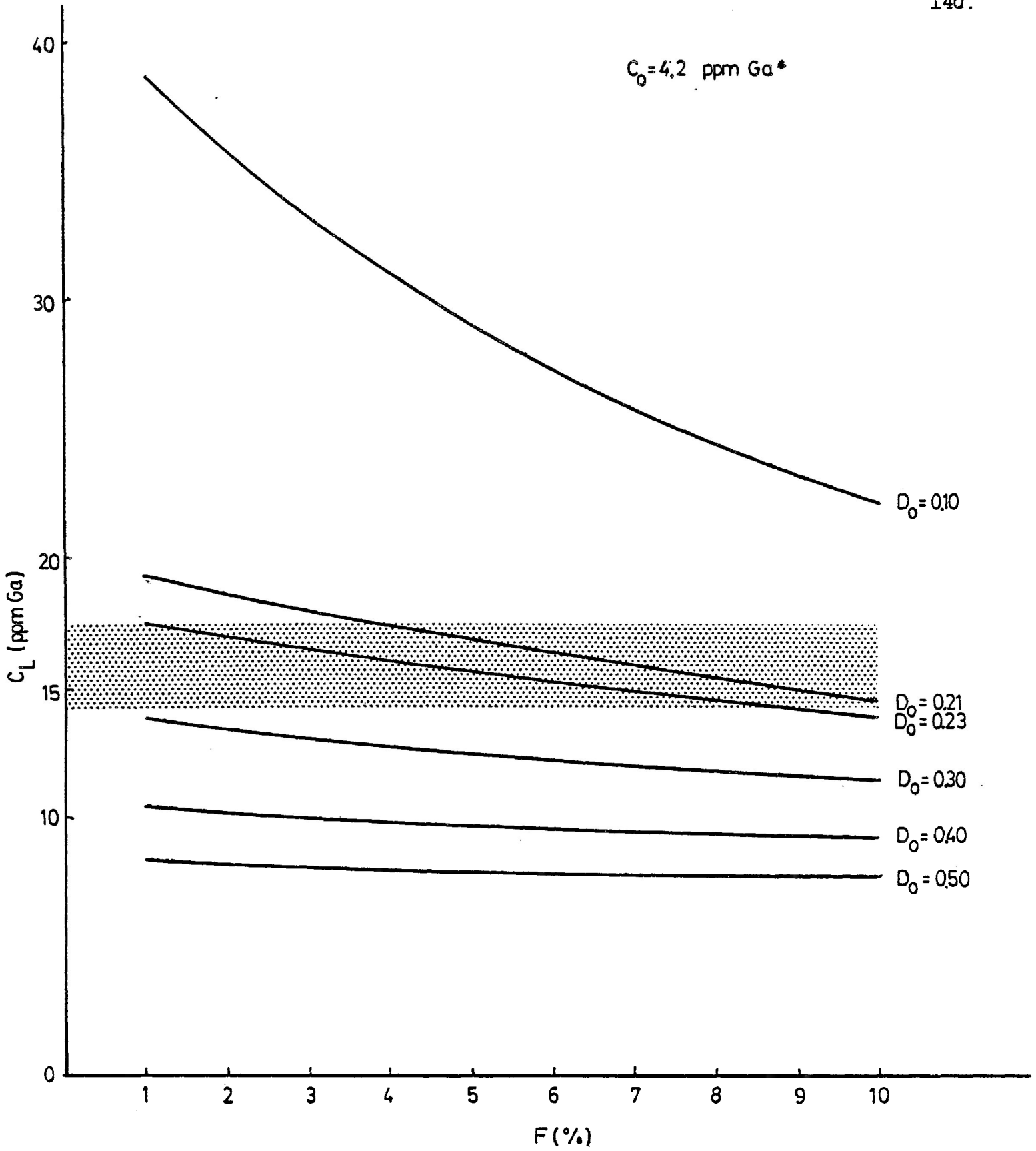

Figure 35. C_L vs. F plot for modal batch melting model. Stippled region defines the range in the abundance of Ga in the Urach primary melts (i.e., 14.20 to 17.33 ppm). * garnet lherzolite based pyrolite estimate of the present study.

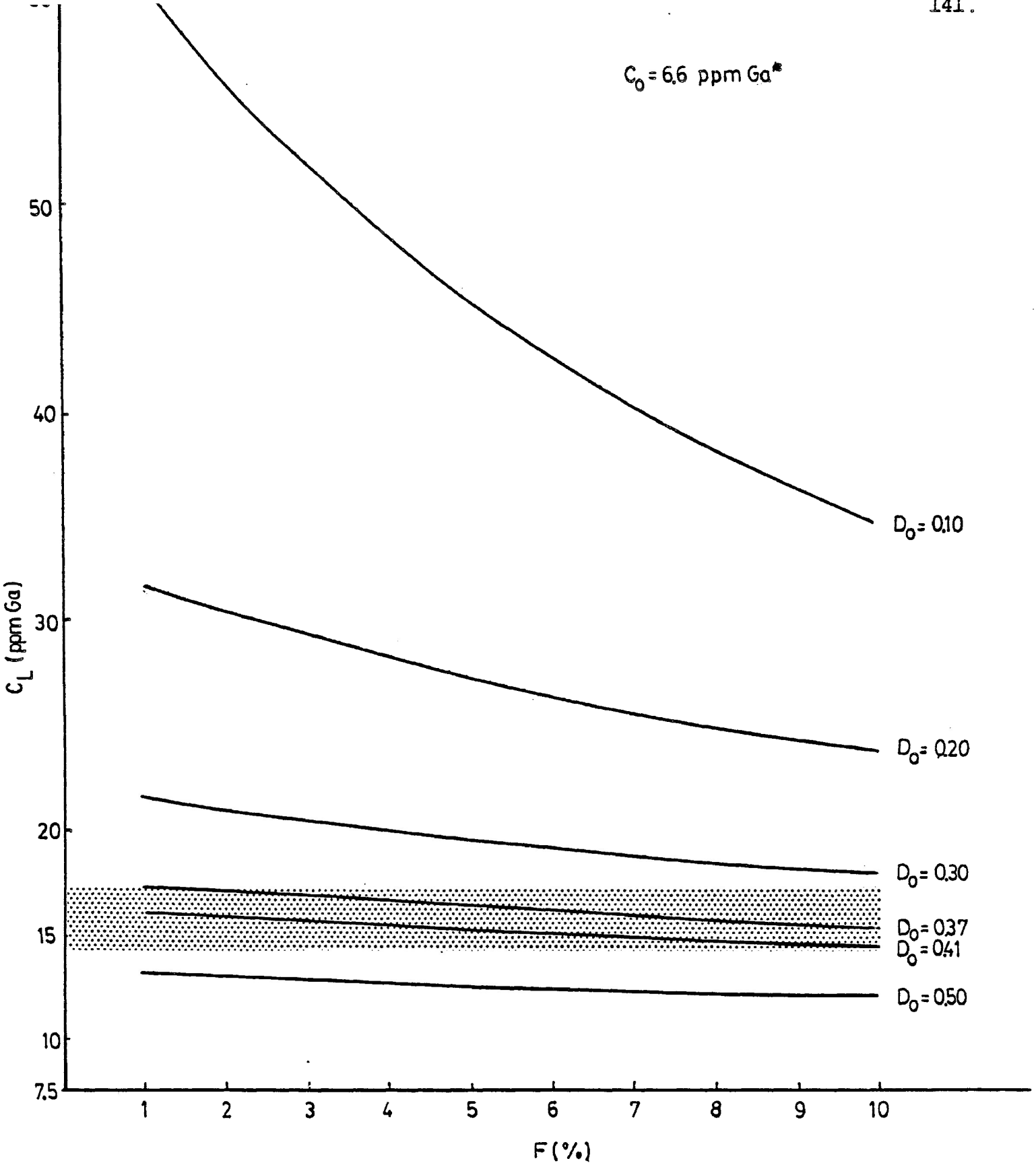

Figure 36. C_L vs. F plot for modal batch melting model. Stippled region defines the range in the abundance of Ga in the Urach primary melts (i.e., 14.20 to 17.33 ppm). * spinel lherzolite based pyrolite estimate of the present study.

Ga) of the present study. The measured ranges for the abundance of Ga in the Balcones, Hegau, and Urach primary melts cannot be duplicated by ranges in model-derived C_L values calculated using the spinel lherzolite based pyrolite source composition estimate (i.e., C_o = 6.6 ppm Ga) of the present study. As a consequence, the constraints calculated using the garnet lherzolite based pyrolite source composition estimate are considered more realistic.

Possible constraints for $D_{Ga}^{bulk-solid/melt}$ calculated using C_o = 4.2 ppm Ga vary from 0.16 (Balcones) to 0.28 (Hegau). These estimates are slightly greater than the estimate of 0.12 given by Frey *et al.* (1985) for the genesis of the Rhonda peridotite, and substantially lower than the estimate of 0.75 given by De Argollo and Schilling (1978(b)) for the genesis of Hawaiian alkaline volcanic rocks.

Assuming a mantle source mineralogy of 55% olivine, 25% opx, 15% cpx, and 5% garnet and using the $D_{Ga}^{mineral/melt}$ estimates of Goodman (1972) and De Argollo and Schilling (1978 (b)), $D_{Ga}^{bulk-solid/melt}$ is calculated to be 0.21. This estimate is within the range of possible constraints for $D_{Ga}^{bulk-solid/melt}$ (i.e., 0.16 to 0.28) calculated for the primary melts of the present study using C_o = 4.2 ppm Ga.

6.5 ADDITIONAL POSSIBLE CONSTRAINTS FOR THE RANGES OF MELTING

Of the incompatible trace elements analyzed for in the present study (i.e., Ga, La, Eu, Hf, Ta, and Th), Th has the widest abundance range in the primary partial melts. The

abundance of Th varies by factors of 2.0, 1.6, 1.7, and 1.2 in the Freemans Cove, Balcones, Hegau, and Urach suites respectively. Since Th has the widest abundance ranges, it is inferred that Th is the most incompatible trace element in the suites of the present study. If Th was not retained by any residual solids during the melting that generated these suites, then the ranges in Th abundance for each suite can be used as a measure of the ranges in the degrees of melting associated with the genesis of each suite (i.e. if $D^{Th} \approx 0$, then $C_L^{Th}/C_o^{Th} \rightarrow 1/F$ for equation (3)). Thus the melting ranges for the Freemans Cove, Balcones, Hegau, and Urach suites are at least over factors of 2.0, 1.6, 1.7, and 1.2 respectively (e.g., from 1% to 2%, 2% to 4%, etc. for the Freemans Cove Suite; 1% to 1.6%, 2% to 3.2%, etc. for the Balcones suite, etc.).

The Th-derived constraints for the ranges of F associated with the genesis of the Freemans Cove and Balcones primary melts (i.e., ranges in F over factors of 2.0 and 1.6 respectively) are consistent with the model-derived constraints for F given in Table 52 for C_o = 4.2 ppm Ga.

For the Th-derived and model-derived constraints for F to be consistent, both C_o and D_o for Hegau and Urach would have to be reduced.

6.6 CONCLUSIONS

1. The ranges in the abundance of Ga in the primary partial melts of the present study can be duplicated using a

simple modal batch melting model.

2. Possible model-derived constraints for $D_{Ga}^{bulk-solid/melt}$ calculated using C_o = 4.2 ppm Ga (the garnet lherzolite based pyrolite composition estimate of the present study) vary from 0.16 (Balcones) to 0.28 (Hegau).

3. $D_{Ga}^{bulk-solid/melt}$ calculated using the $D_{Ga}^{mineral/melt}$ estimates of Goodman (1972) and De Argollo and Schilling (1978(b)) and assuming a mantle source mineralogy of 55% olivine, 25% opx, 15% cpx, and 5% garnet is 0.21. This $D_{Ga}^{bulk-solid/melt}$ estimate is within the range of possible model-derived constraints for $D_{Ga}^{bulk-solid/melt}$ given above.

4. Possible constraints for the ranges in melting associated with the genesis of the Freemans Cove, Balcones, Hegau, and Urach primary melts derived using Th data are over factors of 2.0, 1.6, 1.7, and 1.2 respectively.

5. The Th-derived constraints for the ranges in melting for the Freemans Cove and Balcones primary melts are consistent with the model-derived constraints for F given above.

6. The Th-derived constraints for the ranges in melting for the Hegau and Urach primary melts are not consistent with the model-derived constraints for F given above. For the Th-derived and model-derived constraints for F to be consistent, both C_o and D_o for Hegau and Urach would have to be reduced.

CHAPTER SEVEN

RECOMMENDATIONS FOR FUTURE STUDIES

1. In order to assess the potential of epithermal INAA to generate accurate Ga data it is recommended that a wide variety of geological materials of known Ga content be analyzed using this technique.
2. In order to expand further the data base for Ga in upper mantle-derived materials, and to assess the significance of the relatively low Ga content of the garnet lherzolites of the present study, it is recommended that more garnet lherzolite xenoliths from a wide variety of geographical localities be accurately analyzed.
3. In order to assess the potential of using the distribution of Ga between certain mineral pairs in xenoliths (e.g., $D_{Ga}^{opx/cpx}$) as geothermometers it is recommended that a wide variety of xenoliths and their constituent mineral phases be accurately analyzed.
4. In order to assess further De Argollo and Schilling's (1978) proposals that Ga/Al ratios of basalts might be used to infer the Ga/Al ratios of the mantle sources of the basalts, and to map mantle heterogeneities, it is recommended that the Ga/Al ratios of *coexisting* upper mantle-derived primary partial melts and ultramafic xenoliths from a wide variety of geographical localities be accurately determined.

5. In order to understand better the geochemical behavior of Ga during geological processes, and to facilitate the use of Ga data in solving problems of petrology, it is recommended that Ga distribution coefficients (e.g. $D_{Ga}^{mineral/mineral}$, $D_{Ga}^{bulk-solid/melt}$, etc.) be accurately determined for both natural and artifical samples under controlled experimental conditions.

APPENDICES

APPENDIX 1

NEUTRON ACTIVATION ANALYSIS

A1.1 INTRODUCTION

Neutron activation analysis (NAA) is one of the principal techniques used to determine trace element concentrations in geological samples. Samples to be analyzed by NAA are suspended in the core of a nuclear reactor and exposed to neutrons. Various nuclear interactions occur depending on the kinetic energy of the neutrons involved. Most of the neutrons produced in a nuclear reactor have relatively low kinetic energies, less than or equal to 1.0 KeV, and are termed slow neutrons. Slow neutrons can be subdivided into the following three categories:

1. Thermal Neutrons Thermal neutrons have kinetic energies of approximately 0.025 eV and are in thermal equilibrium with surrounding atoms;
2. Epithermal Neutrons Epithermal neutrons have kinetic energies of about 0.2 eV and are not in complete thermal equilibrium with their environment;
3. Resonance Neutrons Resonance neutrons have kinetic energies in the range of 1.0 to 1000 eV (Dostal and Elson, 1980).

The most common interaction that occurs involves the capture of a single slow neutron by an atom to produce a new isotope (Haskin, 1980). The process of generating radioactive

isotopes by neutron capture is termed neutron activation. If the captured neutrons are thermal neutrons the process is termed thermal neutron activation. If the captured neutrons are epithermal neutrons the process is termed epithermal neutron activation.

Radioisotopes produced by neutron activation undergo radioactive decay. This involves emission of characteristic energies, often gamma rays, at characteristic rates. By analyzing the emitted gamma rays, the identities and concentrations of the decaying radioisotopes and their parent elements can be determined.

Two types of NAA exist:

1. radiochemical neutron activation analysis (RNAA); and
2. instrumental neutron activation analysis (INAA).

RNAA involves chemical separation of radioisotopes of interest prior to gamma ray spectrometry, while INAA does not. If the radioisotopes of interest emit little radiation relative to other elements present, chemical separation orior to spectrometry may be necessary.

A1.2 NAA OF Ga

A1.2.1 Reagents

The reagents used are given in Table 53.

TABLE 53
Reagents Used

Reagent	Manufacturer
HNO_3 (16N)	BDH (B10168)
HF (49%)	FISHER (A-147)
HCl (2N, 6N, 7N, 12N)	AMACHEM (HS75)
$TiCl_3$ (15% W/V)	BDH (30447)
Isopropyl Ether	BDH (B28268)
Gallium (ultra pure)	SPEX (GA03, TMI-1)
NaOH	BDH (ACS816)
Na_2O_2	ANALAR

A1.2.2 Preparation of Ga Carrier

1. Approximately 0.125 grams of ultrapure metallic gallium, weighed to an accuracy of five one-thousandths of a milligram, were placed into a 200 ml glass beaker.
2. Approximately 40 ml of aqua regia were added. The beaker was covered with a watch-glass and placed on a hotplate. The gallium was dissolved overnight at approximately 50°C.
3. Approximately 20 ml of 2N HCl were added. The solution was transparent, colourless, and free of solid material.
4. The solution was transferred to a preweighed self-sealing, screw-top plastic bottle. The beaker was

washed twice with approximately 10 ml of 2N HCl.

5. The plastic bottle was reweighed and the concentration of gallium in solution calculated to be 1995.80 μg/g.

A1.2.3 Preparation of Ga Standard

1. Exactly 1 ml of Ga carrier was transferred to a pre-weighed, self-sealing, screw-top plastic bottle. The bottle was reweighed and the amount of Ga added calculated.
2. Approximately 50 ml of 2N HNO_3 were added, the bottle reweighed, and the concentration of Ga in the diluted solution calculated to be 48.43 μg/g.

A1.2.4 Sample Preparation

A1.2.4.1 RNAA

A1.2.4.1.1 Whole rock samples.

1. A clean diamond rock-saw was used to remove all weathered surfaces from the samples ensuring that only fresh, unaltered material was analyzed.
2. The samples were crushed and ground in a precontaminated tungsten-carbide swing-mill. The resultant powders were hermetically sealed in labelled plastic pouches.
3. Irradiation containers were constructed from smooth pieces of aluminum foil averaging 3 cm square and 60 mg in weight. These containers were weighed to an accuracy of five one-thousandths of a milligram using a Mettler Gram-atic balance.
4. Approximately 100 mg of sample, weighed to an accuracy of five one-thousandths of a milligram, were placed into

each container. The containers were sealed and a fine-tipped felt marker used to imprint each sample's number into the aluminum surface of each container. An additional wrapping of aluminum foil was placed around each container to prevent leakage. The sample's number was imprinted into the surface of this protective covering.

5. Sets of 8 whole rock samples, 2 U.S.G.S. rock standards, and 2 Ga standard samples were prepared. After weighing and packaging, the individual samples comprising each set were stacked together and wrapped in aluminum foil to produce an irradiation package approximately 1.5 cm square and 2.5 cm in height. The standard samples were uniformly distributed in the stacking sequence.

A1.2.4.1.2 Mineral Samples.

1. A clean diamond rock-saw was used to remove all weathered surfaces from the samples ensuring that only fresh, unaltered material was analyzed.
2. The samples were crushed in two stages. In the first stage a tunsten-carbide hammer and anvil were used to reduce the samples to mineral aggregates approximately 0.5 cm in size. The mineral aggregates were then broken into individual mineral fragments by coarse grinding with a precontaminated agate mortar and pestle.
3. The mineral fragements were sieved through a series of brass sieves and the 35 to 60 mesh (.250 mm - .420 mm) fraction collected.

4. The mineral fragments were separated using a Frantz Isodynamic magnetic separator.
5. The fragments comprising each separated mineral phase were carefully examined using a binocular microscope. All fragments with visible (x40 magnification) iron staining, internal inclusions, glass coatings, or attached mineral fragments were discarded.
6. The remaining fragments were ground into fine powders using a precontaminated agate mortar and pestle. The resultant powders were placed in carefully labelled screw-top glass vials.
7. Irradiation containers were prepared, and sample preparation completed as described above for whole rock samples.

A1.2.4.1.3 Ga standard samples. Ga standard samples were prepared by absorbing aliquots of gallium standard onto granular silica. The procedure used is outlined below.

1. Irradiation containers were constructed from aluminum foil as described above for whole rock samples.
2. Approximately 100 mg of granular silica were placed into each container. The combined weight of the container and silica was measured to an accuracy of five one-thousandths of a milligram.
3. Using a micropipette, 100 μl of Ga standard were transferred to, and absorbed onto, the silica.
4. The containers were immediately reweighed and the amount of Ga added calculated.

5. The samples were heated at approximately 50°C on a hotplate until dry. Drying was enhanced using an infra-red heat lamp.

6. The containers were sealed and sample preparation completed as described above for whole rock samples.

A1.2.4.2 Epithermal INAA

A1.2.4.2.1. Whole rock samples.

1. The samples were trimmed, crushed, and ground according to the procedure described above for RNAA whole rock samples.

2. Irradiation containers were prepared from plastic vials approximately 2 cm high and 1 cm in diameter. The vials were labelled and weighed to an accuracy of five one-thousandths of a milligram.

3. Approximately 300 mg of sample, weighed to an accuracy of five one-thousandths of a milligram, were placed into each vial.

4. The vial lids were fused into place to prevent sample loss and contamination.

5. Each vial was placed into a larger plastic vial, and the lids of the larger vials fused into place. The resultant, doubly sealed, irradiation containers were approximately 4 cm high and 1.5 cm in diameter.

6. Sets consisting of 5 whole rock samples and 3 Ga standard samples were prepared. The vials were stacked together to form a circular package approximately 6 cm in diameter. One standard sample was placed in the

center of the package and the others uniformly spaced on the periphery. The package was wrapped with several layers of Scotch-tape.

A1.2.4.2.2 Ga standard samples.

1. Three hundred mg aliquots of Ga standard, weighed to an accuracy of five one-thousandths of a milligram were placed into small plastic vials using a micropipette.
2. The vials were sealed and packaged according to the procedure described above for epithermal INAA whole rock samples.

A1.2.5 Irradiation

Irradiation occurred in the research reactor at McMaster University located in Hamilton, Ontario.

A1.2.5.1 RNAA

The sample sets were irradiated for 7 hours in a thermal neutron flux of 5×10^{12} $n/cm^2/s$. They were allowed to "cool" for approximately 84 hours prior to gamma ray spectrometry.

A1.2.5.2 Epithermal INAA

The sample sets were placed inside a cadmium shield and irradiated for 30 minutes in an epithermal neutron flux of 2×10^{11} $n/cm^2/s$. They were allowed to "cool" for approximately 12 hours prior to gamma ray spectromety.

A1.2.6 Radiochemical Separation of Ga

All work was performed in a lead-lined fumehood. Protective gloves were worn at all times. Tweezers were used to manipulate the active samples.

A1.2.6.1 Whole rock, mineral (excluding spinel), and Ga standard samples.

1. The samples were transferred from their aluminum foil irradiation containers to appropriately labelled 25 ml teflon crucibles. The foil containers were washed with approximately 2 ml of double distilled H_2O.
2. Exactly 1 ml of Ga carrier was added to each crucible using an Eppendorf fixed volume pipette. The carrier provides sufficient quantities of Ga for effective extraction and is used to determine chemical yield.
3. Approximately 1 ml of 16 N HNO_3 was added to each crucible. The HNO_3 wets the sample and provides oxidizing conditions.
4. Approximately 10 ml of 48% HF were added to each crucible. The HF dissolves silicates.
5. The crucibles were placed on an aluminum-foil covered hotplate and heated at approximately 95°C until dry. No boiling or spattering was allowed to occur.
6. Sufficient 6N HCl was added to dissolve the samples. The samples were heated again until dry.
7. Ten ml of 6N HCl were added to each crucible. The samples were heated until dissolved. The solutions were transparent, yellow, and free of solid material.
8. The solutions were transferred to appropriately labelled 125 ml separatory funnels. Each crucible was washed twice with approximately 5 ml of 6N HCl.

9. Approximately 1 ml of $TiCl_3$ was added to each funnel to reduce Fe^{3+} to Fe^{2+}. The funnels were swirled then left undisturbed for approximately 5 minutes. $TiCl_3$ becomes ineffective as a reductant if exposed to air. In the present study, the $TiCl_3$ was stored in a rubber capped flask containing an atmosphere of nitrogen. A hypodermic needle was used to pierce the cap and extract the $TiCl_3$ for use.

10. Fifteen ml of isopropyl ether were added to each funnel to extract Ga. The funnels were vigorously shaken for 3 minutes. The pressure in the funnels was reduced, the lids removed, and the funnels left undisturbed until complete separation of the liquid phases occurred (i.e., no bubbles, clouding or precipitation allowed).

11. The denser acidic phases were drained from the bottoms of the separatory funnels into appropriately labelled 100 ml beakers. The residual ether phases were then drained into different appropriately labelled 100 ml beakers. These beakers were covered with watch-glasses to minimize ether evaporation.

12. The acidic phases were transferred back into their original separatory funnels. The beakers were washed with 15 ml of isopropyl ether and the extraction procedure repeated.

13. The denser acidic phases were drained, discarded as active waste, and the residual ether phases from the first extraction transferred back into the appropriate

separatory funnels containing the ether phases from the second extraction.

14. One drop of $TiCl_3$ was added to each funnel to reduce any remaining Fe^{3+}. The funnels were shaken for 10 seconds, allowing uniform reduction to occur.

15. Ten ml of double distilled H_2O were added to each funnel to back extract Ga. The funnels were vigorously shaken for 3 minutes. The pressure in the funnels was reduced, the lids removed, and the funnels left undisturbed until complete separation of the liquid phases occurred.

16. The denser aqueous phases were drained from the bottoms of the separatory funnels into appropriately labelled 100 ml beakers. The residual ether phases were discarded as active waste.

17. The beakers containing the aqueous gallium solutions were placed on hotplates and carefully evaporated until approximately 5 ml of solution remained in each.

18. The aqueous gallium solutions were transferred to pre-weighed, self-sealing screw-top plastic vials. The beakers were washed with approximately 2 ml of double-distilled H_2O. The liquid levels in the vials were equalized with appropriate amounts of double distilled H_2O. The vials were reweighed, and the weight of the Ga solutions calculated.

A1.2.6.2 Spinel samples. The spinel samples were unaffected by the HF digestion process. Dissolution was accomplished by fusion with Na_2O_2.

1. A 25 ml nickel crucible was prepared for each sample. Two tablets of NaOH were placed in each crucible. The crucibles were covered with nickel lids and heated with a meeker-burner until the NaOH melted. The crucibles were swirled during heating to uniformly coat their inner surfaces with NaOH. The crucibles were cooled to room temperature.
2. Exactly 1 ml of Ga carrier was added to each crucible using an Eppendorf fixed volume pipette.
3. The crucibles were heated on a hotplate at approximately 95°C until dry. Drying was enhanced with an infra-red heat lamp and by allowing a steady stream of pressurized, dry, clean air to flow over the open tops of the crucibles. Once dry, the crucibles were placed in an oven at 55°C until needed.
4. The crucibles were removed from the oven. One pellet of NaOH was placed in each crucible. Approximately 0.5 grams of granular Na_2O_2 were added to, and uniformly distributed within, each crucible.
5. The samples were removed from their aluminum foil irradiation containers and transferred into the nickel crucibles. Approximately 1.5 grams of Na_2O_2 were added to, and uniformly distributed within, each crucible. The crucible lids were replaced.
6. The crucibles were slowly heated with a meeker-burner for approximately 5 minutes until the sample mixtures were almost melted. The heat was increased until the

crucibles were dull-red in colour. The crucibles were maintained at this temperature for approximately 5 minutes to allow complete fusion to occur. Fusion was enhanced by gentle swirling of the crucibles during heating.

7. The crucibles were removed from the burner and cooled for approximately 3 minutes allowing the fusion cakes to separate from the inner surfaces of the crucibles (the separation was accompanied by a distinct, metallic "cracking" sound). Cooling was enhanced by placing the crucibles on lead bricks and by partially removing the crucible lids.

8. The fusion cakes were partially dissolved by placing the crucibles and lids into appropriately labelled 200 ml glass beakers containing 40 ml of distilled H_2O. Watch glasses were placed on the beakers. The beakers were left undisturbed for approximately 5 minutes.

9. Forty ml of 12N HCl were added slowly, in stages, to each beaker. During the addition, a small rubber spatula and a pair of tongs were used to remove all traces of fusion cake from the surfaces of the crucibles and lids. The crucibles and lids were washed with approximately 10 ml of 6N HCl and removed from the beakers. The spatula and tongs were also washed with 6N HCl and removed.

10. The beakers were placed on a hotplate and gently boiled until all solid material was dissolved. The solutions

were transparent and green in colour. Watch-glasses were placed on the beakers to prevent excessive evaporation. Spattering was not allowed to occur.

11. The sample solutions were transferred to appropriately labelled 125 ml separatory funnels. The beakers were washed with approximately 5 ml of 6N HCl.

12. Ga was extracted according to the procedure outlined above for whole rock samples.

A1.2.7 Gamma Ray Spectrometry

The analytical peaks and counting conditions are summarized in Table 54.

TABLE 54
Summary of Analytical Peaks and Counting Conditions

Radio-isotope Analyzed	$T_{\frac{1}{2}}$ (hours)	Measured Photopeaks (KeV)	Count Time (sec)			
			RNAA		Epithermal INAA	
			Sample	Standard	Sample	Standard
Ga^{72}	14.1	630.1 834.1	4000	4000	10000	10000

A1.2.7.1 Whole Rock Samples

Whole rock samples were analyzed at Lakehead University. Detection was performed using an APTEC/NRD PHYGE (passivated Hyperpure Germanium) coaxial spectrometer (resolution of 1.85 KeV FWHM at 1331 KeV) coupled to a Tennelec TC 222 spectroscopic amplifier. The gamma ray spectra were collected on a Norland IT-5400 modular multichannel (4096) analyzer.

A1.2.7.2 Mineral Samples

Mineral samples were analyzed at McMaster University.

Detection was performed using an APTEC/NRD PHYGE (Passivated Hyperpure Germanium) coaxial spectrometer (Model CS20-B31C) coupled to a Canberra Model 2020 spectroscopic amplifier. The gamma ray spectra were collected on a Canberra Series 90 multichannel analyzer.

A1.2.8 Calculations

A1.2.8.1 Decay Correction

Equation 4 was used to correct activity data for decay during analysis.

$$A_o = (A_1)(e^{\lambda \Delta T}) \quad (4)$$

where: A_o is the decay-corrected activity in counts per minute (cpm);

A_1 is the measured activity in cpm;

e is the constant 2.7182818

λ is the decay constant of ^{72}Ga=0.0491594 (i.e., ln(2) divided by the half-life of ^{72}Ga in hours);

ΔT is the time difference, in hours, between the midpoint of each count and a common reference time.

A1.2.8.2 Yield Correction

Equation 5 was used to correct RNAA activity data for chemical yield.

$$A = \frac{A_o}{y} \quad (5)$$

where A is the decay and yield corrected activity in cpm;

A_o is the decay corrected activity in cpm;

y is the chemical yield.

A1.2.8.3 Calculation of Ga Content

Equation 6 was used to calculate gallium content from activity data.

$$C = \left(\frac{A}{W}\right)\left[\frac{(W_s)(C_s)}{(A_s)}\right] \qquad (6)$$

where: C is the gallium content of the sample in μg/g;

A is the corrected activity of the sample in cpm;

W is the sample weight in mg;

C_s is the gallium content of the standard sample in μg/g;

A_s is the corrected activity of the standard in cpm;

W_s is the standard weight in mg.

Since 4 standards were used, 4 calculations were performed for each sample. The results were averaged.

A1.2.8.4 Calculation of Uncertainties Due to Counting Statistics

Equation 7 (Woldseth, 1973) was used to calculate the uncertainty associated with measurement of ^{72}Ga activity due to counting statistics.

$$E = \pm\left(\sqrt{F+B}\right)\left[\frac{100\%}{N}\right] \qquad (7)$$

where: E is the percent relative uncertainty of the measured ^{72}Ga activity at the 1σ confidence;

F is the full peak area of the ^{72}Ga photopeak, measured over 8 channels, in counts;

B is the background activity associated with the ^{72}Ga photopeak, measured over 8 channels, in counts;

N is the net area of the ^{72}Ga photopeak in counts.

Equation 8 (Lyon, 1964) was used to calculate the uncertainty associated with calculating Ga content from activity data.

$$S_c = \pm C\sqrt{E_1^2 + E_2^2 + E_3^2 + E_4^2} \qquad (8)$$

where: S_c is the standard deviation of the calculated Ga content, C;

E_1-E_4 are the percent relative uncertainties of the measured ^{72}Ga activities of:

E_1 the rock or mineral sample,

E_2 the standard sample,

E_3 the yield aliquot,

E_4 the yield standard.

A1.2.9 Determination of Chemical Yield

A1.2.9.1 Preparation of Yield Standard

1. One ml of Ga carrier was placed into a preweighed, self-sealing, screw-top plastic vial.
2. The vial was weighed, to an accuracy of five one-thousandths of a milligram, and the weight of Ga added calculated.
3. Sufficient distilled H_2O was added to equalize the standard volume to that of the sample solutions.
4. The vial was reweighed and the concentration of Ga in solution calculated.

A1.2.9.2 Preparation of Yield Samples

1. A piece of absorbant filter paper, 1 cm square, was prepared for each sample. The filter papers were labelled and suspended on wire hooks attached to a small drying

stand.

2. Seventy-five μl of sample solution were transferred onto each filter paper by micropipette. The filter papers were left undisturbed until dry. Drying was enhanced using an infra-red heat lamp.

3. Irradiation containers were prepared by wrapping each filter paper with 2 layers of aluminum foil. The sample numbers were imprinted into the surfaces of the aluminum foil.

4. Sets of 12 yield samples and 4 yield standards were stacked together and wrapped with aluminum foil to produce an irradition package approximately 1.5 cm square and 2.5 cm in height.

A1.2.9.3 Irradiation

The yield samples and standards were irradiated as described above for RNAA of whole rock samples.

A1.2.9.4 Preparation of Samples for Gamma Ray Spectrometry

1. The samples were unpackaged and the filter papers transferred to self-sealing, screw-top plastic vials using tweezers. The foil wrappings were washed with approximately 5 ml of distilled H_2O. The tweezers were washed with approximately 1 ml of distilled H_2O.

2. The liquid levels in the vials were equalized by addition of distilled H_2O. The samples were then ready for gamma ray spectrometry.

A1.2.9.5 Gamma Ray Spectrometry

The samples were analyzed at Lakehead University using the equipment described above for whole rock samples. Counting times were reduced to 1000 seconds.

A1.2.9.6 Calculation of Chemical Yield

1. The weight of carrier Ga in the yield aliquots was calculated using equation 6 above.

2. The weight of carrier Ga extracted during radiochemistry was calculated using equation 9.

$$W_E = \frac{(W_y)(W_s)}{(W_A)} \qquad (9)$$

where: W_E is the weight of carrier Ga extracted in μg;

W_y is the weight of carrier Ga in the yield aliquot in μg;

W_s is the weight of the original sample solution in g;

W_A is the weight of the 75 μl aliquot in g.

3. The weight of carrier Ga added prior to radiochemistry was calculated using equation 10.

$$W_p = (W_c)(C_c) \qquad (10)$$

where: W_p is the weight of carrier Ga added prior to radiochemistry in μg;

W_c is the weight of carrier solution added, in g;

C_c is the concentration of Ga in the carrier solution, in $\mu g/g$.

4. The chemical yield was calculated using equation 11.

$$y = \left[\frac{W_E}{W_p} \right] (100\%) \qquad (11)$$

where: y is the chemical yield in percent;

W_p is as defined in equation 10 above;

W_E is as defined in equation 9 above.

A1.2.10 Worked Example

The RNAA data used to calculate the Ga content of sample 6-1, a melilite-olivine-nephelinite from Uvalde, Texas, is given in Table 55.

1. Chemical yields for sample 6-1 and standards BCR-1, G-2, Ga_1, and Ga_2 were calculated as follows:

1.1 Equation 4 was used to correct the yield A_1 activity data for decay during analysis.

E.g., for sample aliquot 6-1:

$$A_o = (A_1)(e^{\lambda \Delta T})$$

$$A_o = (209.85002)(2.7182818)^{(.0491594)(9.22778)}$$

$$A_o = 328.21865.$$

for the other aliquots:

BCR-1: $A_o = 335.34184$

G-2: $A_o = 323.78971$

Ga_1: $A_o = 342.33422$

Ga_2: $A_o = 316.46199$

y_1: $A_o = 330.75595$

y_2: $A_o = 338.99412$

y_3: $A_o = 342.79443$

y_4: $A = 341.37242.$

TABLE 55

RNAA Data Used to Calculate the Ga Content of Sample 6-1

Initial Analyses							
Sample	Data						
	Weight (g)	Count Time minutes	ΔT (hours)	Counts F	Counts B	Counts N	A_1 (cpm)
6-1	.10330	66.667	1.20556	3741	1400	2341	35.11500
Standards							
BCR-1	.09265	"	10.02222	2463	784	1679	25.18499
G-2	.09527	"	11.17222	2337	801	1536	23.03999
Ga_1	.10321	"	7.70556	5463	1206	4257	63.85124
Ga_2	.10166	"	8.87222	4968	1099	3869	58.03588
Yield Analyses							
Sample Aliquots	Data						
6-1	.12942	33.333	9.22778	15423	8428	6995	209.85002
BCR-1	.13079	"	6.74444	17147	9086	8061	241.83002
G-2	.12722	"	7.37778	18153	10605	7548	226.44002
Ga_1	.12932	"	5.21111	18615	9751	8864	265.92003
Ga_2	.12798	"	6.07778	17499	9642	7857	235.71002
Standard Aliquots	Data						
Y_1	.12459	33.333	1.19444	24605	14200	10405	312.15003
Y_2	.12770	"	2.47778	23698	13677	10021	300.63003
Y_3	.12909	"	3.19444	23138	13353	9785	293.55003
Y_4	.12859	"	3.91111	22262	12848	9414	282.42003

Standard Concentrations (ppm Ga): BCR-1: 22 ppm

G-2: 23 ppm

Ga_1, Ga_2: 48.43 ppm

Y_1: 212.20 ppm

Y_2: 199.21 ppm

Y_3: 192.42 ppm

Y_4: 186.76 ppm

1.2 Equation 6 was used to calculate the amount of carrier Ga in each aliquot (in this case $A_o = A$).

E.g., for sample aliquot y_1 as the standard:

$$C = \left[\frac{A}{W}\right]\left[\frac{(A_s)(C_s)}{(W_s)}\right]$$

$$C = \left[\frac{328.21865}{.12942}\right]\left[\frac{(.12459)(212.20)}{312.15003}\right]$$

$C = 214.80\ \mu g/g$ Ga

$C = 27.79\ \mu g$ Ga

using the other standards:

y_2: $C = 214.96\ \mu g/g$ Ga
$= 27.82\ \mu g$ Ga

y_3: $C = 214.60\ \mu g/g$ Ga
$= 27.77\ \mu g$ Ga

y_4: $C = 215.65\ \mu g/g$ Ga
$= 27.91\ \mu g$ Ga.

The average calculated amount of carriar Ga present in sample aliquot 6-1 is 27.82 μg.

Similarly, for the other aliquots:

BCR-1: $C = 28.40\ \mu g$

G-2: $C = 27.42\ \mu g$

Ga_1: $C = 28.99\ \mu g$

Ga_2: $C = 26.80\ \mu g$.

1.3 Equation 9 was used to calculate the weight of carrier Ga extracted during radiochemistry.

E.g., for sample 6-1:

$$W_E = \frac{(W_y)(W_s)}{(W_A)}$$

$$W_E = \frac{(27.82)(10.48894)}{(.12942)}$$

$$W_E = 2.25 \text{ mg Ga}$$

Similarly, for the other samples:

BCR-1: $W_E = 2.24$ mg Ga

G-2: $W_E = 2.20$ mg Ga

Ga_1: $W_E = 2.27$ mg Ga

Ga_2: $W_E = 2.15$ mg Ga.

1.4 Equation 10 was used to calculate the weight of carrier Ga added prior to radiochemistry.

E.g., for sample 6-1:

$$W_P = (W_c)(C_c)$$

$$W_P = (1.09458)(2.0887)$$

$$W_P = 2.2862 \text{ mg Ga.}$$

1.5 Equation 11 was used to calculate the chemical yield.

E.g., for sample 6-1:

$$y = \frac{W_E}{W_P}$$

$$y = \left[\frac{2.25}{2.29}\right](100\%)$$

$$y = 98.25\%$$

Similarly, for the other samples:

BCR-1: $y = 97.91\%$

G-2: $y = 96.11\%$

Ga_1: $y = 99.21\%$

Ga_2: $y = 94.26\%$

2. The Ga content of sample 6-1 was calculated as follows:

2.1 Equation 4 was used to correct initial A_1 activity data for decay during analysis.

E.g., for sample 6-1:

$$A_o = (A_1)(e^{\lambda \Delta T})$$

$$A_o = (35.11500)(2.7182818^{(.0491594)(1.20556)})$$

$$A_o = (35.11500)(1.061056)$$

$$A_o = 37.25898$$

for the standards:

$$A_o(\text{BCR-1}) = 40.93737$$

$$A_o(\text{G-2}) = 40.66747$$

$$A_o(\text{Ga}_1) = 92.76417$$

$$A_o(\text{Ga}_2) = 89.22079$$

2.2 Equation 5 was used to correct A_o data for chemical yield.

E.g., for sample 6-1:

$$A = \frac{A_o}{Y}$$

$$A = \frac{37.22811}{0.9825}$$

$$A = 37.8912$$

similarly, for the standards:

BCR-1: $A_s = 41.81293$

G-2 : $A_s = 42.31479$

Ga_1 : $A_s = 93.50379$

Ga_2 : $A_s = 94.64991$

2.3 Equation 3 was used to calculate Ga content.

E.g., for sample 6-1, using BCR-1 as the standard:

$$C = \left(\frac{A}{W}\right)\left[\frac{(W_s)(C_s)}{A_s}\right]$$

$$C = \left(\frac{37.8912}{0.09265}\right)\left[\frac{(0.10160)(22.0)}{41.81293}\right]$$

$$C = 21.86\ \mu g/g$$

similarly, using the other standards:

G-2 : $C = 20.95\ \mu g/g$

Ga_1 : $C = 20.13\ \mu g/g$

Ga_2 : $C = 19.53\ \mu g/g$

the average is 20.62 $\mu g/g$.

3. The uncertainties due to counting statistics were calculated as follows:

3.1 Equation 7 was used to calculate the uncertainties associated with measuring ^{72}Ga activities.

E.g., for the initial analysis of sample 6-1:

$$\Sigma_1 = \frac{\pm\ (\sqrt{F+B}\ )(100\%)}{N}$$

$$\Sigma_1 = \pm 3.06\%$$

similarly, for the standards and aliquots:

initial standards: $\Sigma_2 = \pm 2.74\%$

yield aliquot: $\Sigma_3 = \pm 2.20\%$

yield standards: $\Sigma_4 = \pm 1.90\%$

3.2 Equation 8 was used to calculate the uncertainty associated with calculating Ga content from activity data.

$$S_c = \pm\sqrt{E_1^2 + E_2^2 + E_3^2 + E_4^2}$$

$$S_c = \pm\sqrt{(3.06)^2 + (2.74)^2 + (2.20)^2 + (1.9)^2}$$

$$S_c = 5.03\%$$

The calculated Ga content of sample 6-1 is 20.62 ± 1.03 ppm.

A1.3 INAA OF Sc, Co, La, Sm, Eu, Hf, Ta, Th

A1.3.1 Sample Preparation

The whole rock and mineral samples were prepared as described above in section A1.2.4.1.1.

Four U.S.G.S. rock standards were used as standard samples.

A1.3.2 Irradiation

The sample sets were irradiated for 5 hours in a thermal neutron flux of 4×10^{13} n/cm^2/s. They were allowed to "cool" for approximately three weeks prior to gamma ray spectrometry.

A1.3.3 Gamma Ray Spectrometry

The samples were analyzed using the equipment described above in section A1.2.7.1. The analytical peaks and counting conditions are summarized in Table 56.

TABLE 56

Summary of Analytical Peaks and Counting Conditions

Radio-isotope	$T_{\frac{1}{2}}$	Measured Photopeaks (KeV)	Count Time (sec)		Time Since Irradiation
			Sample	Standards	
^{140}La	40.27 hrs.	487, 1596	1000	4000	3 weeks
^{153}Sm	47.10 hrs.	69, 103	"	"	"
^{46}Sc	83.9 days	889	8000	10000	8 weeks
^{60}Co	5.24 days	1332	"	"	"
^{152}Eu	12.2 yrs.	122	"	"	"
^{181}Hf	44.6 days	482	"	"	"
^{182}Ta	115.1 days	68	"	"	"
^{233}Pa	27.0 days	312	"	"	"

A1.3.4 Calculations

Element abundances were calculated using the procedure described above in section A1.2.8. (No yield correction is required.)

APPENDIX 2

MICROPROBE DATA

A2.1 INTRODUCTION

The major element compositions of the pyroxenes were determined using the automated MAC 500 wavelength dispersive electron microprobe facilities at Purdue University. Data reduction was performed using the Bence-Albee alpha factor method using the data of Albee and Ray (1970). Major elements are believed to be correct to ±2% of the element weight present.

The major element compositions of the olivines, garnets, spinels, and phlogopites were determined using the energy dispersive electron microprobe facilities at Cambridge University. Data reduction was performed using a full ZAF correction procedure as outlined by Stathon (1976). Major elements are believed to be correct to ±2% of the element weight present.

The analytical results are summarized in Table 57.

TABLE 57

Averaged Microprobe Data for Lherzolite Minerals

(N.A. = not analyzed, FeO_T = total iron calculated as FeO, N.D. = not detected)

Sample	# Grains Analyzed	Percent Oxides											
		Na_2O	MgO	Al_2O_3	SiO_2	K_2O	CaO	TiO_2	Cr_2O_3	MnO	FeO_T	NiO	Totals
Garnet Lherzolites													
385 ol	5	N.A.	51.21	N.A.	41.02	N.A.	N.A.	N.A.	N.A	0.12	7.45	0.34	100.14
opx	12	0.21	36.40	0.68	58.09	N.A.	0.47	N.D.	0.29	0.11	4.20	N.A.	100.45
cpx	12	1.74	17.83	1.82	54.84	N.A.	20.53	N.D.	1.42	0.10	2.07	N.A.	100.35
gnt	5	N.A.	20.73	20.47	42.04	N.A.	4.96	N.A.	4.40	0.32	6.78	N.A.	99.70
387 ol	5	N.A.	50.42	N.A.	40.89	N.A.	N.A.	N.A.	N.A.	0.12	8.49	0.33	100.24
opx	13	N.D.	35.34	0.81	58.46	N.A.	0.29	0.02	0.25	0.15	5.09	N.A.	100.41
cpx	12	3.05	15.79	3.26	54.01	N.A.	19.47	0.10	1.83	0.10	2.53	N.A.	100.11
gnt	5	N.A.	19.98	22.00	41.11	N.A.	4.40	N.A.	2.52	0.44	8.40	N.A.	99.86
phl	5	0.52	24.95	13.35	40.39	9.08	N.A.	0.55	0.64	N.A.	2.81	0.19	92.48
390 ol	5	N.A.	50.83	N.A.	40.94	N.A.	N.A.	N.A.	N.A.	0.12	7.40	0.35	99.63
opx	12	0.05	35.48	0.71	58.24	N.A.	0.47	N.D.	0.32	0.10	4.49	N.A.	99.86
cpx	11	1.23	17.94	1.46	55.17	N.A.	21.27	N.D.	1.25	1.90	0.06	N.A.	100.28
gnt	5	N.A.	20.33	19.86	41.91	N.A.	5.66	N.A.	4.86	0.31	6.82	N.A.	99.75

Spinel Lherzolites		Na_2O	MgO	Al_2O_3	SiO_2	CaO	TiO_2	Cr_2O_3	MnO	FeO_T	NiO	Totals
VSL-5 ol	5	N.A.	49.97	N.A.	40.51	N.A.	N.A.	N.A.	0.12	8.62	0.34	99.55
opx	10	0.22	33.19	3.97	55.63	0.73	0.10	0.55	0.17	5.53	N.A.	100.09
cpx	14	1.86	15.73	5.98	52.89	19.35	0.45	1.23	0.12	2.51	N.A.	100.12
sp	10	N.A.	20.09	48.35	N.A.	N.A.	0.21	20.54	0.23	11.21	0.25	100.87
VSL-6 ol	5	N.A.	49.11	N.A.	40.62	N.A.	N.A.	N.A.	0.12	9.98	0.25	99.49
opx	15	0.23	32.32	4.84	54.58	0.74	0.12	0.42	0.21	6.25	N.A.	99.71
cpx	8	1.64	15.29	7.24	51.94	19.92	0.53	0.86	0.14	3.06	N.A.	100.62
sp	12	N.A.	21.03	58.45	N.A.	N.A.	N.A.	9.31	0.17	10.35	0.31	99.73
VSL-7 ol	5	N.A.	49.92	N.A.	40.44	N.A.	N.A.	N.A.	0.13	8.66	0.29	99.44
opx	18	0.15	33.65	3.63	55.42	0.73	0.02	0.56	0.17	5.46	N.A.	99.79
cpx	10	0.82	17.13	4.10	53.46	21.53	0.09	0.94	0.12	2.57	N.A.	100.76
sp	9	N.A.	19.83	47.63	N.A.	N.A.	N.A.	21.72	0.23	11.30	0.26	100.97

APPENDIX 3

INAA REE DATA

The abundances of La, Sm, Eu, Hf, Ta, and Th in the lherzolite xenoliths are given in Table 58.

TABLE 58

Abundances of La, Sm, Eu, Hf, Ta, and Th in the Lherzolite Xenoliths

(N.A. = not analyzed; N.D. = not detected)

Sample	Abundances (ppm)		
Garnet Lherzolites	La	Sm	Eu
385 Whole Rock	2.15±0.24	0.23±0.04	N.D.
ol	N.A.	N.A.	0.16±0.08
opx	0.80±0.10	0.15±0.02	0.17±0.15
cpx	3.14±0.38	2.09±0.10	0.25±0.01
gnt	N.D.	1.24±0.17	0.31±0.19
	Hf	Ta	Th
385 Whole Rock	0.27±0.14	0.66±0.14	N.D.
ol	0.48±0.13	N.D.	0.08±0.08
opx	N.D.	0.10±0.04	0.38±0.15
cpx	0.37±0.14	0.22±0.07	N.D.
gnt	N.D.	N.D.	N.D.

TABLE 58 (Cont'd)

Sample	Abundances (ppm)		
Garnet Lherzolites	La	Sm	Eu
387 Whole Rock	10.44±0.47	1.59±0.06	0.54±0.19
ol	0.13±0.06	N.D.	0.22±0.10
opx	1.87±0.09	0.20±0.01	N.D.
cpx	14.58±0.28	6.10±0.05	1.78±0.17
gnt	N.A.	N.A.	0.50±0.20
phl	N.A.	N.A.	N.D.
	Hf	Ta	Th
387 Whole Rock	0.51±0.13	0.39±0.05	1.21±0.28
ol	N.D.	N.D.	N.D.
opx	N.D.	0.10±0.04	0.38±0.15
cpx	0.37±0.14	0.22±0.07	N.D.
gnt	N.D.	N.D.	N.D.
phl	N.D.	0.61±0.06	1.97±0.20
	La	Sm	Eu
390 Whole Rock	1.77±0.12	0.42±0.13	0.11±0.07
ol	N.A.	N.A.	N.D.
opx	0.37±0.06	0.05±0.01	N.D.
cpx	3.07±0.13	3.87±0.03	0.60±0.12
gnt	0.44±0.37	1.44±0.82	1.06±0.32
	Hf	Ta	Th
390 Whole Rock	0.28±0.14	0.42±0.06	N.D.
ol	N.D.	N.D.	N.D.
opx	N.D.	0.11±0.04	N.D.
cpx	N.D.	N.D.	N.D.
gnt	0.62±0.52	0.28±0.20	N.D.

Sample	Abundances (ppm)		
Spinel Lherzolites	La	Sm	Eu
VSL-5 Whole Rock	2.99±0.23	N.D.	0.27±0.09
ol	N.A.	N.A.	N.D.
opx	0.12±0.06	0.02±0.01	0.21±0.12
cpx	24.19±0.38	1.35±0.04	0.72±0.22
sp	N.D.	N.D.	N.D.

TABLE 58 (Cont'd)

Sample	Abundances (ppm)		
Spinel Lherzolites	Hf	Ta	Th
VSL-5 Whole Rock	N.D.	1.43±0.04	0.53±0.24
ol	N.D.	N.D.	N.D.
opx	N.D.	N.D.	N.D.
cpx	1.20±0.37	N.D.	3.83±0.52
sp	N.D.	N.D.	N.D.
	La	Sm	Eu
VSL-6 Whole Rock	0.51±0.18	N.D.	0.55±0.62
ol	N.A.	N.A.	N.D.
opx	N.A.	N.A.	N.D.
cpx	N.A.	N.A.	0.45±0.14
sp	N.A.	N.A.	0.30±0.13
	Hf	Ta	Th
VSL-6 Whole Rock	N.D.	1.48±0.04	N.D.
ol	N.D.	N.D.	N.D.
opx	N.D.	N.D.	N.D.
cpx	0.87±0.27	N.D.	N.D.
sp	N.D.	N.D.	N.D.
	La	Sm	Eu
VSL-7 Whole Rock	1.38±0.21	N.D.	N.D.
ol	N.A.	N.A.	N.D.
opx	0.15±0.08	N.D.	N.D.
cpx	N.A.	N.A.	N.D.
sp	N.D.	N.D.	0.21±0.13
	Hf	Ta	Th
VSL-7 Whole Rock	N.D.	1.09±0.04	N.D.
ol	N.A.	N.D.	0.53±0.16
opx	N.D.	0.06±0.05	N.D.
cpx	N.D.	N.D.	0.95±0.35
sp	N.D.	N.D.	N.D.

APPENDIX 4

INAA DATA FOR OTHER GARNET LHERZOLITES FROM KIMBERLEY, SOUTH AFRICA

The abundances of La, Sm, Eu, Sc, and Co in 3 garnet lherzolite xenoliths from the Bultfontein Floors mine dump in Kimberly, South Africa, were determined by Dr. R.H. Mitchell using INAA (see Appendix 3, section A1.3.1). The data are given below in Table 59.

TABLE 59

Abundances of La, Sm, Eu, Sc, and Co in Garnet Lherzolite Xenoliths (N.D. = not detected)

Sample		Abundances (ppm)				
		La	Sm	Eu	Sc	Co
GL-1	ol	0.40	0.03	N.D.	0.45	141.80
	opx	4.51	0.38	0.01	2.22	53.81
	cpx	18.28	4.81	1.32	36.65	17.02
	gnt	1.08	0.78	0.42	103.80	40.91
GL-2	ol	0.13	0.01	N.D.	0.36	142.10
	opx	3.30	0.27	0.04	1.59	54.06
	cpx	18.01	4.29	1.13	31.64	18.12
	gnt	0.39	0.35	0.18	87.63	45.31
GL-3	ol	0.11	0.02	N.D.	0.42	134.00
	opx	1.27	0.12	0.02	1.30	53.73
	cpx	14.57	3.70	0.91	26.25	16.07
	gnt	0.36	0.58	0.19	72.80	34.00

REFERENCES

Abbey, S. (1983) Studies in "Standard Samples" of silicate rocks and mineral 1969 - 1982. Geological Survey of Canada paper 83-15, p.30.

Ahrens, L.H. (1951) Quantitative spectrochemical analysis of silicate rocks, silicate minerals, and allied minerals. Spectrochim. Acta. 4, 302-306.

Ahrens, L.H. (1965) *Distribution of Elements in Our Planet*. New York: McGraw Hill.

Albee, A.L. and L. Ray. (1970) Correction factors of electron proble microanalysis of silicates, oxides, carbonates, phosphates, and sulfates. Anal. Chem. 42, #12.

Allegre, C.J. and J.F. Minster. (1978) Quantitative models of trace element behaviour in magmatic processes. Earth Planet Sci. Lett. 38, 1-25.

Anders, E. (1968) Chemical processes in the early solar system, as inferred from meteorites. Acc. Chem. Res., 1, 289-2-98.

Anders, E. and M. Ebihara. (1982) Solar-system abundances of the elements. Geochim. et Cosmochim. Acta. 46, 2363-2380.

Arculus, R. and J. Delano. (1981) Siderophile element abundances in the upper mantle: evidence for a sulphide signature and equilibrium with the core. Geochim. et Cosmochim. Acta. 45, 1331-1343.

Arth, J.G. (1976) Behaviour of trace elements during magmatic processes: a summary of theoretical models and their application. J. Res. U.S. Geol. Surv. 41, 41-47.

Baedecker, P.W., R. Schaudy, J.L. Elzie, J. Kimberlin, and J.T. Wasson. (1971) Proc. Lunar Sci. Conf. 2nd, pp.1037-1061.

Baedecker, P.A., J.J. Rowe and E. Steinnes. (1977) Application of epithermal neutron activation in multi-element analysis of silicate rocks employing both coaxial Ge(Li) and low energy photon detector systems. J. Radioanal. Chem. 40, 115-146.

Bailey, D.K. (1974) "Continental rifting and alkaline magmatism." In *The Alkaline Rocks*, (editor H.Sorenson). New York: Wiley, pp.148-159.

Barker, D.S. and K.P. Young. (1979) A marine Cretaceous nepheline basanite volcano at Austin, Texas. J. Science 31, 5-24.

Barker, D.S., R.H. Mitchell and D.B. McKay. (1985) Late Cretaceous nephelinite to phonolite magmatism in the Balcones Province, Texas. In papers presented at the G.S.A. South Central Section Meeting Symposia on Alkalic Rocks and Kimberlites, April, 1985.

Borisenok, L.G. (1959) Raspredelenie galliya v gornykh porodakh Sovetskogo Soyuza (The distribution of gallium in rocks of the Soviet Union). 1, 46-59.

Boyd, F.R. and P.H. Nixon. (1978) Ultramafic nodules from the Kimberley pipes, South Africa. Geochim. et Cosmochim. Acta. 42, 1367-1382.

Brett, R. (1970) The Earth's core: speculations on its chemical equilibrium with the mantle. Geochim. et Cosmochim. Acta. 35, 203-221.

Brett, R. (1976) The current status of speculations on the composition of the core of the Earth. Rev. Geophys. Space Phys. 14, 375-383.

Brett, R. (1984) Chemical equilibration of the Earth's core and upper mantle. Geochim. et Cosmochim. Acta. 48, 1183-1188.

Brey, G. (1978) Origin of olivine melilitites - chemical and experimental constraints. J. Volc. Geo. Res. 3, 61-88.

Brey, G. and J. Keller. (1982) Hegau Volcanic Province: Excursion Guide. Third International Kimberlite Conference, Clermont-Ferrand, France.

Brunfelt, A.O. and E. Steinnes. (1969) Instrumental neutron activation analysis of silicate rocks with epithermal neutrons. Anal. Chim. Acta. 48, 13-24.

Burton, J.D., F. Culkin and J.P. Riley. (1959) The abundances of gallium and germanium in terrestrial materials. Geochim. et Cosmochim. Acta. 16, 151-180.

Cameron, A.G.W. (1982) "Elementary and nuclidic abundances in the solar system." In *Essays in Nuclear Astrophysics* (eds. C.A. Barnes, D.N. Charamm, and D.D. Clayton), Cambridge University Press.

Carswell, D.A. and F.G.F. Gibb. (1980) Geothermometry of garnet lherzolite nodules with special reference to those from the Kimberlites of Northern Lesotho. Contrib. Mineral Petrol. 74, 403-416.

Chou, C.-L. (1978) Fractionation of siderophile elements in the Earth's upper mantle. Proc. Lunar. Planet. Sci. Conf. 9th, pp.219-230.

Chou, C.-L. (1980) "Radiochemical neutron activation analysis." In *Neutron Activation Analysis in the Geosciences* (editor G.K. Muecke). Mineralogical Assoc. of Canada, Short Course Handbook Volume 5, pp.133-166.

Chou, C., P. Baedecker and J. Wasson. (1973) Distribution of Ni, Ga, Ge, and Ir between metal and silicate portions of H-group chondrites. Geochim. et Cosmochim. Acta. 37, 2159-2171.

Chou, C.-L., P.A. Baedecker and J.T. Wasson. (1975) Allende inclusions: volatile-element distribution and evidence for incomplete volatilization of presolar solids. Geochim. et Cosmochim. Acta. 40, 85-94.

Chou, C.-L., D.M. Shaw and J.H. Crocket. (1983) Siderophile trace elements in the Earth's oceanic crust and upper mantle. J. Geophys. Res. 88, supplement, pp.A507-A518.

Clague, D.A. and F.A. Frey. (1982) Petrology and trace element geochemistry of the Honolulu Volcanics, Oahu: implications for the oceanic mantle below Hawaii. J. Petrol. 23, Part 3, 447-504.

Culkin, F. and J.P. Riley. (1958) The spectrometric determination of gallium in rocks and minerals. Analyst. 83, 208-212.

Day, F.H. (1963) *The Chemical Elements in Nature.* London: George G. Harrap and Co. Ltd., pp.203-205.

De Argollo, R.M. (1974) *Ga-Al and Ge-Si in Volcanic Rocks.* Unpublished Master's Thesis, University of Rhode Island.

De Argollo, R. and J.G. Schilling. (1978(a)) Ge-Si and Ga-Al fractionation in Hawaiian volcanic rocks. Cheochim. et Cosmochim. Acta. 42, 623-630.

De Argollo, R.M. and J.G. Schilling. (1978(b)) Ge/Si and Ga/Al variations along the Reykjanes Ridge and Iceland. Nature. 276, 24-28.

De Soete, D., R. Gijbels and J. Hoste. (1972) *Neutron Activation Analysis* (editors P.J. Elving and I.M. Kolthoff). London: John Wiley and Sons.

Dostal, J. and C. Elson. (1980) "General principles of neutron activation analysis." In *Short Course in Neutron Activation Analysis in the Geosciences*, (editor G.K. Muecke), Mineralogical Assoc. of Canada, Short Course Handbook Volume 5, pp.21-42.

Drake, M.J., H.E. Newsom, S.J.B. Reed and M. Clare Enright. (1984) Experiemental determination of the partitioning of gallium between solid iron metal and synthetic basaltic melt: electron and ion microprobe study. Geochim. et Cosmochim. Acta. 48, 1609-1615.

Ewing, T.E. and S.C. Caran. (1982) Late Cretaceous volcanism in south and central Texas - stratigraphic, structural, and seismic models. Gulf Coast Assoc. of Geological Societies Transactions. 32, 137-145.

Frey, F.A. and D.H. Green. (1974) The mineralogy, geochemistry and origin of lherzolite inclusions in Victorian Basanites. Geochim. et Cosmochim. Acta. 38, 1023-1059.

Frey, F.A., D.H. Green and S.D. Roy. (1978) Integrated models of basalt petrogenesis: a study of quartz tholeiites to olivine melilitites from southeastern Australia utilizing geochmeical and experimental petrological data. J. Petrol. 19, 463-513.

Frey, G.A., C.J. Suen and H.W. Stockman. (1985) The Rhonda high temperature peridotite: geochemistry and petrogenesis. Geochim. et Cosmochim. Acta. 49, 2469-2491.

Gabrielson, O. (1945) Studier over element-fordelningen: zinkblanden fran svenska fyndorter. Sveriges Geol. Undersokn., Ser. C, Avhandl. och Uppsat., No. 468, Arsbok 39, No.1.

Ganapathy, R. and E. Anders. (1974) Bulk compositions of the Moon and Earth, estimated from meteorites. Proc. Lunar Sci. Conf. 5th, pp.1181-1206.

Garati, G., C. Gorgoni and G.P. Sighinolfi. (1984) Sulphide mineralogy and chalcophile and siderophile element abundances in the Ivrea-Verbano mantle peridotites (Western Italian Alps). Earth Plant. Sci. Lett. 70, 69-87.

Gast, P.W. (1968) Trace element fractionation and the origin of tholeiitic and alkaline magma types. Geochim. et Cosmochim. Acta. 32, 1057-1086.

Goldberg, E., A. Uchiyama and H. Brown. (1951) The distribution of Ni, Co, Ga, Pd and Au in iron meteorites. Geochim. et Cosmochim. Acta. 2, 1-25.

Goldschmidt, V.M. and C. Peters. (1931) Zur Geochemic des Ga. Nachr. Ges. Wiss. Gottingen, Math.-phys. Kl.1, 165-183.

Goldschmidt, V.M. (1937) The principals of distribution of chemical elements in minerals and rocks. J. Chem. Soc., 1937, 655-673.

Goles, G.G. (1967) In *Ultramafics and Related Rocks* (editor P.J. Wyllie). New York: John Wiley and Sons, Inc., pp.352-362.

Goodman, R.S. (1972) The distribution of Ga and Rb in co-existing groundmass and phenocryst phases of some basic volcanic rocks. Geochim. et Cosmochim. Acta. 36, 303-317.

Harvey, P.K., D.M. Taylor, R.D. Hendry and F. Bancroft. (1973) An accurate fusion method for the analysis of rocks and chemically related materials by X-Ray fluorescence spectrometry. X-Ray Spectrom. 2, 33-44.

Haskin, L.A. (1980) "An overview of neutron activation analysis in geochemistry." In *Short Course in Neutron Activation Analysis in the Geosciences* (editor G.K. Muecke). Mineralogical Assoc. of Canada, Short Course Handbook Volume 5, pp.1-19.

Harte, B. (1977) Rock nomenclature with particular relation to deformation and recrystallization textures in olivine bearing xenoliths. J. Geology. 85, 279-288.

Hertogen, J. and R. Gijbels. (1976) Calculation of trace element fractionation during partial melting. Geochim. et Cosmochim. Acta. 40, 313-322.

Jagoutz, E., H. Palme, H. Baddenhausen, K. Blum, M. Cendales, G. Dreibus, B. Spettel, V. Lorenz and H. Wanke. (1979) The abundances of major, minor and trace elements in the Earth's mantle as derived from primitive u/m nodules. Proc. Lunar Plant. Sci. Conf. 10th, pp.2031-2050.

Jones, J.H. and M.J. Drake. (1982) "An experimental approach to early planetary differentiation." In *Lunar and Planetary Science*, 13, pp.369-370. Houston: Lunar and Planetary Inst.

Kallemeyn, G.W. and J.T. Wasson. (1981) The compositional classification of chondrites - I. The carbonaceous chondrite groups. Geochim. et Cosmochim. Acta. 45, 1217-1230.

Keays, R.R., D.K.B. Sewell and R.H. Mitchell. (1981) Platinum and palladium minerals in upper mantle-derived lherzolites. Nature. 294, No. 5842, 646-648.

Kerr, J. (1974) *Geology of Bathurst Island Group and Byam Martin Island, Arctic Canada.* Geological Survey of Canada, Memoir 378.

Kimura K., R.S. Lewis and E. Anders. (1974) Distribution of gold and rhenium between nickel-iron and silicate melts; implications for abundance of siderophile elements on the Earth and Moon. Geochim. et Cosmochim. Acta. 38, 683-701.

Kurat G., H. Palme, B. Spettel, H. Baddenhausen, H. Hofmeister, C. Palme and H. Wanke. (1980) Geochemistry of ultramafic xenoliths from Kapfestein, Austria: evidence for a variety of upper mantle processes. Geochim. et Cosmochim. Acta. 44, 45-60.

Langmuir, CH., R.D. Vocke, G.N. Hanson and S.P. Hart. (1978) A general mixing equation with applications to Icelandic basalts. Earth Plant. Sci. Ltt. 37, 380-392.

Lederer, C.M., J.M. Hollander and I. Perlman. (1967) *Table of the Isotopes*, 6th Edition. New York: John Wiley and Sons, Inc., p.207.

Lonsdale, J.T. (1927) *Igneous Rocks of the Balcones Fault Region of Texas.* University of Texas Bulletin 2744, 178 p.

Lyon, W.S. (1964) *Guide to Activation Analysis.* Princeton, New Jersey: Van Nostrand.

Maurice, P. (1987) "Geologese." In *Geolog*, Newsletter of the Geological Assoc. of Canada, Vol.16, Part 1, p.46.

McIntire, W.L. (1963) Trace element distribution coefficients: a review of theory and applications to geology. Geochim. et Cosmochim. Acta. 27, 1209-1264.

McKay, D.B. (1984) *Application of Ion Exchange to N.A.A. of REE in Geologic Samples (a comparative study).* Unpublished Honors Thesis, Lakehead University, Thunder Bay.

McKenzie, R.M., A.C. Oertel and K.G. Tiller. (1958) Analyses of the standard rocks G1 and W1. Geochim. et Cosmochim. Acta. 14, 68-72.

Meinke, W.W. (1955) Trace-element sensitivity: comparison of activation analysis with other methods. Science. 121, 177-184.

Mellor, J.W. (1924) *A Comprehensive Treatise on Inorganic and Theoretical Chemistry*, Vol.5. Longmans, Green and Co.

Minster, J.F. and C.J. Allegre. (1978) Systematic use of trace elements in igneous process, Part 3: inverse problem of batch partial melting in volcanic suites. Contrib. Mineral. Petrol. 68, 37-52.

Mitchell, R.H., D.A. Carswell and D.B. Clarke. (1980) Geological implications and validity of calculated equilibration conditions for ultramafic xenoliths from pipe 200 Kimberlite, Northern Lesotho. Contrib. Mineral. Petrol. 72, 205-217.

Mitchell, R.H. and R.R. Keays. (1981) Abundance and distribution of gold, palladium, and iridium in some spinel and garnet lherzolites: implications for the nature and origin of precious metal-rich intergranular components in the upper mantle. Geochim. et Cosmochim. Acta. 45, 2425-2442.

Mitchell, R.H. and R.G. Platt. (1983) Primitive nephelinitic volcanism associated with rifting and uplift in the Canadian Arctic. Nature. 303, 609-612.

Mitchell, R.H. and R.G. Platt. (1984) The Freemans Cove volcanic suite: field relations, petrochemistry and tectonic setting of nephelinite-basanite volcanism associated with rifting in the Canadian Arctic Archipelago. Can. J. Earth Sci. 21, No.4, 428-436.

Moller, P., P. Dulski and H.J. Schneider. (1983) "Interpretation of Ga and Ge content in sphalerite from the Triassic Pb-Zn deposits of the Alps." In *Mineral Deposits of the Alps and of the Alpine Epoch in Europe* (editor H.J. Schneider). Berlin-Heidelberg: Springer, 313-322.

Morgan, J.W. (1986) Ultramafic xenoliths: clues to Earth's late accretionary history. J. Geophys. Res. 91, 12375-12387.

Morgan, J.W. and G.A. Wandless. (1979) Terrestrial upper mantle: siderophile and volatile trace element abundances. (Abstract) Lunar Sci. Conf. 10, p.855.

Morgan, J.W., G.A. Wandless, R.K. Petrie and A.J. Irving. (1980) Composition of the Earth's upper mantle - I. Siderophile trace elements in ultramafic nodules. In *Evolution of the Upper Mantle* (editors R.E. Zartman and S.R. Taylor), Tectonophysics. 75, 47-67.

Mori, T. and D.H. Green. (1975) Pyroxenes in the system $Mg_2Si_2O_6$-$CaMgSi_2O_6$ at high pressure. Earth Planet. Sci. Lett. 26, 277-286.

Morris, D.F.C. and F.M. Breuer. (1954) The occurrence of Ga in blende. Geochim. et Cosmochim. Acta. 5, 134-141.

Morris, D.F.C. and M.E. Chambers. (1960) The determination of Ga in rocks by neutron-activation analysis. Talanta. 5, 147-153.

Muecke, G.K. (1980) *Short Course in Neutron Activation Analysis in the Geosciences.* Mineralogical Assoc. of Canada, Short Course Handbook Volume 5.

Mukherjee, B. (1948) Spectrographic determination of gallium in Indian bauxite by the carbon arc cathode layer method. Proc. Natl. Inst. Sci. India, 14, 169-175.

Nehru, C.E. and P.J. Wyllie. (1974) Electronmicroprobe measurements of pyroxenes coexisting with H_2O undersaturated liquid in the join $CaMg_2Si_2O_6$-H_2O at 30 kbar with application to geothermometry. Contrib. Mineral. Petrol. 48, 221-228.

Newsom, H.E. and H. Palme. (1984) The depletion of siderophile elements in the Earth's mantle: new evidence from molybdenum and tungsten. Earth Planet. Sci. Lett. 69, 354-364.

Nixon, P.H., O. von Knorring and J.N. Rooke. (1963) Kimberlites and associated inclusions of Basutoland, a mineralogical and geochemical study. Amer. Mineral. 48, 1090-1132.

Oftedal, I. (1940) Untersuchungen uber die Nebenbestandteile von Erzmineralien norwegischer zinkblende-fuhrender Vorkommen. Skrif, Norsdke. Vid-Akad. (Oslo) 1. Mat-Nat. Kl., No.8.

Rayleigh, J.W.S. (1896) Theoretical considerations respecting the separation of gases by diffusion and similar processes. Philos. 42, 493-499.

Rhodes, J.M. and J.B. Dawson. (1975) Major and trace element chemistry of peridotite inclusions from the Lashaine volcano, Tanzania. Phys. Chem. Earth. 9, 545-557.

Ringwood, A.E. (1955) The principles governing trace element distribution during magma crystallization: Part 1. Geochim. et Cosmochim. Acta. 7, 189-202.

Ringwood, A.E. (1965) Chemical evolution of the terrestrial planets. Geochim. et Cosmochim. Acta. 30, 41-104.

Ringwood, A.E. (1975) *Composition and Petrology of the Earth's Mantle.* New York: McGraw-Hall, 618 p.

Ringwood, A.E. and S.E. Kesson. (1977) Basaltic magmatism and the bulk composition of the Moon 2: siderophile and volatile elements in Moon, Earth and chondrites: implications for lunar origin. Research School Earth Sciences, Publication 1222: pp.425-464.

Sandell, E.B. (1947) Determination of gallium in silicate rocks. Anal. Chem. 19, 63-65.

Sandell, E.B. (1949) The Ga content of igneous rocks. Amer. J. Sci. 247, 40-48.

Saunders, A.D. and J. Tarney. (1979) The geochemistry of basalts from a back-arc spreading centre in the East Scotia Sea. Geochim. et Cosmochim. Acta. 43, 555-572.

Schiller, E.A. (1987) "The elements of the future". In *Investment News*, Vol.1, Issue 2, p.14.

Schilling, J.G. and J.W. Winchester. (1967) "Rare-Earth fractionation and magmatic processes." In *Mantles of the Earth and Terrestrial Planets* (editor S.K. Runcorn). Interscience, pp.267-283.

Shaw, D.M. (1957) The geochemistry of gallium, indium, thallium: a review. Phys. Chem. Earth. 2, 164-211.

Shaw, D.M. (1970) Trace element fractionation during anatexis. Geochim. et Cosmochim. Acta. 34, 237-243.

Shaw, D.M. (1977) "Trace element melting models." In *Physics and Chemistry of the Earth, Volume II: Origin and Distribution of the Elements* (editor L.H. Ahrens). Pergamon Press, pp.577-586.

Sick, U. (1970) *Uber Melilith-Nephelinite der Schwabischen Alb.* Ph.D. Thesis, University of Tubingen, Tubingen (Unpublished).

Smales, A.A. (1965) "The place of activation analysis in a research establishment dealing with pure materials." In *Trends in Activation Analysis.* Texas A&M University, College Station, pp.186-188.

Spencer, A.B. (1969) Alkalic igneous rocks of the Balcones Province, Texas. J. Petrol. 10, 273-306.

Statham, P.J. (1976) A comparative study of techniques for quantitative analysis of the X-ray spectra obtained with a Si(Li) detector. X-Ray Spectrometry. 5, 16-28.

Steinnes, E. (1971) "Epithermal NAA of geological material". In *Activation Analysis in Geochemistry and Cosmochemistry* (editors A.O. Brunfelt, E. Steinnes). Oslo: Universitetsforlaget, pp.113-128.

Stosch, H.-G. (1981) Sc, Cr, Co and Ni partitioning between minerals from spinel peridotite xenoliths. Contrib. Mineral Petrol. 78, 166-174.

Strock, L.W. (1945) *Quantitative Spectrographic Determination of Minor Elements in Zinc Sulphide Ores.* A.I.M.M.E. Tech. Pub. No. 1866.

Strominger, D., J.M. Hollander and G.T. Seaborg. (1958) Rev. Mod. Phys. 30, 585.

Sun, S.S. and G.N. Hanson. (1975) Origin of Ross Island basanitoids and limitations upon the heterogeneity of mantle sources for alkali basalts and nephelinites. Contrib. Mineral. Petrol. 52, 77-106.

Sun, S.S. and R.W. Nesbitt. (1977) Chemical heterogeneity of the Archean mantle, composition of the Earth and mantle evolution. Earth Planet. Sci. Lett. 35, 429-448.

Sun, S.S. (1981) Chemical composition and origin of the Earth's primitive mantle. Geochim. et Cosmochim. Acta. 46, 179-192.

Temple, P.G. (1965) *Geology of the Bathurst Island Group, District of Franklin, Northwest Territories.* Ph.D. Thesis, Princeton University, Princeton, N.J.

Treuil, M. and J.-L. Joron. (1975) Utilisation des elements hygromagmatophiles pour la simplification de la modelisation quantitative des processus magmatiques. Exemples de L'Afar et de la Dorsale Medioatlantique. Soc. Ital. Mineral. Petrol. 31, 125-174.

Turekian, K.K. and S.P. Clark. (1969) Inhomogeneous accumulation of the Earth from the primitive solar nebula. Earth Plant. Sci. Lett. 6, 346-348.

Van der Walt, T.N. and F.W.E. Strelow. (1984) Accurate determination of Ga in South African primary and secondary reference samples by ion exchange chromatography and atomic absorption spectrometry. Geostandards Newsletter. 8., No. 2, 163-167.

Vincent, E.A. and G. Nightingale. (1974) Gallium in rocks and minerals of the Skaergaard Intrusion. Chemical Geology. 14, 63-73.

Vinogradov, A.P. (1962) Srednie soderzhaniya khimicheskikh elementov v glavnykh tipakh izverzhennykh gornykh porad zemnoi kury (Average Contents of Elements in the Main Types of Igneous Rocks in the Earth's Crust). Geokhimiya, No. 7: 1962.

Vlasov, K.A. (1966) *The Geochemistry and Mineralogy of Rare Elements and Genetic Types of Their Deposits, Volume 1: Geochemistry of Rare Elements* (editor K.A. Vlasov). Monson Wiener Bindery Ltd., pp.437-673.

Wagner, P.A. (1914) "The diamond fields of Southern Africa." *The Transvaal Leader*, Johannesberg (2nd impression C. Struik (PTY) Ltd., Cape Town, 1971).

Wass, S.Y. (1980) Geochemistry and origin of xenolith-bearing and related alkali basaltic rocks from the Southern Highlands, New South Wales, Australia. Amer. J. Sci. 280-A, 639-666.

Wasson, J.T. (1970) Ni, Ga, Ge and Ir in the metal of iron-meteorites-with-silicate inclusions. Geochim. et Cosmochim. Acta. 34, 957-964.

Wasson, J.T. and J. Kimberlin. (1966) Determination by neutron activation of gallium and germanium in iron meteorites. Radiochim. Acta. 5, 170-174.

Wells, P.R.A. (1977) Pyroxene thermometry in simple and complex systems. Contrib. Mineral. Petrol. 62, 129-139.

Wimmenauer, W. (1970) Zur Petrologie der Magmatite des Oberr heingrabens. Fortschr. Mineral. 47, 242-262.

Wittaker, E.J.W. and R. Muntus. (1970) Ionic radii for use in geochemistry. Geochim. et Cosmochim. Acta. 34, 945-956.

Wittur, G. (1987) Minor metals. Canadian Mining Journal. 108, No. 2, 60.

Woldseth, R. (1973) *All You Ever Wanted to Know About X-ray Energy Spectrometry*. Burlingame, California: Kevex Corporation.

Wood, B.J. (1974) The solubility of alumina in opx coexisting with garnet. Contrib. Mineral. Petrol. 146, 1-5.